SURFACE ACOUSTIC WAVE BANDPASS FILTER SYNTHESIS AND DESIGN

By

MONIR H. EL-DIWANY
B.Sc.(Eng.), B.Sc.(Math.)(Hons.)

A Thesis

Submitted to the School of Graduate Studies

in Partial Fulfilment of the Requirements

for the Degree

Master of Engineering

McMaster University

May 1975

SURFACE ACOUSTIC WAVE BANDPASS FILTER SYNTHESIS AND DESIGN.

MASTER OF ENGINEERING(1975) McMaster University
(Electrical Engineering) Hamilton, Ontario.

TITLE: Surface Acoustic Wave Bandpass Filter Synthesis and Design.

AUTHER: Mohir H. El-Diwany, B.Sc.(Eng.) (Cairo University)
B.Sc.(Math.)(Hons.)(Ain Shames University)

SUPERVISOR: Professor C. K. Campbell.

NUMBER OF PAGES: (x) , 145.

SCOPE AND CONTENTS:

The design and fabrication of a Surface Acoustic Wave(SAW) TV-IF Filter .

ABSTRACT

Theory, design and fabrication of a Surface Acoustic Wave (SAW) TV-IF filter is presented in this thesis. The filter is a linear phase bandpass filter with a passband extending from 41.25 to 47.25 MHz. Optimization techniques were used for designing the filter impulse response. Conventional photolithography was used for the device fabrication. The results obtained correspond very well to the theoretical design.

ACKNOWLEDGEMENTS

The auther would like to express his indebtiness to Dr. C.K.Campbell for his technical advice and continuous encouragement throughout the course of this project.

I also wish to express my sincere appreciation to my colleagues at the CRL for valuable discussions. In particular I wish to single out Mr. M. Suthers for his invaluable help.

Messrs D. Seiler and P. Nolan deserve special thanks for numerous helpful suggestions and for their critical proof reading of this thesis.

Finally thanks are due to Mrs. Peggy Johnstone for the typing of the thesis.

TABLE OF CONTENTS

LIST OF FIGURES

CHAPTER I

INTRODUCTION

1.1 Background

The Rayleigh wave or Surface Acoustic Wave (SAW) that is found near the surface of a piezoelectric material has been employed to build a new family of electronic devices known as SAW Devices. Because the velocity of these acoustic waves is much less than the velocity of electromagnetic waves, a relatively long time delay can be achieved using these devices. Data storage, signal recognition, coding and separation of one signal from another are some of the applications that have been achieved using these devices [1], [2], [3].

The surface wave is neither a longitudinal nor transverse wave. It has both shear and longitudinal components, i.e. the particle motion associated with a Rayleigh wave is elliptical in the plane which is perpendicular to the surface of the substrate and parallel to the direction of propagation. Most of the acoustic energy is contained within a distance of 1.5λ_o of the crystal surface (λ_o is the wave length). Dissipation of acoustic energy (to the adjacent air medium) depends on the irregularity of the surface of the crystal substrate. Very smooth surface substrates are required to build these devices.

To generate and detect these waves, a certain type of transducer, known as the Interdigital Transducer (IDT) is used. Two simple IDTs consisting of two pairs of metal electrodes (fingers), deposited on the

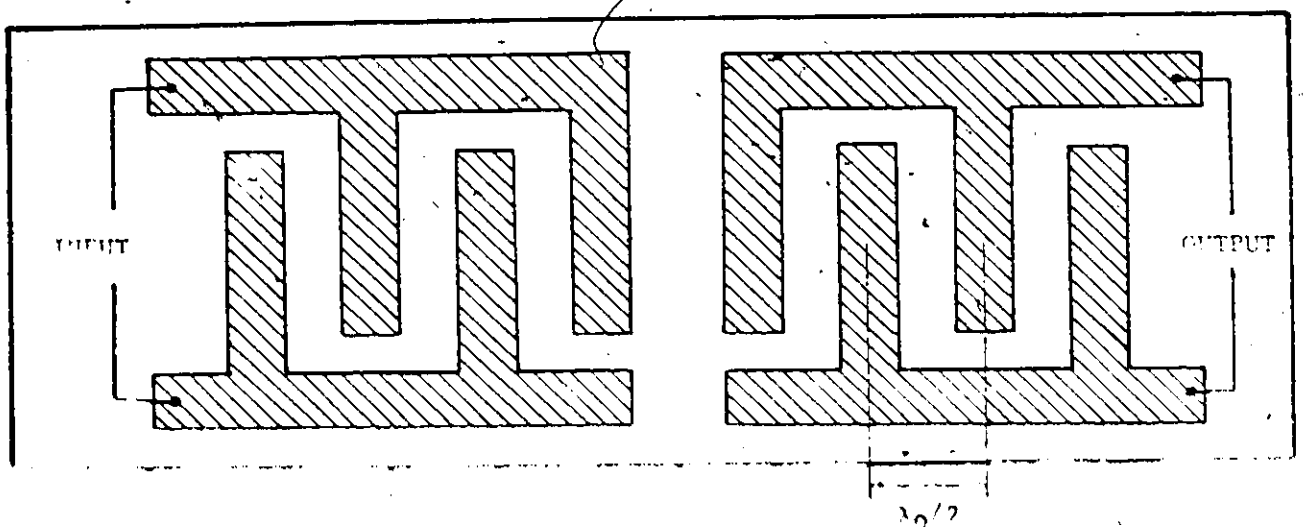

Fig. 1 Transmitter/Receiver pair of Interdigital Transducers deposited on [illegible]

surface of a piezoelectric material are shown in Fig.1.1. One of these transducers functions as a transmitter and the other as a receiver. An electric signal applied to one of these transducers will create an electric field between its electrodes. This electric field will be accompanied by a mechanical stress in the piezoelectric substrate. A rapidly changing electric signal will produce a sound wave that will travel on the surface of the crystal along certain axes. When this wave reaches the output transducer, the electric field associated with the travelling sound wave will induce an Rf voltage signal between the finger electrodes.

There is a certain frequency f_o, known as the synchronous frequency at which the transducer has a maximum efficiency. This frequency is related to the dimensions of the transducer by the relation

$$f_o = v/\lambda_o \qquad (1.1)$$

where $\lambda_o/2$ - repeat distance of the IDT (Fig 1.1)

v - SAW velocity in the substrate

At this frequency the voltages induced at the electrode fingers will be in phase and the output will be maximum. The characteristics of an IDT are determined by the number of finger pairs, their arrangement and the substrate material.

1.2 Scope of this Thesis

The theory, design and fabrication of a SAW TV-IF filter are presented in this thesis. The filter under consideration has a center frequency of approximately 44 MHz and a bandwidth of 6 MHz.

SAW transducers are best described in terms of the "Equivalent

Circuit Model". The model describes the sources of distortion, insertion loss and the effect of the substrate and transducer parameters on the resulting device response. Analysis of IDTs based on this model is presented in Chapter II with special emphasis on the design considerations. However, complete modelling for the device using this model is outside the scope of this thesis. The Equivalent Circuit Model was extended to explain the theory and design of a SAW component known as the Multistrip Coupler (MSC). MSCs are usually used in SAW filter design. The theory and design of the MSC are presented in Chapter III.

Another model for the IDT, known as the δ-function model or the impulse response model was used for the filter synthesis. This model is described in Chapter IV. An optimization scheme [20], designed originally for finite impulse response digital filters, was suggested in [17] and by the author (separately at the same time) to be used for optimizing the filter response given by the δ-function model.

The TV filter specifications, design and fabrication are given in Chapter V. Conventional photolithography was used for the device fabrication. The experimental results, conclusions and recommendations are given in Chapter VI.

CHAPTER II

ANALYSIS OF INTERDIGITAL SURFACE ACOUSTIC WAVE TRANSDUCERS.

2.1 General

The equivalent circuit model for SAW interdigital transducers (IDT) has proved to be the most efficient model for describing an IDT. The IDT could be visualized as a 3-port network (two acoustic ports and one electrical). Using the equivalent circuit model the transfer matrices for the input and output transducers can be found and hence the total transfer function between the electrical terminals can be determined as a function of frequency. Quantities like insertion loss, reflections from the input and output transducers, effect of device matching and electrical loading on the amplitude and phase responses, .. etc., can be found or included in this model.

2.2 The Equivalent Circuit Model

Consider the prototype IDT shown in Fig.2.1a. Applying an electrical voltage between its electrodes, the instantaneous electric field distribution will be as shown in Fig.2.1b. The electric field tangential and vertical components are both strong near the finger edges. Under the metal electrodes, the vertical component is much greater than the tangential and the opposite condition occurs in the interelectrode spacings. Two kinds of approximation for the electric field distribution problem are shown in Fig.2.2. These are called the

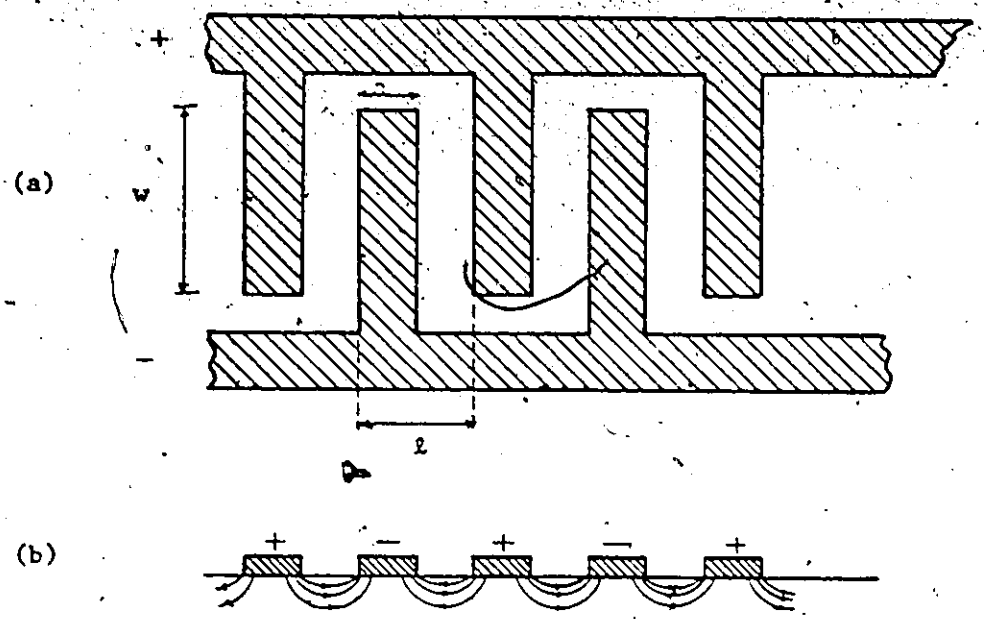

Fig 2.1 (a) SAW Interdigital Transducer
(b) Fingers cross section

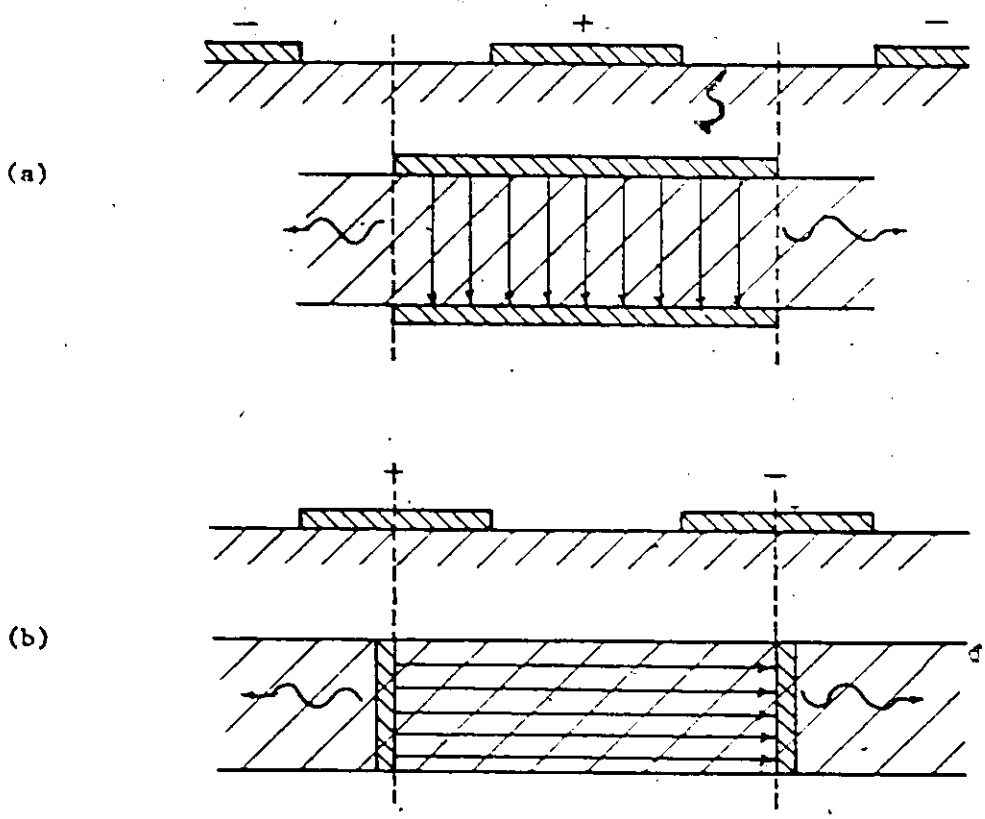

Fig 2.2 (a) Crossed-Field Approximation.
(b) In-Line Field Approximation.

crossed field and the in-line field approximations. Consequently there are two equivalent circuit models, namely the "in-line" model and the "crossed field" model. The choice between these two models is based on the contribution of the vertical and tangential field components to the Rayleigh waves. This in turn depends on the substrate material and the metallization ratio ($\eta = a/\ell$). For Lithium Niobate ($LiNbO_3$), the piezoelectric material extensively used for SAW devices, with a metallization ratio $\eta = 0.5$, the "crossed field" model is adopted. The only model which shall be considered in this work is the crossed field model.

The Mason equivalent circuit [4] for one electrode section is shown in Fig.2.3. The circuit elements are expressed in terms of two important parameters; the substrate electromechanical coupling coefficient k and the interelectrode capacitance C_n. The coupling coefficient k is defined for bulk wave transducers as the ratio of mutual elastic and dielectric energy to the geometric mean of elastic and dielectric self energies [4]. However, for SAW transducers, it is still a measure for the energy conversion efficiency. Lithium Niobate is the most favourable material for SAW devices because of its high coupling coefficient. The value of k for SAW transducers is given by [4].

$$k^2 \approx 2F \left|\frac{\Delta v}{v}\right| \qquad (2.1)$$

where Δv is the change in SAW velocity between the case of a free surface substrate and that with the surface coated by a very thin metal film. The factor F is a filling factor and depends on the metallization degree of the surface. For transducers deposited on Lithium Niobate ($LiNbO_3$), with metallization ratio $\eta = 0.5$ the measured value of the filling

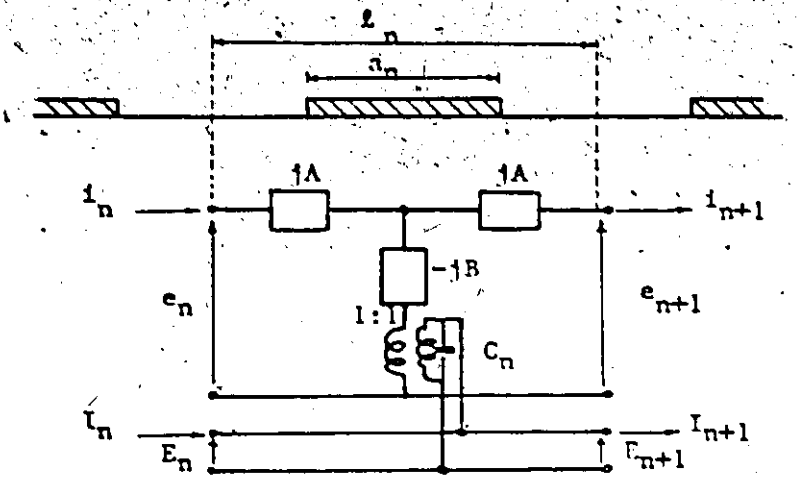

Fig 3.3 Mason Equivalent Circuit for one electrode section.

$A=R_0 \tan \theta_n/2$

$B=R_0/\sin\theta_n$

R_0=substrate characteristic mechanical impedance in electrical units.

ℓ_n =periodic length of the n^{th}section.

θ_n=transit angle of the n^{th}section.

C_n=electrode capacitance of the n^{th}section.

k =electromechanical coupling coefficient.

$R_0=1/G_0= \pi/\omega_n C_n k^2$

$\theta_n=2\pi f \ell_n/v$

$f_n=\omega_n/2\pi= v/2\ell_n$=the n^{th}section synchronous frequency.

factor is F = 1 ± 0.2 .

The capacitance per unit length of an electrode section C depends on the value of η rather than the separation between fingers. Its value is given by the empirical formula [6].

$$C = [(1 + \varepsilon_{PR}^{T})\ (6.5(a/\ell)^2 + 1.08(a/\ell) + 2.37]10^{-12}\text{F/m} \quad (2.2)$$

where $a/\ell = \eta$ is the metallization ratio [Fig.2.1],

$$\varepsilon_{PR}^{T} = \frac{1}{\varepsilon_o}\sqrt{\varepsilon_{11}\varepsilon_{33} - \varepsilon_{13}^2}$$

ε_{PR}^{T} is the relative permittivity at constant stress and the ε_{ij} are the actual dielectric constants at constant stress with the 1 direction being the direction of propagation. The values of k and C both depend on the orientation of the crystal and the direction of wave propagation on the surface. For example, the YZ - $LiNbO_3$ (Y cut - Z propagation) has a coupling coefficient $k^2 = 0.045$ and C = 464 pF/m for a metallization ratio $\eta = 0.5$.

The transfer function matrix for one electrode section of Fig.2.3 is given by [5].

$$\begin{bmatrix} e_n \\ i_n \\ E_n \\ I_n \end{bmatrix} = [T] \begin{bmatrix} e_{n+1} \\ i_{n+1} \\ E_{n+1} \\ I_{n+1} \end{bmatrix} \quad (2.3a)$$

where

$$[T] = \begin{bmatrix} \cos\theta_n & jR_o\sin\theta_n & 2\sin^2\theta_n/2 & 0 \\ jG_o\sin\theta_n & \cos\theta_n & -jG_o\sin\theta_n & 0 \\ 0 & 0 & 1 & 0 \\ -jG_o\sin\theta_n & 2\sin^2\theta_n/2 & (jwC_n + jG_o\sin\theta_n) & 1 \end{bmatrix} \quad (2.3b)$$

The transfer function matrix for the whole transducer will simply be the multiplication of the transfer matrices of its electrodes. The polarity of the circuit transformers should correspond to the polarity of their corresponding electrodes. In general, the electrode sections need not be identical. The value of w and ℓ of Fig.2.1a could differ from one section to another and hence θ_n, C_n and R_o would vary.

2.2.1 N Identical Sections Transducer

The uniform transducer of N identical electrode sections having the same overlapping w and periodic length ℓ of Fig.2.1a will be considered in this section. The transducer equivalent circuit parameters will be

$C_n = C_s$ = electrode capacitance per section.

$\ell_n = \ell$ = periodic length

$\theta_n = \theta = 2\pi f(\frac{\ell}{v}) = \pi(\frac{f}{f_o})$ = periodic section transit angle.

$f_o = v/2\ell$ = synchronous frequency of the transducer.

$R_o = 1/G_o = \pi/\omega_o C_s k^2$ = substrate mechanical characteristic impedance in electrical units.

The IDT as a 3 port network with two acoustic ports and one electrical (see Fig.2.4) will have the admittance matrix [Y] given by [4].

$$\begin{bmatrix} I_1 \\ I_2 \\ I_3 \end{bmatrix} = [Y] \begin{bmatrix} E_1 \\ E_2 \\ E_3 \end{bmatrix} \qquad (2.4a)$$

where

$$[Y] = \begin{bmatrix} -jG_o \cot N\theta & jG_o \csc N\theta & -jG_o \tan \theta/2 \\ jG_o \csc N\theta & -jG_o \cot N\theta & jG_o \tan \theta/2 \\ -jG_o \tan \theta/2 & jG_o \tan \theta/2 & j(\omega C_T + 2G_o N \tan \frac{\theta}{2}) \end{bmatrix} \qquad (2.4b)$$

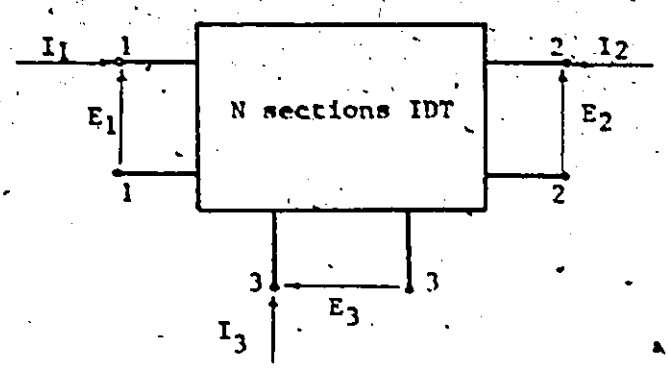

Fig 2.4 An N-identical sections IDT as a 3-port network.

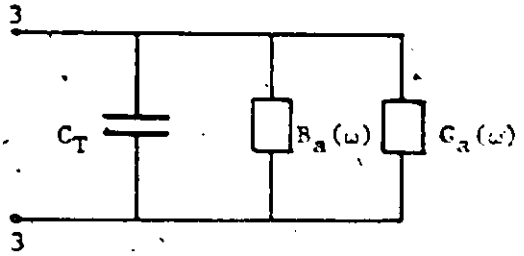

Fig 2.5 Shunt representation for transducer electrical input immittance.

Assuming that the transducer radiates into an infinite medium, or equivalently that the two acoustic ports are terminated by the characteristic impedance R_o, the input admittance of the transducer will be * (see Fig 2.5 [4]).

$$Y = G_a(\omega) + j[B_a(\omega) + \omega C_T] \tag{2.5}$$

where

$$G_a(\omega) = 2G_o[\tan \theta/2 \text{ in } N\theta/2]^2$$

$$B_a(\omega) = G_o \tan \frac{\theta}{2} [2N + \tan \frac{\theta}{2} \sin N\theta]$$

$$C_T = NC_s$$

For frequencies near the synchronous frequency

$$G_a(\omega) \cong \hat{G}_a \left(\frac{\sin x}{x} \right)^2 \tag{2.6a}$$

$$B_a(\omega) = \hat{G}_a \left(\frac{\sin 2x - 2x}{2x^2} \right) \tag{2.6b}$$

where $$x = \frac{N\pi}{2} \left(\frac{f-f_o}{f_o} \right) \tag{2.6c}$$

$$\hat{G}_a = \frac{2N^2\omega_o C_s k^2}{\pi} \tag{2.6d}$$

At the synchronous frequency f_o

$$G_a(\omega_o) = \hat{G}_a \tag{2.7a}$$

$$B_a(\omega_o) = 0 \tag{2.7b}$$

---

* $G_a(\omega)$ & $B_a(\omega)$ are not independent of each other. $B_a(\omega)$ is the Hilbert transform of $G_a(\omega)$ [24].

It is obvious that the input admittance is a function of the overlapping finger length w. By adjustment of this length the input conductance could be adjusted to match the output conductance of the driving source [6].

2.2.2 General SAW Transducer

The general SAW tranducer with both non uniform finger overlap and periodic length is shown in Fig.2.6a. To analyze this type of transducer it should first be divided into a number of imaginary strips [5] as illustrated by the dotted lines. The transducer of Fig.2.6a is represented schematically by Fig.2.6b. The shaded boxes represent electrode sections with finger overlap, each having the equivalent circuit of Fig.2.5. The open boxes represent the non-overlapping electrode sections which behave exactly as transmission lines for the surface waves. Such an electrode section of length ℓ_n will have the equivalent circuit of Fig.2.7 with the transfer function matrix [5].

$$\begin{bmatrix} e_n \\ i_n \\ E_n \\ I_n \end{bmatrix} = \begin{bmatrix} \cos\theta_n & jR_o\sin\theta_n & 0 & 0 \\ jG_o\sin\theta_n & \cos\theta_n & 0 & 0 \\ 0 & 0 & 1 & 0 \\ 0 & 0 & 0 & 1 \end{bmatrix} \begin{bmatrix} e_{n+1} \\ i_{n+1} \\ E_{n+1} \\ I_{n+1} \end{bmatrix} \qquad (2.8)$$

Multiplication of the transfer function matrices of the different sections of a certain strip will give the transfer function matrix of that strip. Again assuming that the transducer radiates into an infinite medium, the acoustic ports of each strip are equivalently terminated by the characteristic impedance R_o. The input admittance of each strip and hence of

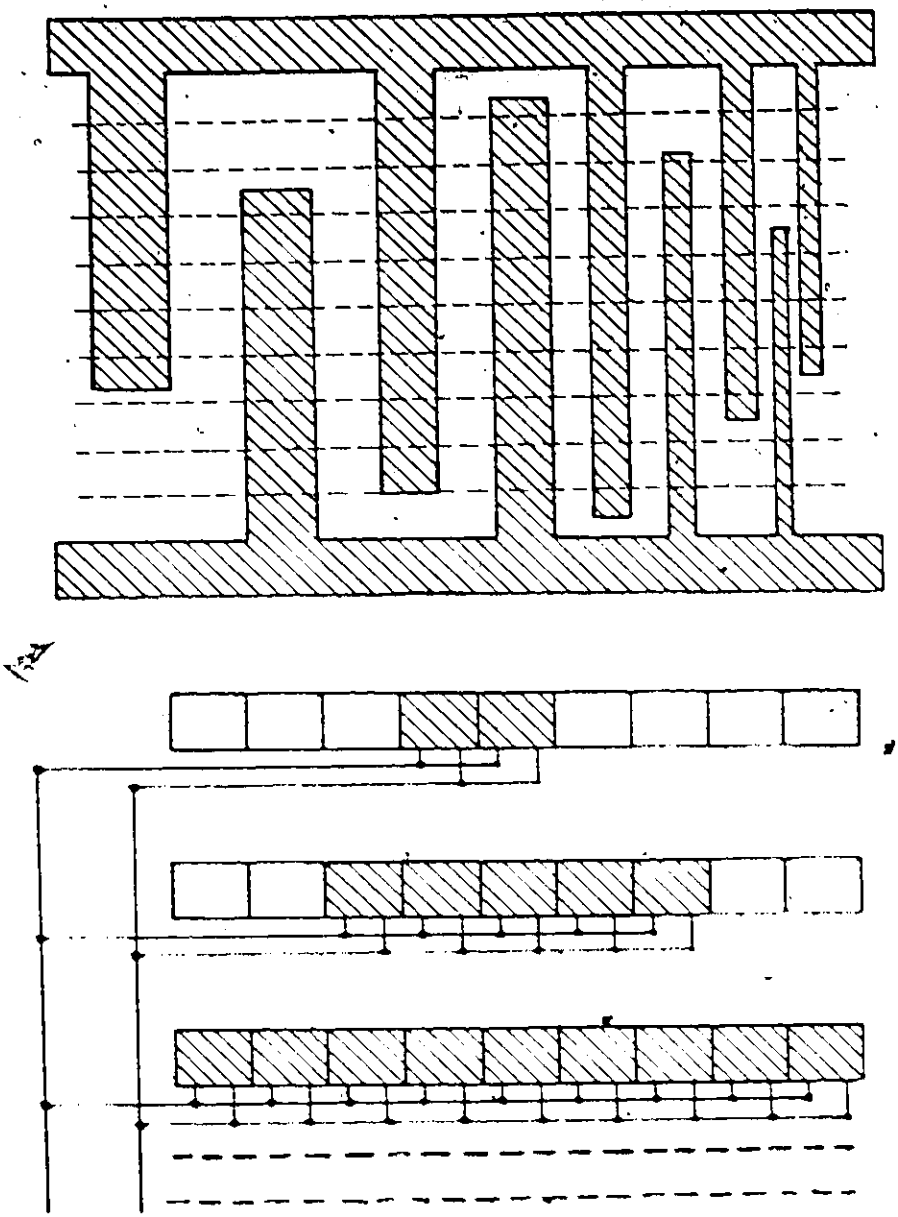

Fig 2.6 (a) General SAW transducer,
(b) Strip representation of the transducer in (a).

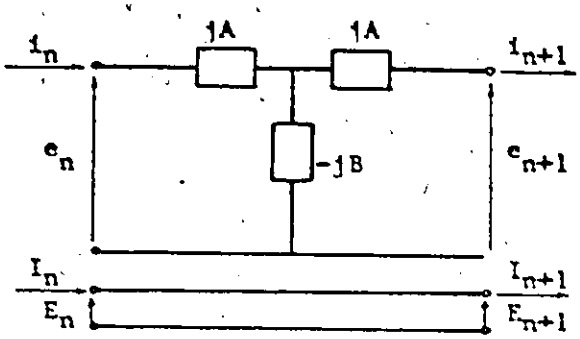

$A=R_0 \tan\theta/2$

$B=R_0/\sin\theta$

$\theta_n=2\pi f l_n/v$

$R_0=v/C_n\omega_n k^2$

Fig 7.7 Equivalent circuit for section of line with no finger overlap

the transducer could then be found. It is clear that the output waves from the different strips will neither have the same magnitude nor the same phase. If a uniform transducer is used as a receiver the input to its acoustic ports will be the vectorial sum of the output "voltages" of the different strips. The electrical terminals of each section are all connected in parallel to the driving source. The interaction between the different strips through the source impedance or the matching network makes the frequency response sensitive to the electrical loading and the extent of matching specially for high values of k.

The advantage of using the equivalent circuit model is that many of the secondary effects in SAW transducers can be encompassed in this model.

Scattering and Transmission Properties of Interdigital Transducers

The power scattering coefficients [1] for a three port network are defined as:

$$\Gamma_{ij} \qquad \frac{P_i}{(P_{av})_j}$$

where P_i is the power transmitted or reflected from port i and $(P_{av})_j$ is the power available from a matched generator at port j. Thus, Γ_{ii} is the fraction of power reflected when power is incident at port i, and $\Gamma_{ij}(i \neq j)$ is the fraction of power transmitted from port i when power is incident at port j. The two cases of uniform and apodized transducers will be considered separately to determine the effect of electrical loading on these coefficients.

2.3.1 N identical Sections Transducer

Consider the transmitter-receiver pair of Fig.2.8. The transmitted "voltage" from the input transducer will be the driving voltage of the output transducer at port 1. Port 2 is acoustically terminated by the impedance R_o while port 3 is electrically terminated in Y_L. From the symmetry and reciprocity of the uniform IDT,

$$p_{11} = p_{22}, \quad p_{13} = p_{23}, \quad p_{ij} = p_{ji} \quad i \neq j$$

If $Y_L = G_L + jB_L$, such that $B_L = -\omega_o C_T$ then [4]

$$p_{11} = \frac{1}{(1+b)^2}, \quad p_{21} = \frac{b^2}{(1+b)^2}, \quad p_{31} = \frac{2b}{(1+b)^2} \qquad (2.9)$$

where $b = G_L/\hat{G}_a$

These results can be reached by using the [Y] matrix for the uniform IDT or from the scattering matrix analysis for a lossless, symmetrical 3 port network. Minimum acoustic to electric conversion loss is obtained for $b = 1$, i.e. when $Y_L = \hat{G}_a - j\omega_o C_T$; a conjugate matched load.

The transmitter input impedance could be matched to the driving source impedance by using a series or shunt coil to tune out the input reactance and making the series input resistance equal to the generator resistance R_g. The input conductance can be adjusted by adjusting the finger length [6]. The minimum insertion loss, will then be 6 dB as illustrated in Fig.2.8.

The Triple Transit Echo (TTE) is defined as the portion of the output due to a double reflection between the input and output transducers

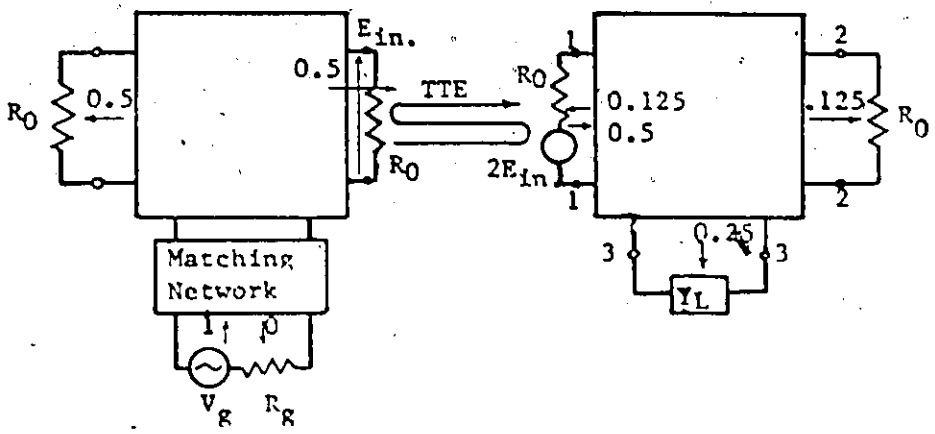

Fig 2.8 Power flow in a device consisting of two uniform transducers.

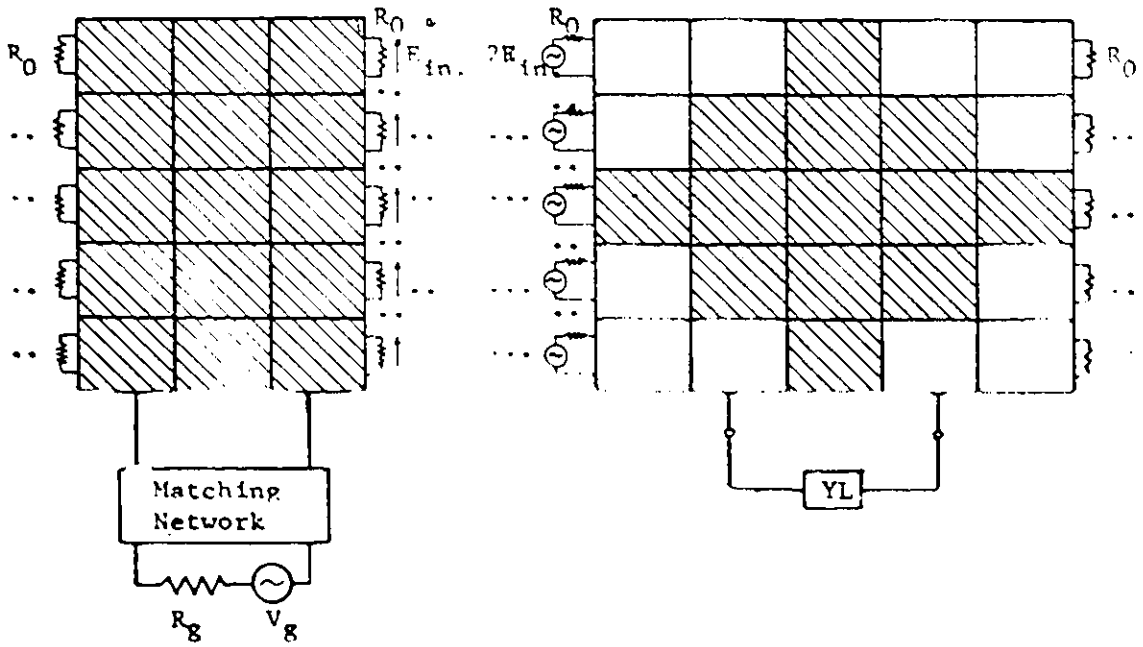

Fig 2.9 Strip representation of a SAW filter consisting of a uniform input transducer and an apodized output transducer.

as shown in Fig.2.8. With the matching conditions of the input and output transducers the TTE is -12 dB below the output signal.

To find the effect of the transducer matching on the frequency response, first define the radiation Q_r as [4]

$$Q_r = \omega_o C_T / \hat{G}_a \qquad (2.10a)$$

Substituting for $\hat{G}_a$ & C_T from (2.2), (2.5) & (2.6d),

$$Q_r = \frac{\pi}{2 N k^2} \qquad (2.10b)$$

For large values of $N k^2$ the radiation or the tuned circuit Q_r is smaller than the untuned bandwidth Q. ($Q = f_o/\Delta f$). Hence matching has negligible effect on the shape of the frequency response. Generally for high coupling coefficient materials such as YZ-$LiNbO_3$, the shape of the frequency response is determined primarily by the transducer structure.

2.3 General SAW Transducer

Consider a set of two transducers, one uniform and the other apodized. The pair is shown diagramatically in Fig.2.9. Let the uniform transducer be the transmitter and the apodized transducer the receiver. All the incident voltages at the receiver are in phase and have the same amplitude. The strips of the apodized transducer are connected in parallel (electrically) and have Y_L as a common load. Each strip possesses an internal impedance different from the other strips, hence when matching the transducer by putting Y_L equal to the conjugate of the transducer input impedance, this will provide unequal acoustic-to-electrical conversion efficiency for the different strips. Such an interaction between

the transducer fingers will make the response sensitive to the electric loading and the result is that ripples are introduced in the amplitude and phase responses of the transducer [7].

Reflected waves from the different strips of the apodized transducer are not in phase. Hence the TTE for apodized transducers is less than that of uniform transducers, i.e. less than -12 dB below the signal. At the same time the minimum insertion loss for apodized transducers is greater than that of uniform transducers.

The ripples in the amplitude and phase responses, the TTE and the minimum insertion loss are all functions of the electric loading and could be predicted only by the equivalent circuit model.

2.4 Design Considerations of Surface Acoustic Wave Transducers

In this section most of the factors that affect the generation of a SAW filter are discussed. These factors can be grouped into three design considerations.

2.4.1 Distortion Effects.

2.4.2 Insertion Loss

2.4.3 Substrate Choice

2.4.1 Distortion Effects.

Distortion in the amplitude and phase responses are mainly due to:

(1) Triple Transit Echo (TTE).

(2) Wave diffraction.

(3) Wavefront distortion in apodized transducers.

Some other sources of distortion which could affect the performance of a

SAW device are:

(4) Harmonic content of the output signal.

(5) Bulk wave generation by an IDT.

The TTE and the beam spreading due to wave diffraction are the major sources of distortion. Wave reflection by an IDT is caused by (a) wave regeneration by the transducer, (b) wave reflection from the finger edges. Wave regeneration by the voltage induced in the receiver was explained in the previous section. The TTE due to this wave regeneration was found to be -12 dB below the signal at matching conditions for uniform transducers. This could be reduced by choosing $b > 1$ in (2.9), i.e., by mismatching the device with a low impedance to reduce the induced voltage in the output load. Wave reflection from the finger edges is due to the sudden change of wave velocity at these edges. The change of wave velocity is caused partially by the mechanical loading of the metal fingers and partially by the electric shorting of the surface. The mechanical or mass loading tends to bring the SAW velocity closer to the bulk wave velocity, i.e., to increase the SAW velocity. The mechanical discontinuity can be reduced by using a light metal such as aluminum and reducing its thickness to the limit imposed by the ohmic losses. Aluminum thin films of thickness between 500 & 5000 Å can be used for SAW devices with negligible mass loading effects. The electric shorting in the metallized region will reduce the SAW velocity. The difference in wave velocity between the metallized and unmetallized regions is proportional to k^2 (2.1). This change in wave velocity is translated into change of the characteristic impedance R_o in the equivalent circuit model. Beside wave reflection due

to acoustic mismatch at the finger edges, the electric shorting has another serious effect which is the reduction of the average wave velocity in the finger region. This will decrease the center frequency of the transducer.

Wave reflections from the finger edges of a transducer having a metallization ratio $\eta = 0.5$ are shown in Fig.2.10. It is clear that these reflections add in phase at the synchronous frequency of the transducer for the case of $\eta = 0.5$. Unfortunately the value of $\eta = 0.5$ is a requirement imposed by other design considerations. A common technique to reduce the wave reflection from the finger edges is splitting each finger into two fingers, as shown in Fig.2.11a. The total reflection from each pair of fingers will be zero. This technique on the other hand will reduce the finger widths to half the previous value, adding more burden on the fabrication technology.

Wave diffraction due to limited aperture of the transducer introduces ripples in the amplitude profile of the wave. This effect will be discussed in detail in Section 2.4.3.

The surface wave launched from an apodized transducer has a concave rather than straight wave front. This wave front distortion is caused by the change in wave velocity which is due to the change of the metallization degree of the surface within the transducer region. In other words, because the wave velocity in a metallized region is less than that in a non metallized region of a piezoelectric substrate, the average phase velocity along the transducer axis, where there is the highest number of metal fingers, will be less than the average phase velocity along axes at the extremities of the transducer. However this

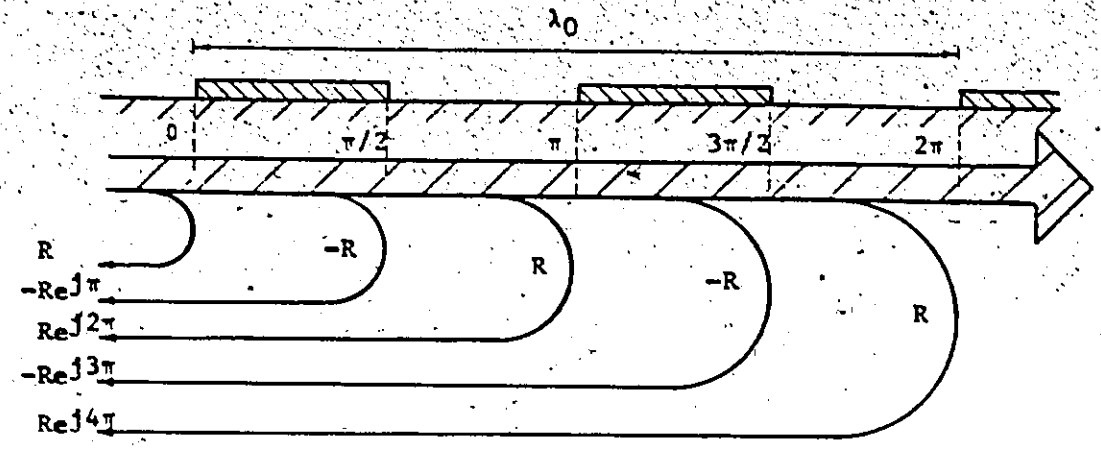

Fig 2.10 Wave reflection at the finger edges due to discontinuity.

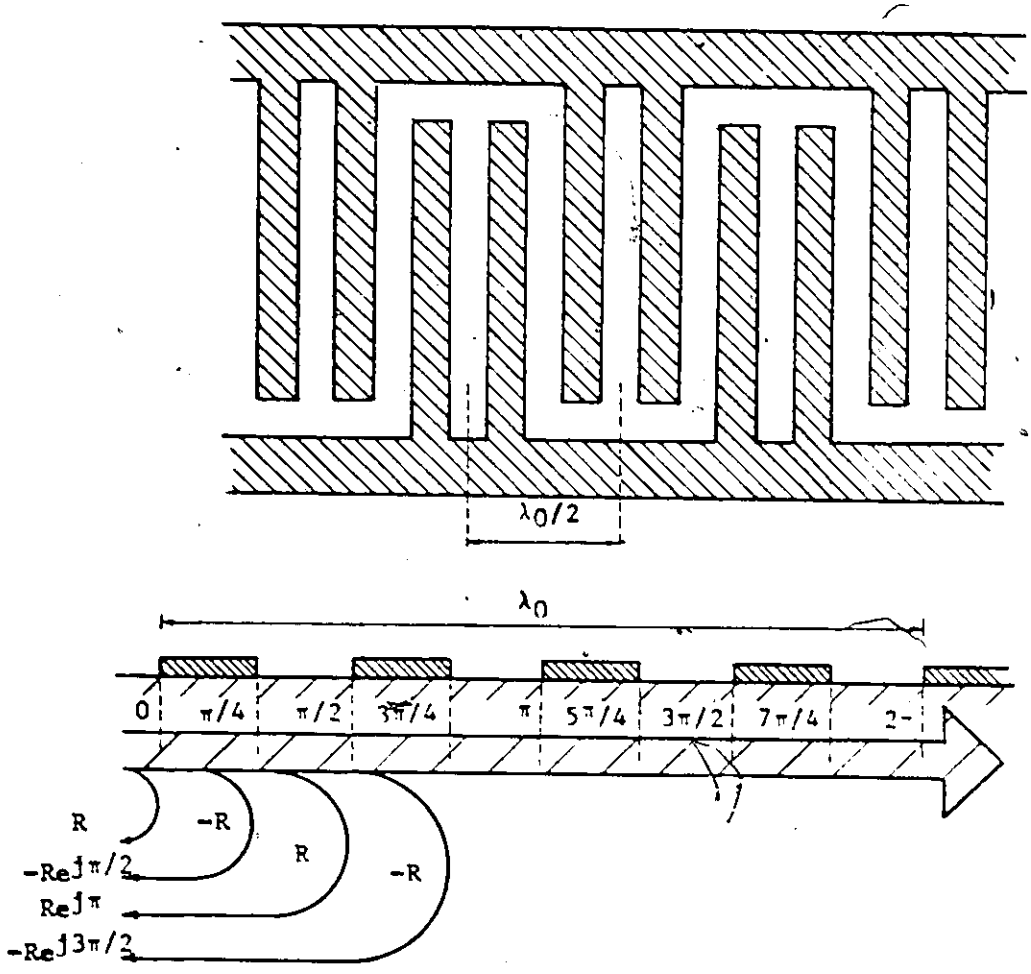

Fig 2.11 (a)Uniform split electrode transducer.
(b)Wave reflections from the transducer fingers.

kind of distortion can be removed simply by adding dummy electrodes (Fig.2.12). These electrodes do not contribute to the wave generation but give a uniform metallization in the transducer region so that the phase velocity will be the same along any axis parallel to the transducer axis.

Excitation of surface waves at the harmonic frequencies of the transducer synchronous frequency depends on the electric field distribution resulting from the applied voltage to the transducer. Only the odd harmonics are excited. Their amplitudes are proportional to the corresponding Fourier coefficients of the electric field. The electric field distribution depends on the transducer geometry and the metallization ratio η (the metal to space ratio). For single electrode transducers, the amplitudes of the different harmonics are determined by the value of η [11]. The optimal value of η for minimum overall harmonic content is $\eta = 0.5$.

The generation of bulk waves by interdigital transducers [12] occurs at discrete frequencies and is in the order of 50 dB below the excitation of the Rayleigh made for crystals with strong electromechanical coupling like $LiNbO_3$. However under certain circumstances [12], the excitation can be stronger, on the order of 20 dB below the excitation of the Rayleigh mode. The mechanism of bulk wave generation by interdigital transducers is beyond the scope of this thesis. However bulk waves can be suppressed by the use of multistrip couplers as will be seen in Chapter III.

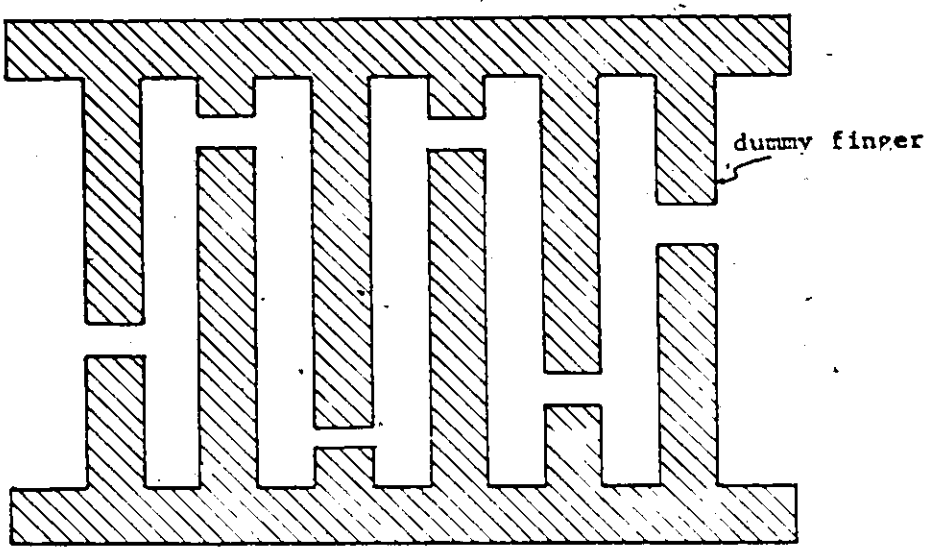

Fig 2.12 Apodized transducer with dummy electrodes.

2.4.2 Insertion Loss

Losses in SAW devices are due to:

(1) Bidirectionality of Interdigital Transducers.

(2) Electrical mismatch.

(3) Losses in matching network.

(4) Losses due to finger resistance.

(5) Propagation losses in the substrate.

(6) Losses due to beam spreading and beam steering.

Bidirectionality and mismatch are the main sources of insertion loss in SAW devices. For two matched uniform transducers the minimum insertion loss is 6 dB. However for apodized transducers the insertion loss is larger than 6 dB even with matching conditions. The insertion loss due to bidirectionality can be reduced by 3dBs with the use of unidirectional transducers [16]. Electrical mismatch also increases the insertion loss. However, the mismatch might be a requirement to reduce the TTE.

Losses introduced by the matching network are usually very small. Ohmic losses due to finger resistance are also insignificant unless the film thickness is very small. Propagation loss of surface acoustic waves is usually negligible below 100 MHz. Losses due to beam spreading and beam steering do not exceed 2dB.

2.4.3 Substrate Choice

The choice of the substrate material and orientation for a particular application is usually a compromise between a number of parameters. The important characteristics of a piezoelectric material are:

(1) Phase Velocity and Electromechanical Coupling Coefficient.

(2) Diffraction and Beam Steering Properties.

(3) Acoustic Attenuation.

(1) Phase Velocity and Electromechanical Coupling Coefficient: The phase velocity of SAW waves determines the interdigital period $\lambda_o/2$. For high frequency devices it is desirable to use high velocity substrates so that the fabrication becomes simpler. On the other hand for long time delays it would be more convenient to use low velocity substrates. The phase velocity of $LiNbO_3$ ranges between 3480 m/sec. and 4000 m/sec. depending on the orientation. In Table 2.1, the phase velocity of different materials with different orientations are listed.

The electromechanical coupling constant was defined in SEC.2.2 and its value was given by (2.1) which could be rewritten as:

$$k^2 = 2 \frac{|\Delta v|}{v} \qquad (2.11)$$

where Δv is the change of surface wave velocity produced by shorting the free surface with a thin conducting film. From Table 2.1, it is seen that $LiNbO_3$ provides the highest coupling coefficient (or $\Delta v/v$) of all the available piezoelectric materials.

(2) Diffraction, Beam Spreading and Beam Steering [13]: Wave diffraction is caused by the limited aperture of the surface waves launched from an IDT. It has two effects on the surface waves (see Fig.2.14):

(a) In the region closer to the source (Fresnel Region), wave diffraction introduces ripples in the amplitude profile of the wave. The beam width will be almost constant in this region.

TABLE 2.1 [9]

SUMMARY OF DESIGN DATA FOR MICROWAVE ACOUSTIC SURFACE WAVE DEVICES

Material	$LiNbO_3$	$LiNbO_3$	$LiNbO_3$	$LiNbO_3$	$Bi_{12}GeO_{20}$	$Bi_{12}GeO_{20}$	$LiTaO_3$	$LiTaO_3$	Quartz	Quartz
Orientation	Y Cut Z Prop	16 1/2° Double Rotated Cut	41 1/2° Rotated Cut X Prop	X Cut Z Prop	001 Cut 110 Prop	111 Cut 110 Prop	Z Cut Y Prop	Y Cut Z Prop	Y Cut X Prop	ST Cut X Prop
Surface Wave velocity v(m/sec)	3488	3503	4000	3483	1681	1708	3329	3230	3159	3158
Estimate of Electromagnetic to Acoustic coupling $\Delta v/v$	0.0241	0.0268	0.0277	0.0252	0.0068	0.0082	0.0059	0.0033	0.0009	0.00058
Power Flow Angle ϕ (deg)	0	0	0	-1.726	0	0	0	0	0	0
Slope of Electro-mechanical Power Flow Curve, $\partial\phi/\partial\theta$	-1.083	-1.087	-0.445	-0.610	-0.304	+0.366	-1.241	-0.211	0.653	0.378
SW ATTN In Air at 1 GHz(dB/μsec)	1.07	..15	1.05	-	1.64	1.64	1.0	1.14	2.6	3.09
Temp.Coefficient of Delay $\frac{1}{\tau}\frac{\partial\tau}{\partial T}$	94.	96.	72.	93.	-	-	69.	35.	-24.	0

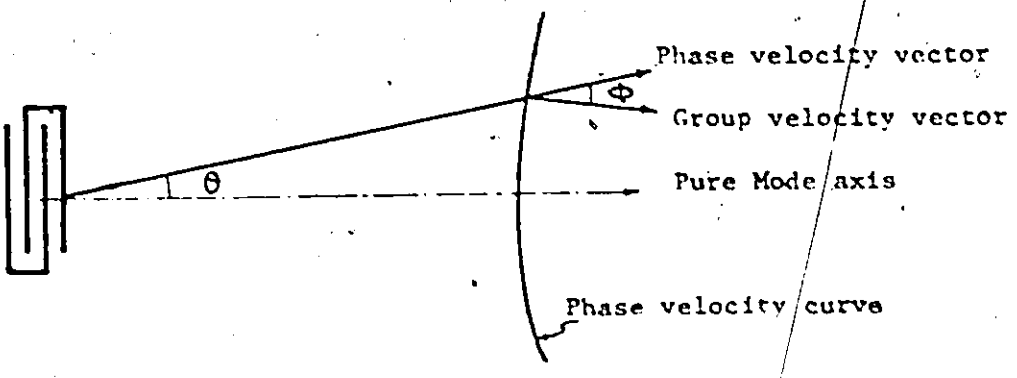

Fig 2.13 Variation of the phase velocity near the pure mode axis of the substrate

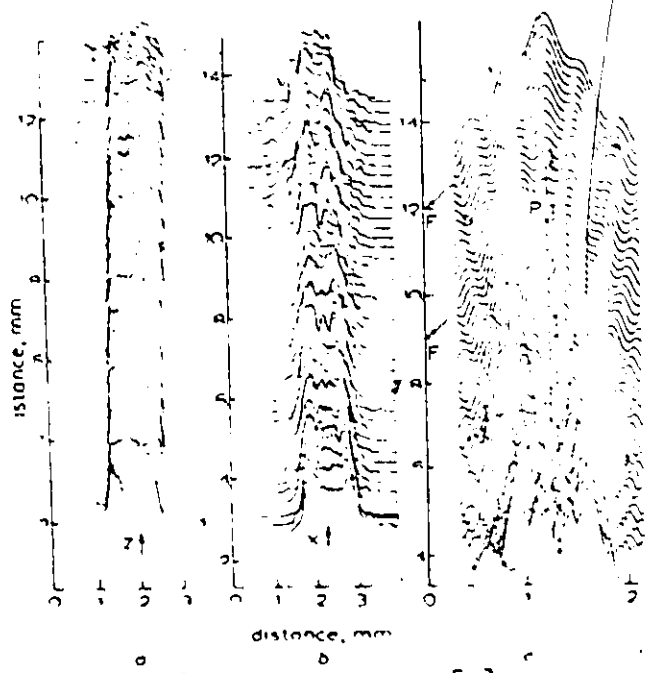

Fig 2.14 *Intensity and amplitude profiles* [13]

a and b Intensity profiles for surface waves propagating along the x and z axes, respectively, of Y cut $LiNbO_3$. Waves were launched from transducers of aperture 4mm operating at 100 MHz. The profiles were measured at intervals of 0.25 mm, and vertical axis indicates distance of profile from midpoint of transducers

c Computer simulation of amplitude profiles for similar transducer on isotropic material for profiles measured at intervals of 0.25 mm for distances of 2-13 mm

(b) Away from the source (Fraunhofer Region), the wave amplitude profile becomes more uniform but the beam width is considerably increased.

Beam spreading will contribute to the total loss since not all the radiated power will be intercepted. The ripples in the beam amplitude will add a new source of distortion especially if the output transducer is an apodized one.

The line separating the two regions is determined by the aperture of the transducer and the anisotropy of the substrate. The anisotropy of the wave velocity will either increase or decrease the beam spreading depending on the pure mode direction chosen. The pure mode axes are defined as the axes along which the power flow is colinear with the wave vector, i.e. the phase velocity vector and the group velocity vector coincide. Let ϕ represent the angle between these two vectors. The variation of phase velocity with the angle θ measured from the pure mode axis where the velocity is v_o is given by [9]:

$$v = v_o(1 + b\theta^2) \qquad (2.12)$$

The parameter b is a measure of anisotropy while $\frac{\partial\phi}{\partial\theta}$ is a measure of collimation. When $\frac{\partial\phi}{\partial\theta} = 0$, the case of isotropic propagation near the pure mode axis exists. When $\frac{\partial\phi}{\partial\theta} = 1$ this corresponds to the case of large collimation. From Fig 2.13, it can be shown that:

$$b = \frac{1}{2}\frac{\partial\phi}{\partial\theta} \qquad (2.13)$$

The self collimation produced by the anisotropy of the wave velocity will increase the extent of the Fresnel Region. The effective Fresnel distance, defined as the distance from the source to the point

on the beam axis from which the main lobe appears to emerge (point P in Fig.2.14), is given by [13]

$$r_{Fres.} = \frac{0.75a^2 \sec \phi}{\lambda(1 + \frac{\partial \phi}{\partial \theta})} \qquad (2.14)$$

where 2^a = launched beam width. The far field divergence half angle is given by

$$\psi_{anis} = \frac{\lambda}{2a} \left(\frac{1 + \partial\phi/\partial\theta}{\sec \phi} \right) \qquad (2.15)$$

Losses due to beam spreading are negligible if the output transducer is in the Fresnel Region of the input transducer. This is an important factor in choosing the aperture width of a transducer. However for apodized transducers, the diffraction from the region with small aperture could be minimized by increasing the total relative overlap. In Fig.2.14 the intensity profiles for waves propagating along the z axis of Y cut $LiNbO_3$ are shown. It is clear that self collimation is another important feature of $LiNbO_3$ which can be seen by comparing the value of $\frac{\partial \phi}{\partial \theta}$ for different substrate materials.

Beam steering refers to the angular misalignment of the acoustic beam with respect to the axis of the transducer. Beam steering is a result of misalignment of the transducer axis with the pure mode axis on anisotropic crystals. Due to beam steering, part of the generated beam will not be intercepted by the output transducer and hence will result in additional power losses.

For a high anisotropic material such as YZ $LiNbO_3$ a misalignment of 1° of the transducer axis causes a considerable shift in the transverse position of the beam. Beam steering losses are considerable for long

time delay devices. Alignment between the substrate axis and the transducer axis should be within 0.1° Losses due to beam steering and beam spreading can be reduced also by introducing multistrip couplers in the design.

(3) Acoustic Attenuation: Propagation attenuation is caused by transfer of energy into heat in the lattice structure of the crystal. For surface waves, the attenuation constant due to this form of loss, "Vacuum Attenuation", is proportional to the square of the frequency. An additional term could be added to the attenuation constant due to losses in the adjacent air. This term, "Air Loading" is proportional to the frequency. For $LiNbO_3$ the attenuation constant α is given by the empirical expression [9]

$$\alpha = 0.88f^{1.9} + 0.19f \qquad \text{dB/}\mu\text{ sec.} \qquad (2.16)$$

where f is in GHz. It is seen that propagation loss is negligible below about 200 MHz. Attenuation constants for different substrates are listed in Table 2.1.

(4) Temperature Coefficient of Delay: The temperature affects the performance of SAW devices through the temperature dependance of surface wave velocity and the thermal expansion of the substrate. The temperature coefficient of delay $\frac{1}{\tau}\frac{\partial \tau}{\partial T}$ is the best measure for the temperature sensitivity, where τ is the time delay while T is the temperature. In some applications such as delay lines, the coefficient of delay is perhaps the predominant factor in choosing the substrate material. In Table 2.1 values of temperature coefficient of delay are given for different substrate materials and orientations. $LiNbO_3$ has a relatively high coefficient

(90 pp m/C°) whereas ST.-cut quartz has a temperature coefficient equal to zero. The high temperature coefficient of YZ $LiNbO_3$ is one of the few characteristics in which YZ-$LiNbO_3$ is inferior to other low-loss piezoelectrics.

CHAPTER III

SURFACE ACOUSTIC WAVE MULTISTRIP COUPLER

3.1 General

The Multistrip Coupler (MSC) is an array structure of metal strips deposited on the surface of a piezoelectric substrate. Shown in Fig.3.1 is the simplest form of a MSC. A surface acoustic wave launched by transducer 1 will travel along track A_1 inducing a potential difference between adjacent metal strips. These potentials also appear in track B_2 where a second surface wave is generated.

A large number of applications and devices based on the MSC have been developed [14]. In this chapter the only scheme that will be discussed is that of Fig.3.1. The equivalent circuit model for the MSC will be presented. Also the design considerations and advantages of the MSC will be discussed.

3.2 Principle of Operation of Multistrip Couplers.

The design criterion for the MSC is the 100% transfer of energy, within a certain frequency band, from one track to the other. The equivalent circuit model leads finally to the design equations of the MSC.

Consider the case of the parallel, equal aperture tracks of Fig.3.1. A uniform wave generated by transducer No.1 can be resolved into two modes; the symmetric and the antisymmetric modes. The sum of these two modes gives the total SAW at any point on the surface (Fig.3.2).

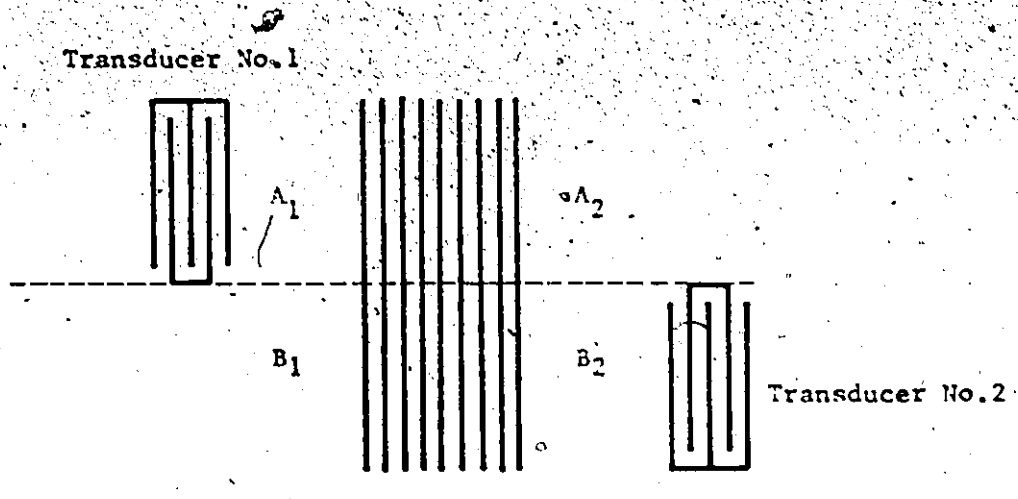

Fig 3.1 Two transducers coupled with a Multistrip Coupler.

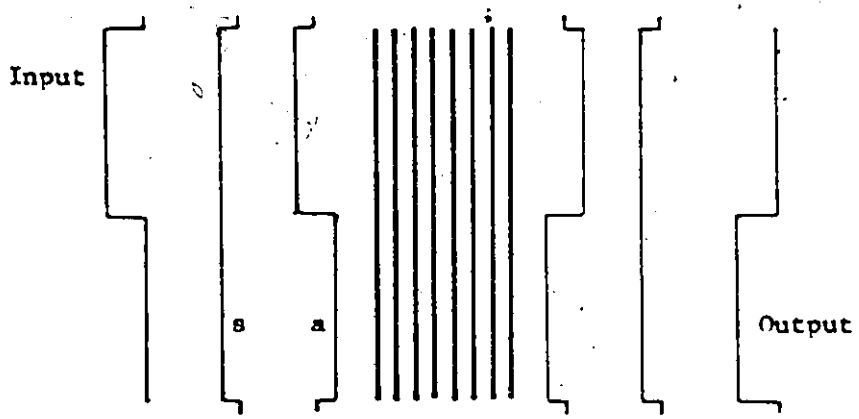

Fig 3.2 The symmetric mode(s) and antisymmetric mode (a) of the input and ouput waveforms.

In the tracks A_1, B_1, A_2 & B_2 (the metal free regions), the two modes have the same velocity which is equal to the SAW velocity of the substrate. In the MSC region, however, the two modes have two different velocities, which is the essence of the MSC behaviour.

The symmetric mode will induce equal inphase voltages in each metal strip in both tracks. Therefore, there is no current associated with this mode. Hence the symmetric mode velocity v_s will be equal to the free surface wave velocity. However, because of the finite width of the metal strips in the direction of wave propagation, the electric field associated with the acoustic wave will not have exactly the same distribution as in the case of a free surface. Hence v_s will be slightly less than the free surface velocity (the stiffened velocity).

The antisymmetric mode would introduce two equal 180° out of phase voltages in each strip if the strips are disconnected along the dotted line separating the two tracks. However, when these strips are connected together, as is the case, the charges on the two halfs of one strip will cancel out and the potential of each strip will remain zero. This mode will be associated with currents flowing in each strip back and forth. Hence the wave velocity of this mode v_a, is close to the unstiffened wave velocity, the surface wave velocity with the substrate covered with a thin metallic film.

As a result of the difference in the phase velocity between the two modes, a phase difference will be introduced between the two modes as they travel along the MSC. This phase difference is proportional to the number of strips of the MSC. A 100% transfer of energy between the two tracks will occur when the phase difference is equal

to π. The two modes being in phase in track A_1 and 180° out of phase in track B_1, will give zero output in track A_2 and a full output in track B_2.

If λ is the beat wavelength for the modes, i.e.

$$1/\lambda = 1/\lambda_a - 1/\lambda_s = f\left(\frac{1}{v_a} - \frac{1}{v_s}\right)$$

$$= f\,\frac{v_s - v_a}{v_s\, v_a} \qquad (3.1)$$

then, the 100% transfer of energy occurs when the MSC length $L_T = \lambda/2$ i.e. [15]

$$L_T = \frac{1}{2f}\,\frac{v_s\, v_a}{v_s - v_a} \qquad (3.2)$$

A simple expression can be obtained by making the approximation $v_s - v_a = \Delta v$ where Δv is the difference between free and metallized propagation velocities. Substituting for Δv using (2.11) yields

$$L_T = \frac{\lambda}{k^2} \qquad (3.3)$$

The number of strips N_T, assuming $\lambda_o/2 = d$ the repeat distance of the MSC will be [15]

$$N_T = \frac{\lambda}{k^2 d} = \frac{2}{k^2}\left(\frac{f}{f_o}\right)^{-1} \qquad (3.4)$$

This simple expression for N_T is an approximate expression and does not show the important fact that at f_o, the synchronous frequency, a stop band is introduced by the MSC.

The equivalent circuit model gives a full description of the performance of the coupler. One repeat distance of the MSC is represented by two circuits, one for each track. Each circuit (see Fig.3.3) consists of two T sections representing the two surface wave conditions along one repeat distance. The two circuits are electrically coupled through their electrical ports. Notice that the circuit elements are in mechanical units.

The circuit of Fig.3.3 reduces to those of Fig.3.4. for the symmetric and antisymmetric modes. The modes in one track can now be analyzed using the circuits of Fig.3.4. If $\phi_{(s)}$ & $\phi_{(a)}$ are the symmetric and antisymmetric phase shifts across each section then

$$N_T = \frac{\pi}{\phi_{(s)} - \phi_{(a)}} \qquad (3.5)$$

The complete expression for $\phi_{(s)}$ & $\phi_{(a)}$, given in [15], shows that at $f = f_o$, a stop band is introduced by the MSC. A simple expression for N_T is given by [15]

$$N_T = \frac{\pi}{F\,k^2} \frac{\theta/2}{\sin^2\theta/2} \qquad (3.6)$$

where $\theta = \frac{2\pi f a d}{v}$

and F is a filling factor which depends on the metallization ratio. This expression is not valid in the region of the stopbands but it works almost perfectly in the main frequency range of interest which lies in a broad band below the synchronous frequency. For frequencies above the first stop band the coupling to bulk modes makes the coupler of less interest.

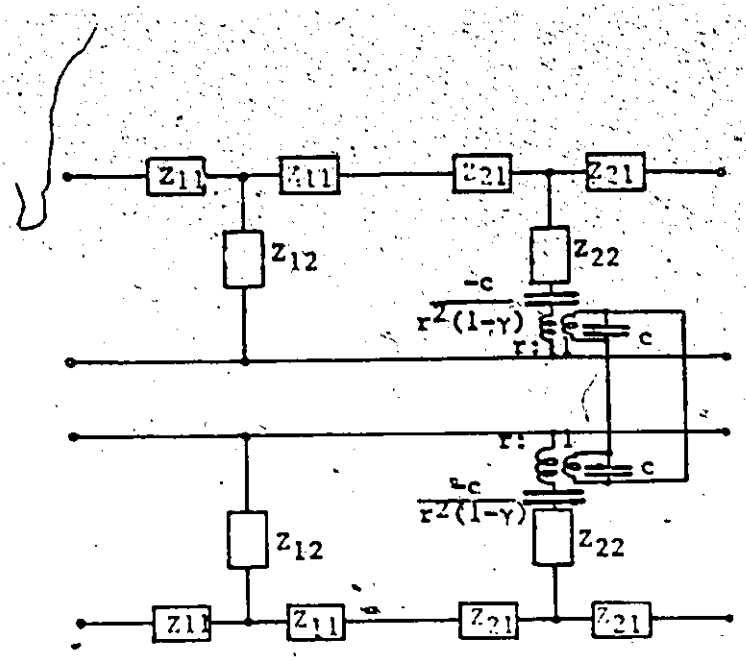

$Z_{i1} = jZ_i \tan\theta_i/2$

$Z_{i2} = jZ_i \operatorname{cosec}\theta_i$

where

$$\theta_1 = \frac{2\pi f(1-\alpha)d}{v_1} \qquad \theta_2 = \frac{2\pi f \alpha d}{v_2}$$

α is the active fraction of one repeat distance.

v_1&v_2 are the wave velocities in the passive and active regions.

d is the repeat distance of the coupler.

Z_i is the mechanical characteristic impedance of the substrate.

$$Z_i = \rho A v_i$$

ρA is the substrate mass per unit track length.

γ is a variable:

$\gamma = 1$	for the in-line model,
$\gamma = 2$	for the crossed-fieldmodel,
$0 < \gamma < 1$	for a mixed model.

c is the capacitance between adjacent strips for individual track aperture.

Fig 3.3 Equivalent Circuit of one repeat distance of a MSC.

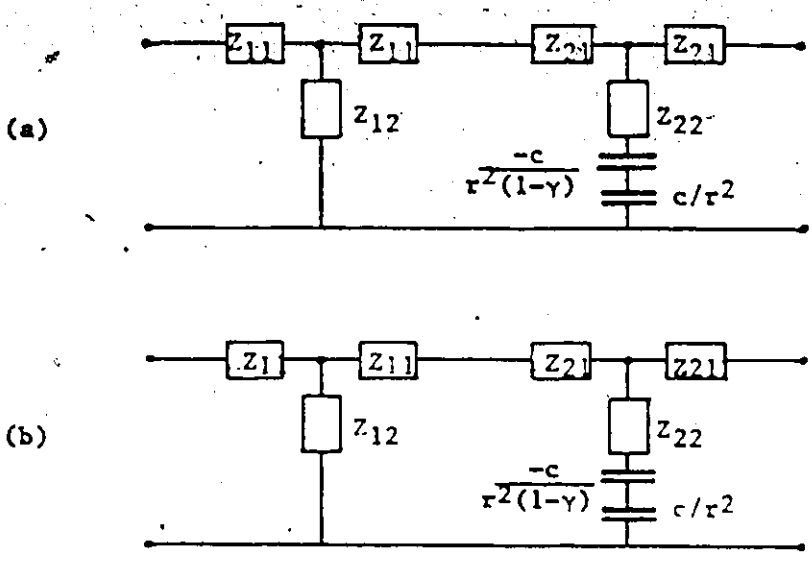

Fig 3.4 Single track equivalent circuit,
(a) For symmetric mode,
(b) For antisymmetric mode.

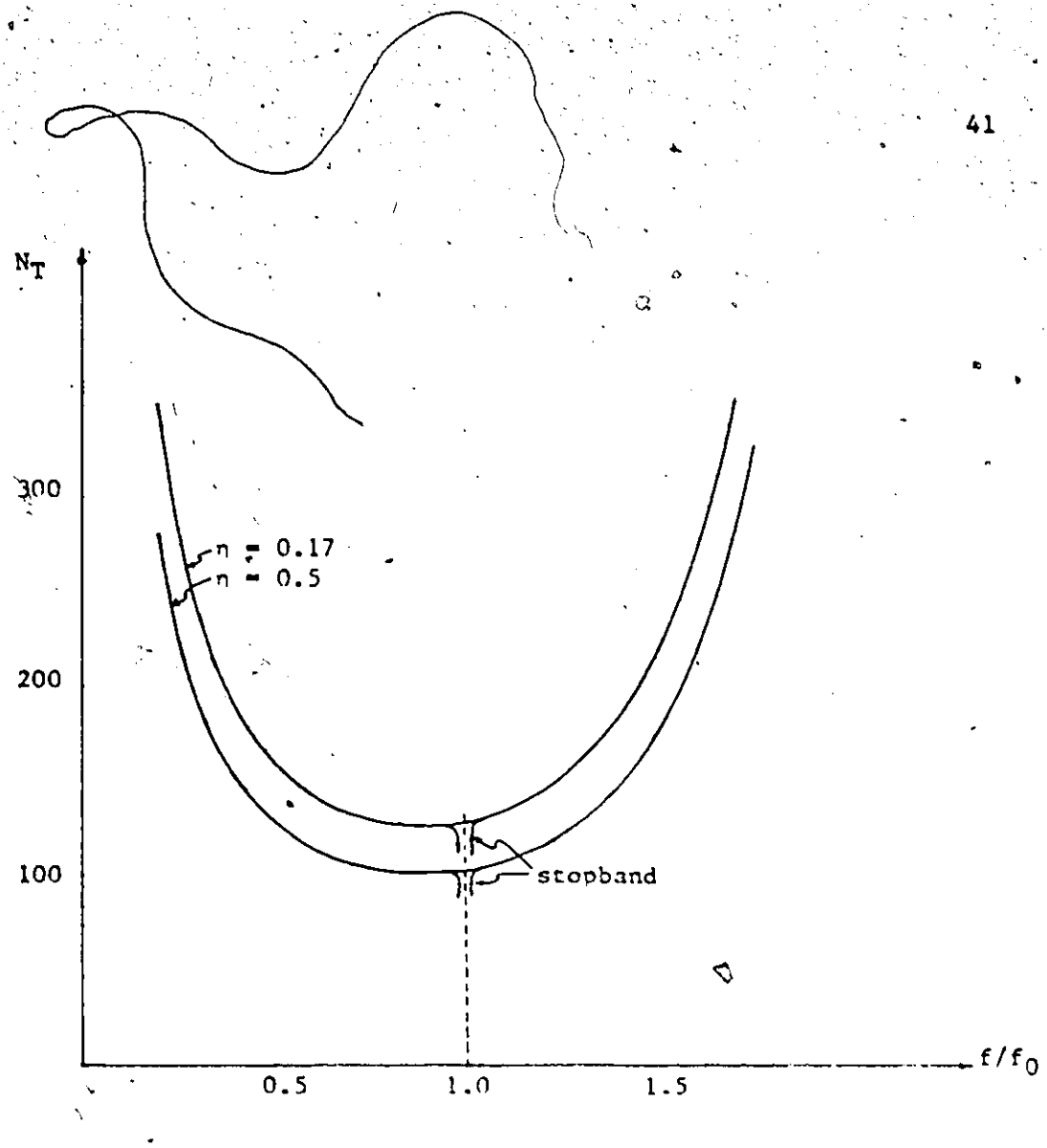

Fig 3.5 Number of strips for transfer N_T plotted against frequency normalized to the first stop band frequency for different metalization ratio η on YZ-$LiNbO_3$ substrate.

3.3 Design Considerations of Multistrip Couplers [15], [16].

The general shape of a plot of N_T vs f/f_o, where f_o is the synchronous frequency, is a U-shaped curve as shown in Fig.3.5. This of course disregards the effect of the stop band. There is a value of f/f_o at which N_T has a minimum. The pass band of the coupler will be around this frequency where N_T is almost constant. In other words, below the first stop band there is a frequency range along which the number of strips required for 100% transfer of energy is almost constant. The value of f/f_o for minimum N_T is controlled by the factor α. The minimum value of N_T is determined by the factor Fk^2. There is a direct relation between the effective coupling Fk^2 and the metallization ratio η (the ratio between the width of a metal strip and the repeat distance d). For $\eta = 0.5$ the value of Fk^2 is maximum and hence the number of strips required for 100% transfer of energy is minimum. High value of k^2 on the effective coupling Fk^2 also increases the band width of the MSC. The ratio η has also a direct relation with γ the field model which in turn determines the shape of the stop band of the coupler. Optimum performance of the coupler is obtained for $\eta = 0.5$. A plot of (3.6) for a MSC deposited on YZ $LiNbO_3$ with activity factor $\alpha = 0.85$ is shown in Fig.3.5.

As a result of the presence of the MSC, there are changes in the characteristic impedance of the "Transmission line" all along the coupler. These changes in the characteristic impedance will cause wave reflections which will add constructively at the synchro-

nous frequency of the coupler. However, these reflections become insignificant at frequencies away from the stop band. The signal losses by the MSC are mainly due to the ohmic losses in the metal strips and the conversion to bulk waves. The thickness and composition of the metal strips are not very significant factors unless the thickness is very small so that the ohmic losses become effective. Also if the thickness is very large then through mass loading the bulk mode conversion and the reflections from the MSC become significant. For aluminum strips of thickness between 2000 $\mathring{A}$ and 5000 $\mathring{A}$, the above effects can be entirely neglected.

A practical formula for the design of MSC on YZ-$LiNbO_3$ is given by [16]

$$N_T = \frac{195\ f/f_o}{1 - \cos(153\ f/f_o)} \qquad (3.7)$$

where f is the frequency of operation and the cosine angle is in degrees. The above expression is obtained by substitution in (3.6) for the parameter values. The variables a & F were used as fitting parameters between theoretical and experimental results. The values adopted in the above expression are for the case of metallization ratio $\eta = 0.5$. The operating frequency is usually taken as $0.75\ f_o$ where the band width is approximately 120% and the wave reflection by the coupler is negligible.

Example: The design of a MSC on YZ-$LiNbO_3$ to work in the frequency range 41.25 MHz to 47.25 MHz (The TV IF frequency range)

$f/f_o = 0.75$

hence from (3.7) $\therefore N_T = 103$ strips

The synchronous frequency of the coupler $f_o = 58.3$ MHz

For YZ-$LiNbO_3$ $v = 3488$ m/s

$\therefore \lambda_o = 59.88$ μm

For metallization ratio $\eta = 0.5$,

the strip width $= \frac{d}{2} = \frac{\lambda_o}{4}$

$\therefore$ Strip width $= 14.955$ μm

The choice of f_o becomes crucial only when the band width is important. In this example the band width is relatively small so the value of f_o is tolerable.

It is obvious from the above example that YZ $LiNbO_3$ is an ideal material for the utilization of MSCs. The large bandwidth and the relatively small number of strips of the couplers are direct consequences of the high coupling coefficient k^2 of YZ $LiNbO_3$.

3.4 Use of Multistrip Couplers in Surface Acoustic Wave Devices

Consider the device configuration of Fig 3.6. The impulse response of the apodized transducer will be a wave propagating on the surface of the crystal having the shape of the apodization and of constant amplitude. If this "space modulated" wave is the input to the MSC, then the output will be an "amplitude modulated" wave. In other words, the output wave in track B corresponding to an input wave of span χ in track A will be uniform across B and have an

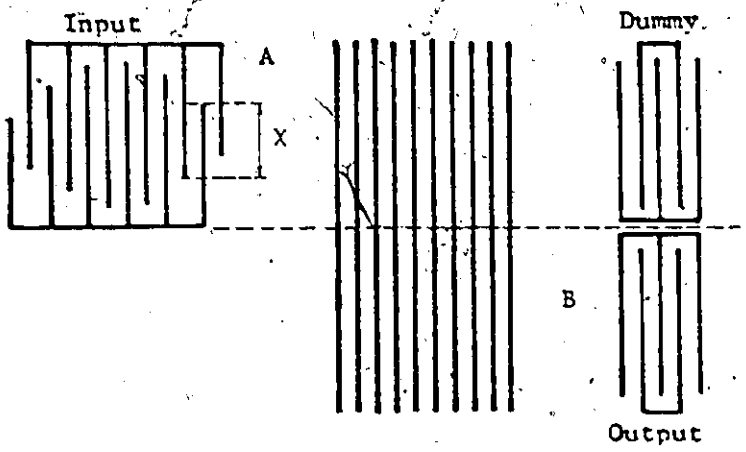

Fig 3.6 Using the MSC with apodized transducers.

amplitude proportional to χ. This can be easily explained by considering the case of a MSC with unequal tracks. In this case the number of strips required for maximum transfer of energy will be the same as before but the maximum fraction of energy transferred will now be given by [15]

$$F_T = \frac{4\ell_1 \ell_2}{(\ell_1 + \ell_2)^2} \qquad (3.8)$$

where ℓ_1 and ℓ_2 represent track aperture widths. Considering our case as the case of two unequal apertures with $\ell_1 = \chi$ and $\ell_2 = L-\chi$, then output power from the track $(L-\chi) = F_T$ x Input power to the track χ. The input power to track χ will be proportional to χ only because the amplitude of the input wave is constant while the output power from track $(L-\chi)$ is proportional to both the length $(L-\chi)$ and the square of the amplitude of the output wave. It can be easily shown that the amplitude of the output wave is proportional to χ.

The importance of this property could be appreciated if we are using two apodized transducers in the configuration of Fig.3.6. In this case the total frequency response will be the product of the individual responses of each transducer. That will not be the case if the two apodized transducers are placed side by side. This fact is extremely important in SAW filter design and will be implemented in the design given in Chapter VI.

Rejection of spurious waves generated by the input transducer

in track A will be incident to the dummy output transducer only. Also the triple transit signals are suppressed because reflection from the MSC outside the stop band is generally small. Suppression of bulk acoustic waves and triple transit signals is important in the design of SAW filters and delay lines.

CHAPTER IV

SURFACE ACOUSTIC WAVE FILTER SYNTHESIS.

4.1 General

Surface acoustic wave filters are best described in the time domain, i.e. by their impulse response. There is a quite distinct relation between the transducer configuration and its impulse response. Since filter specifications are usually given in the frequency domain, a valuable tool to determine the filter response in both the frequency and time domains is the Discrete Fourier Transform (DFT) using the Fast Fourier Transform technique.

Conceptually SAW filters are transversal filters in which the signal is repetitively delayed and added to itself. There is an obvious analogy between such filters and the non recursive, Finite Impulse Response (FIR) digital filters. Hence many aspects of the design techniques of FIR digital filters can be applied to SAW filters.

In this chapter the mathematical formulation for the relation between the transducer configuration and the impulse response is presented. Two approaches for SAW filter synthesis, both based on the design of the impulse response are also presented. The first approach uses directly the DFT with a weighting function to approximate the optimum inpulse response. The second approach uses the optimization techniques to find the optimum filter response.

4.2 The δ Function Model: [5], [17].

The SAW Transducer could be represented by a number of sources of acoustic energy. These sources are placed at the finger edges, as shown in Fig.4.1, where the gradient of the electric field created by the applied voltage is maximum. Let $e^{j\omega t}$ be the applied voltage to the transmitter comb. Each finger radiates an acoustic plane wave along the surface perpendicular to the finger edge. Neglecting acoustic wave diffraction [Sec.2.4.3], the wave is considered to be uniform along the length of the finger. The amplitude and phase of this wave is proportional to the electric field gradient at that finger edge. The wave radiated from the finger edge at x_n in the x direction will be

$$I_n \, e^{j\omega \, (x_n - x)/v} \, e^{j\omega t}$$

where I_n is the wave amplitude and v is the SAW velocity. The sum of these radiated waves at a receiver finger edge of position y_m, say, is given by:

$$\sum_{n=1}^{N} I_n \, e^{j\omega(x_n - y_m)/v} \, e^{j\omega t}$$

where N is the total number of edges in the transmitter comb. The induced voltage in the output transducer will be the sum of the induced voltages at its finger edges and is given by:

$$v_o(t) = \sum_{m=1}^{M} I_m \sum_{n=1}^{N} I_n \, e^{j\omega(x_n - y_m)/v} \, e^{j\omega t} \qquad (4.1)$$

where I_m is similar to I_n and M is the number of finger edges of the receiver. Since both I_m and I_n are proportional to the electric

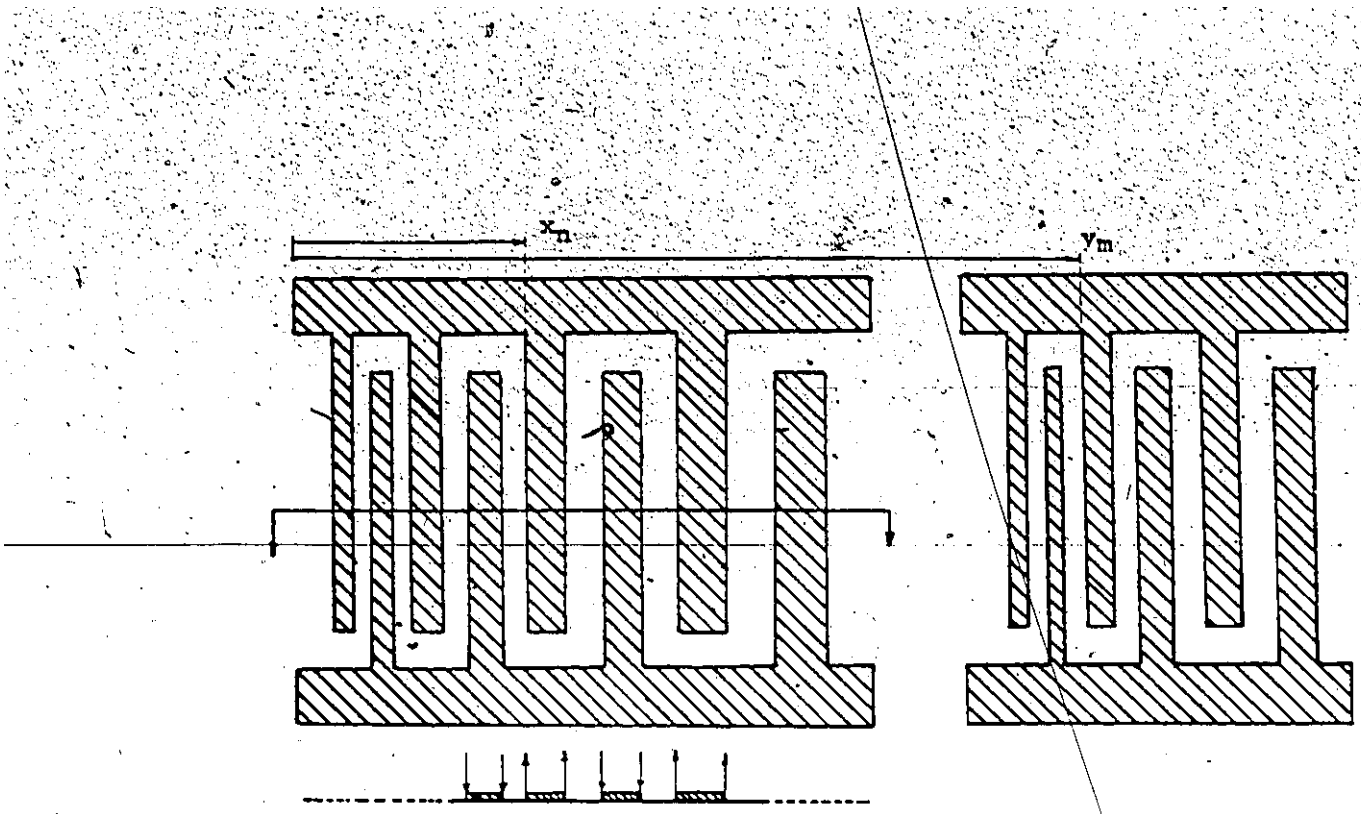

Fig 4.1 Two non-apodized transducers with representation of the electric field gradient as δ -function sources at the finger edges.

field gradient at the finger edges, they change their signs in pairs, i.e. if I_1 and I_2 are positive, then I_3 and I_4 should be negative and so on. AIso their amplitudes depend on the metallization ratio (metal to space ratio). This amplitude dependence is usually very small, so it cannot be used as a design variable to achieve certain characteristics for the transducer response. The transfer function will then be

$$H(f) = \left[\sum_{n=1}^{N} I_n \; e^{j\omega x_n/v} \right] \left[\sum_{m=1}^{M} I_m \; e^{j\omega y_m/v} \right] \qquad (4.2)$$

It is seen that the terms between brackets are the Fourier Transforms of $\sum_n I_n \; \delta(x - x_n)$ where the Dirac delta functions represent the sources at the finger edges at x_n with associated amplitudes I_n. Hence the total frequency response of the transducers configuration of Fig.4.1 is the product of the individual responses of the two transducers.

Certain types of frequency responses could be realized by coding only the phase (i.e. position) of each finger, since I_n is approximately constant, $\pm$ 1. Generally, to achieve any arbitrary frequency responses H(f), the amplitude of the δ-sources at each finger edge must also be adjustable. This cannot be achieved unless each finger is fed separately from a different source, which is not a practical solution. A simpler solution, rather than changing the amplitude, is to change the beam width by changing the finger overlap. Consider the system of two apodized transducers shown in Fig.4.2. To find

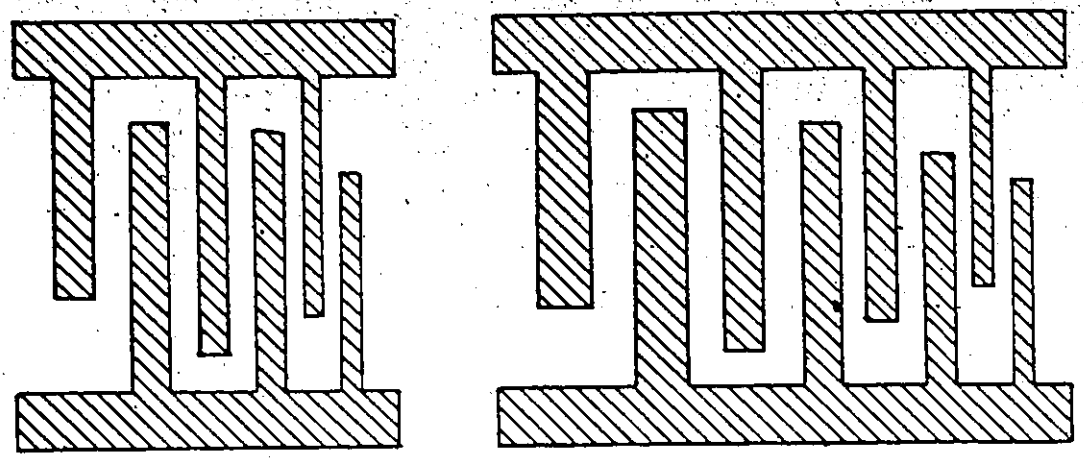

Fig 4.2 Two apodized transducers.

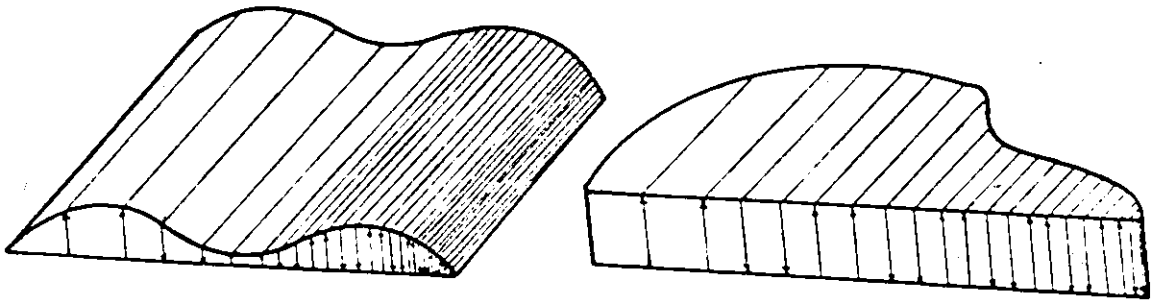

(a) (b)

Fig 4.3 Wave forms launched from different transducers
(a)From one of the trarsducers of Fig 4.1,
(b)From the apodized transducer of Fig 4.4.

their transfer function, consider the response caused by an (n,m) pair. It takes the form

$$I_n\ I_m\ e^{j(x_n-y_m)\omega/v} \quad x \text{ (weighting factor } C_{nm}).$$

The weighting factor is proportional to the beam width intercepted by the "active" part of the finger edge at y_m. In other words, if $w(x)$ represents the overlap function of the transmitter and $g(y)$ for the receiver, the weighting factor $C_{nm} = w(x_n)$ or $g(y_m)$ whichever is smaller. The transfer function will then be

$$H(f) = \sum_{n}^{N} \sum_{m}^{M} C_{nm}\ I_n\ I_m\ e^{j\omega(x_n-y_m)/v} \qquad (4.3)$$

Because of the binding term C_{nm}, the above double summation does not split into two separate summations as for the case of two unapodized transducers of Fig.4.1. This will make the above configuration of less interest for the design of SAW filters, since it is extremely difficult to visualize the comb's design from the entire transfer function. Now consider the case where only one of the transducers is apodized while the other has uniform overlap whose length is equal to or greater than the largest overlap in the apodized transducer, such as the configuration of Fig.4.4. In this case the double summation of (4.3) can be split into two summations. The transfer function will then be

$$H(f) = \left[\sum_{n}^{N} w(x_n)\ I_n \exp(j\ x_n\ \omega/v)\right]\left[\sum_{m}^{M} I_m \exp\ j\ y_m\ \omega/v\right]$$

..... (4.4)

If the uniform transducer(Fig4.4) consists of a small number of fingers, then it will have a flat broad band response and can be treated as a constant, i.e., the total response will be

$$H(f) = \sum_{n=1}^{N} A_n \exp j x_n \frac{2\pi f}{v} \qquad (4.5)$$

where $A_n = w(x_n)\, I_n$

It is clear that the coefficients A_n in this case are adjustable through the function $w(x_n)$, rather than I_n. It is important to notice the difference between varying the coefficient A_n through $w(x_n)$ and I_n (see Fig. 4.3). Variation of A_n through I_n is more difficult to achieve but it has the advantage of using two "active" transducers, as illustrated in (4.2). Variation of A_n by apodization is much easier but it puts the whole burden of the transfer function on only one transducer. It is possible, by using a multistrip coupler to change the spatial variations into amplitude variations as it was explained in Sec.3.4. This allows using two apodized transducers at the input and output so that more complicated responses could be achieved.

Any transfer function H(f) should be realizable through the variation of the coefficients A_n and the finger positions x_n in (4.5) However, there are two restrictions on the impulse response of SAW devices; the finite response, due to the finite number of fingers that could be used and the sign of the real coefficients A_n which should be changing in pairs.

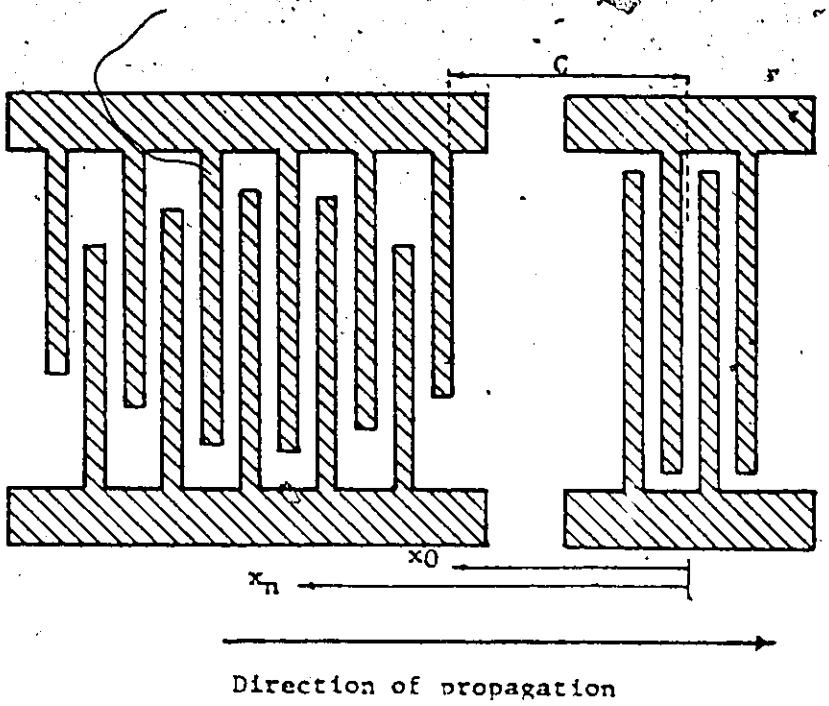

Fig 4.4 A simple filter consisting of one apodized transducer and a uniform broad band transducer.

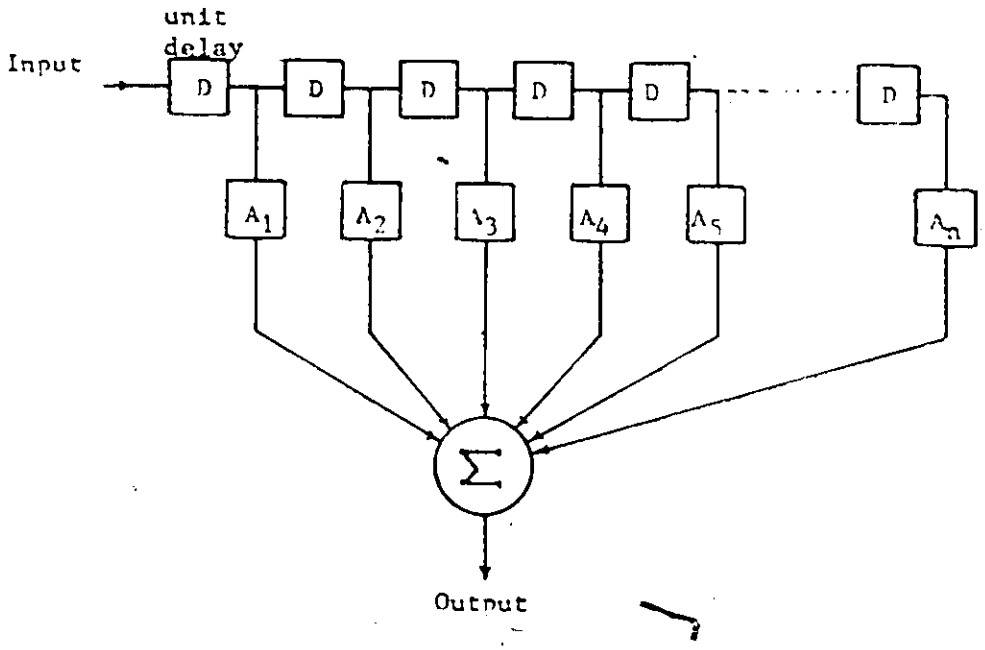

Fig 4.5 Schematic diagram of transversal filter.

A special case of that of Fig.4.2 is shown in Fig.4.4. For band pass filter application, this transducer configuration is used and only this configuration will be considered in the rest of this thesis. Its transfer function is given by

$$H(f) = \sum_{n=0}^{N-1} A_n \, e^{-j2\pi fnT} \qquad (4.6)$$

where T is the time period between two successive δ-impulses and $A_n = w(nT)$. The common term $e^{-\frac{j2\pi fC}{V}}$ has been omitted. The transfer function given by (4.6) is exactly the same as that of a Finite Impulse Response (FIR), non-recursive digital filter [17]. Both of these are represented schematically by Fig.4.5., with the major difference that the input and output in each case is different. For a SAW filter which is an analogue filter, the input and output are continuous signals (notice that, by definition, analogue filters do not necessarily have continuous impulse responses). As a digital filter the input and output are digital signals. In either case the impulse response is a sequence of impulses $\{A_n\}$ delayed from each other by unit delay T. The Fourier Transform (or more precisely the standard z-transform on the unit circle of the z plane) of this sequence is, as expected, given by (4.6).

Conceptually a SAW filter and a non recursive digital filter are transversal filters in which the signal is repetitively delayed and added to itself. The synthesis of transversal filters is completely different from that of the conventional RLC filters. The transfer function of an RLC filter is generally a rational function

having a number of poles and zeros. The synthesis of such a filter is merely distributing these poles and zeros in the S-plane to achieve the best approximation to the desired response (e.g. Chebyshev approximation for equal ripple response). The transfer function for a transversal filter on the other hand is a polynomial so it has only zeros. Usually it takes a larger number of zeros to achieve certain amplitude characteristics than that if poles were allowed. Hence new procedures should be found to locate the zeros for the transversal filters. There are generally two approaches for synthesizing a transversal filter: an approximate technique using the Discrete Fourier Transform (DFT) together with a weighting function and another approach using optimization techniques. These approaches will be discussed in details throughout the rest of this chapter.

Impulse Model Design of Surface Acoustic Wave Filters

The impulse response of the transducer [illegible] sequence of impulses [illegible]

$$H_p(f) = \sum_{n=0}^{N-1} A_n \, e^{-j2\pi f n T}$$

There are three important restrictions on the impulse response $\{A_n\}$ which are [8]:

*The coefficients A_n must be real and alternate their signs in pairs.

**The discrete nature of the impulse response.

***The finite duration of the impulse response.

To examine more closely the effect of these restrictions on the frequency response, they have to be separated from each other. First assume A(t) to be a real-time continuous version of the response $\{A_n\}$ which may have infinite duration. This assumption is valid because the coefficients A_n are all real since all fingers are driven from the same source. The periodically alternating sign of $\{A_n\}$ restricts the response A(t) to have the form of an amplitude modulated signal, i.e.

$$A(t) = h_\ell(t) \cos 2\pi f_o t \qquad (4.7)$$

where f_o is the center frequency of the band pass filter. The corresponding frequency response is a symmetrical band pass filter[18]. The $h_\ell(t)$ is called the equivalent low pass filter response and has the frequency response $H_\ell(f)$ [Fig.4.6a]. Hence A(t) and its Fourier Transform will be as shown in Fig.4.6b. Now sampling the continuous response A(t) at a sampling rate f_s samples/sec, the Fourier Transform of the resulting sequence will be given by

$$Hp(f) = \sum_{n=-\infty}^{\infty} H(f - nf_s) \qquad (4.8)$$

To prevent aliasing between adjacent spectra of Hp(f), the sampling frequency f_s should be equal to or greater than the Nyquist rate. However, due to the periodicity of the structure the sampling frequency must have particular values to allow for the finger positioning such that they alternate their signs in pairs. If $f_s = 4f_o$, the finger positioning will be as shown in Fig.4.6c. Note that the overlap between two fingers will be proportional to the sum of the absolute

values of the corresponding impulses.

In the special case using double electrodes where the fingers change sign in pairs, the sampling frequency is chosen equal to $8f_o$. In this case the impulses should be changing signs in quadruple which is not feasible by the interdigital transducers. The only impulses that will be generated are those adjacent impulses with the different polarity as shown in Fig.4.6d. However, designing the transducer(the finger overlapping) according to these generated impulses, the frequency response will show a third harmonic due to the suppressed impulses. The effect of these suppressed impulses on the original response is to increase the ripples amplitude in the pass band.

The fact that the same response is generated theoretically at the odd harmonics of f_o can be used to generate some frequency response at one of its subharmonics. However, there are limitations on this because of the phase cancellation in the pass band due to phase error produced by error in finger positioning.

The effect of the finite impulse response can be seen as follows [17]. Assume that a certain frequency response could be realized by an infinite sequence $\{A_n\}_{-\infty}^{\infty}$. Truncating this sequence by taking only the N "predominant" elements, $\{A_n\}_N$ is equivalent to multiplying the sequence $\{A_n\}_{-\infty}^{\infty}$ by a window function w(t) as shown in Fig.4.6d & e. Multiplication in the time domain is convolution in the frequency domain. Hence if W(f) is the Fourier Transform of the window w(t), then the resulting frequency response will be the convolution of the desired response with the function W(f).

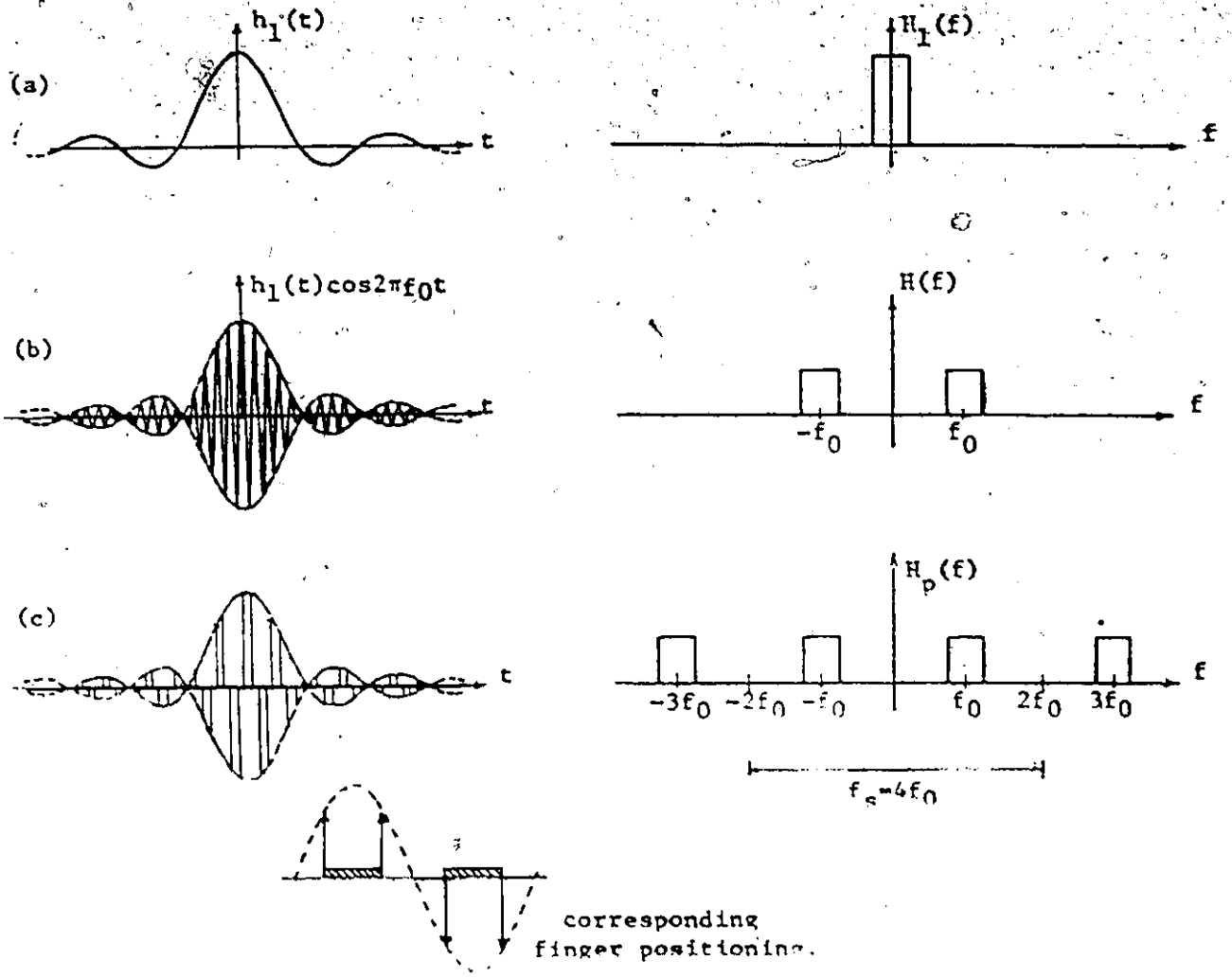
(a)
$h_1(t)$
t
$H_1(f)$
f
(b)
$h_1(t)\cos 2\pi f_0 t$
t
H(f)
f
$-f_0$
f_0
(c)
t
$H_p(f)$
f
$-3f_0$ $-2f_0$ $-f_0$ f_0 $2f_0$ $3f_0$
$f_s=4f_0$
corresponding
finger positioning.
(d)
t
$H_p(f)$
f
$-5f_0$ $-3f_0$ $-f_0$ f_0 $3f_0$ $5f_0$
$f_0=8f_0$
corresponding
finger positioning.

Fig 4.6

(Cont. Fig 4.6)

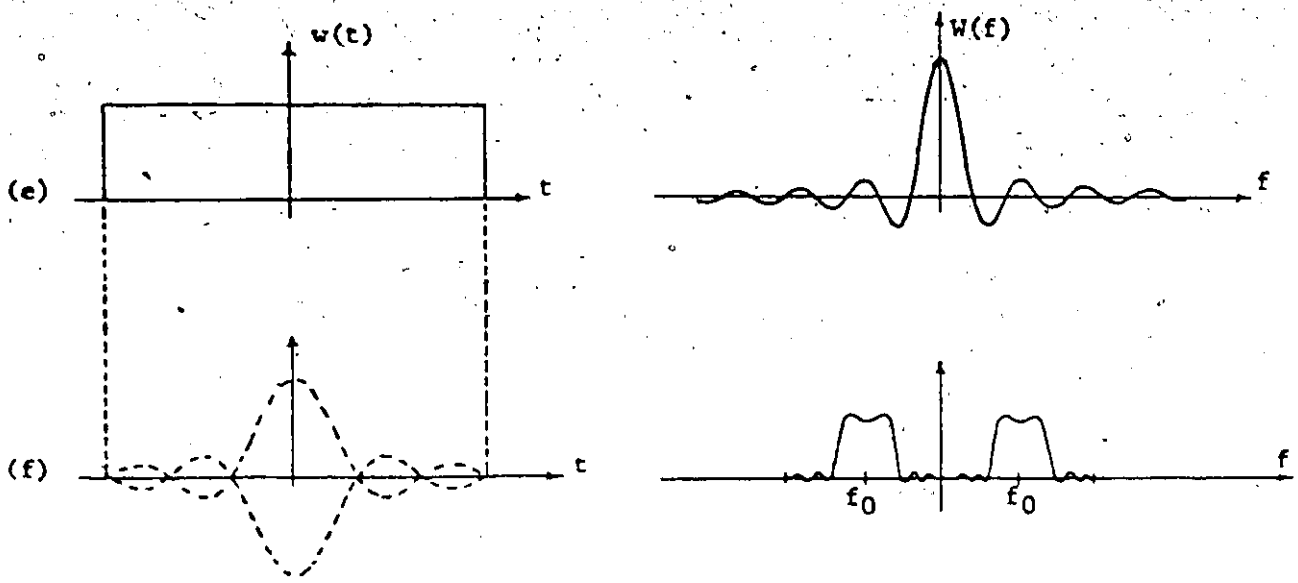

Fig 4.6 The Impulse Response Design.

This will introduce ripples in the pass band, known as Gibbs Oscillations, which distort both the amplitude and phase responses. The truncation might also increase aliasing effects between adjacent spectra. However, aliasing effects are negligible because the band width is usually much less than $2f_o$.

There are two approaches to find the coefficients A_n which give the optimum response. One approach uses a weighting function (window function) which varies slowly rather than the rectangular in order to terminate the infinite impulse response. This in effect will reduce the Gibbs ripples in the frequency response. The other approach optimizes the filter response by iterating the coefficients A_n for minimum ripples in the amplitude response.

4.3.1 The Discrete Fourier Transform Approach Using Window Function Technique.

The design procedure is as follows (see Fig.4.7)

(1) The desired frequency response is sampled using a large number of samples (M samples) over the frequency range $4f_o$ where f_o is the center frequency of the symmetric band pass filter [the samples are generally complex and in conjugate pairs from the positive and negative sides of the spectrum].

(2) Using the Fast Fourier Transform (FFT), one can obtain the Inverse Discrete Fourier Transform (IDFT) which is an M sample impulse response. [the number of samples M must be of the form 2^m, where m is an integer. This condition is imposed by the FFT technique].

(3) To truncate this impulse response down into N samples, multiply

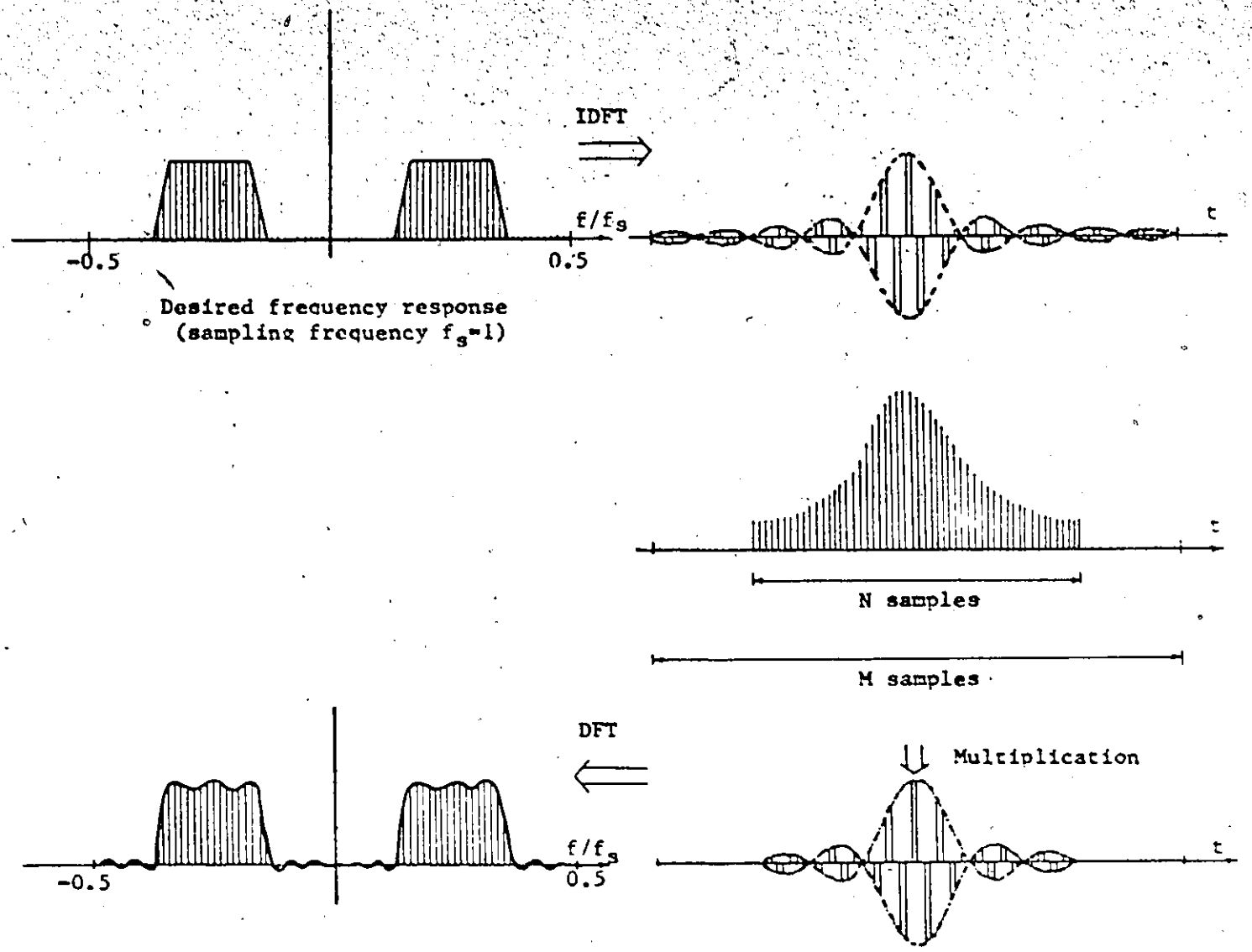

Fig 4.7 The DFT approach for designing the impulse response of a SAW band pass filter.

by the chosen window function which is usually available in a sampled form in the time domain. The length of the window function is set equal to N and is completed to M by adding zero samples to its ends. The product of the window function and the M samples impulse response will give the required impulse response.

(4) The resulting frequency response follows easily by taking the DFT of the impulse response.

It is seen that the design problem then becomes one of finding an "optimum" weighting function which achieves the smallest ripple size. Many window functions have been suggested [17], and the choice among them depends on the desired frequency response.

This design technique is a straightforward technique and often yields results which are within 10 percent of the optimum. However in this technique the designer cannot specify the pass band and the stop band ripples independently.

4.3.2 Optimization Techniques - Equiripple Designs.

In this approach the filter response is optimized by iterating the coefficients A_n in (4.7). Several schemes have been developed which differ in the algorithm used and the number of variables which are allowed to vary.

In the scheme by Parks and McClellan [20], the coefficients A_n are all allowed to vary to achieve a minimum deviation. The magnitude of the ripples in the pass band and stop band can be specified independently. The Lagrange interpolation formula is used to obtain a polynomial with extremes of these ripple amplitudes. The parameters involved in the formulation are the length of the impulse response,

the magnitude of the ripples in the pass band and stop band and the transition width. Only one of these parameters is left free while the others are fixed. In that scheme, the amplitude of the ripples in the pass band and stop bands is the parameter which is left free. The scheme, its flow charts and its computer program are well documented in [20]. The program is originally for designing optimum finite impulse response, linear phase digital filters. The program is listed in Appendix A, with minor adjustments for the CDC 6400. Complete designs of two band pass filters using this program have been worked out in Chapter V.

The number of fingers (or the length of the impulse response) required to achieve certain characteristics depends on the transition width and the ripple size. As a "rule-of-thumb" themminimum value of N, the number of fingers, for deviation in the pass band and stop band of 0.01 is given by the empirical formula [17].

$$N \left(\frac{\text{Transition Width}}{\text{Center frequency}}\right) = 2 \qquad (4.9)$$

However, the number of fingers N could always be increased to reduce the tolerance required on the individual element values. The band width that could be implemented by SAW filters is limited by the maximum allowable number of fingers for small band widths. For large band widths, the impulse response coefficients are changing very rapidly which cannot be implemented by apodization of an interdigital transducer since overlap weighting is only accurate when the changing is small from element to element. Band widths ranging from 1 to 30 percent are practically achievable by using any of the above procedures.

CHAPTER V

DESIGN AND FABRICATION OF SURFACE ACOUSTIC WAVE TV-IF FILTER

5.1 General

The design and fabrication flow chart of SAW filters is shown in Fig.5.0. The optimization techniques give the optimum impulse response which is used to design the δ-function model of the filter. "The δ-function model gives a very good first-order estimate of the frequency response and is quite useful because of its simplicity"[5]. The equivalent circuit model, however, gives almost the exact response of the filter. Hence the δ- function model should be checked using the equivalent circuit model. One or two iterations might be necessary before getting the required response. However, modelling the device using the equivalent circuit model is outside the scope of this thesis and hence this step was by-passed in the design process. The δ-function model was used directly to design the filter. Conventional photolithography was used for the device fabrication. Wiring and matching are the last steps in the fabrication process. All the design and fabrication steps are included in this chapter.

5.2 Filter Specification and Realization.

An ideal TV-IF filter response is a linear phase response with the amplitude specifications [25] shown in Fig.5.1a. A more realistic response is given by Fig.5.1b whose specifications are as follows:

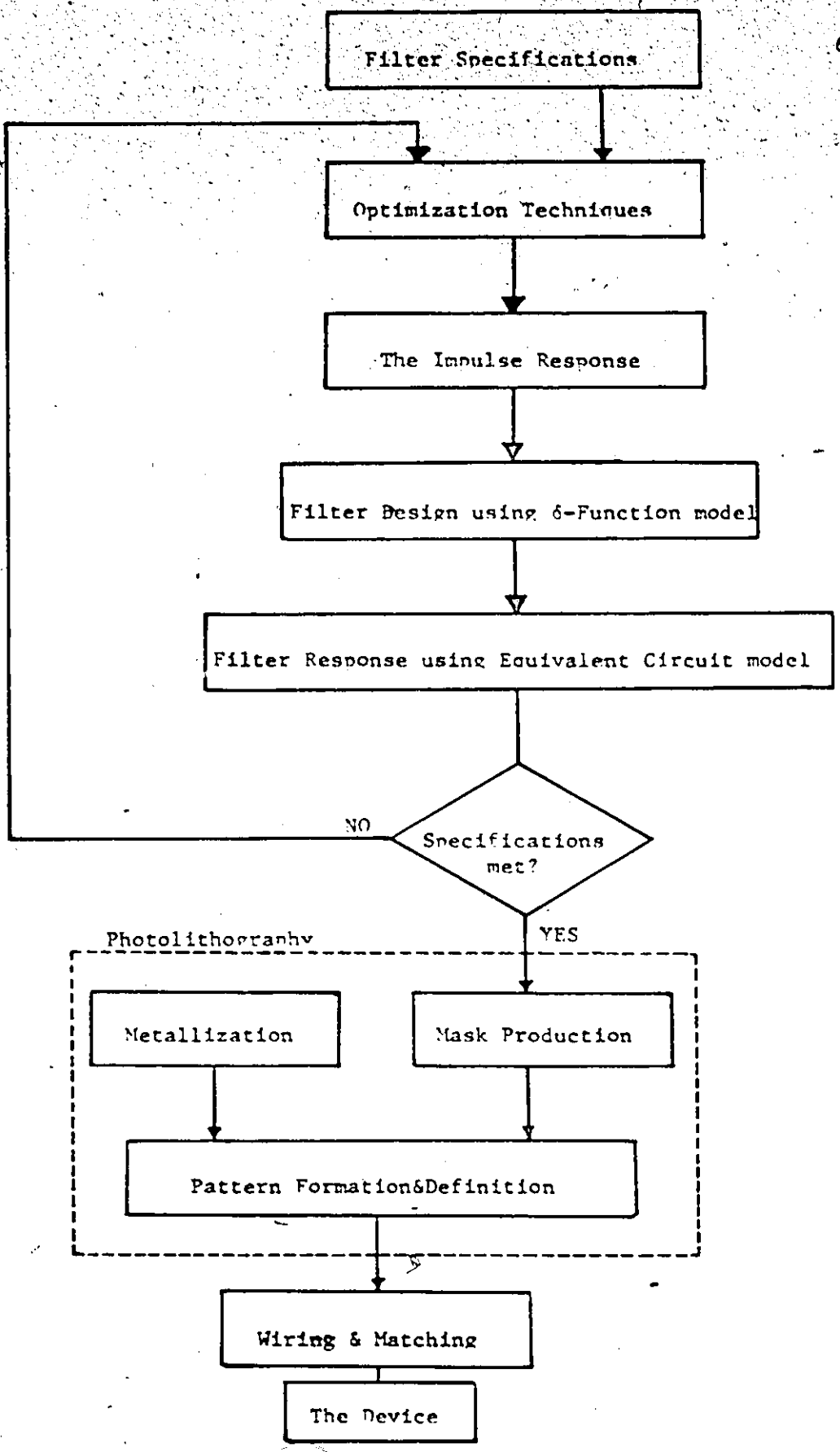

Fig 5.0 Flow chart of design and fabrication process.

(a)

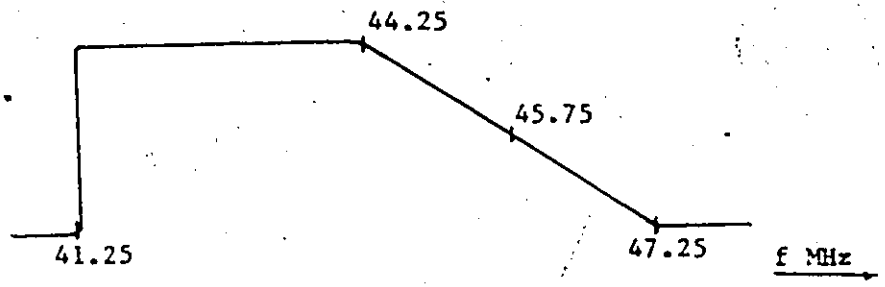

(b)

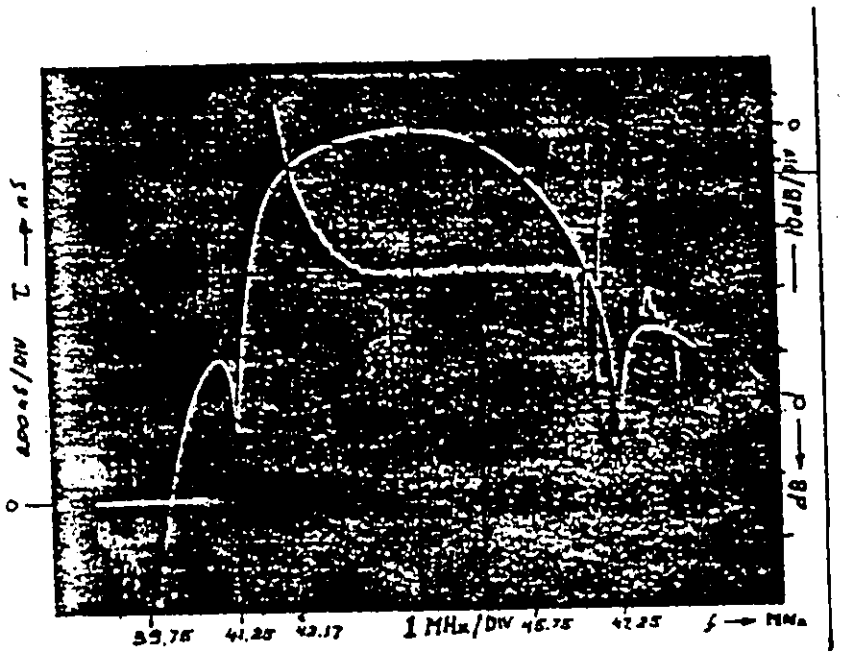

Fig 5.1 (a) Ideal TV-IF filter response,
(b) Specifications of the fiter response as given by Electrohome Co.

AMPLITUDE SPECIFICATIONS:

Selectivity ≈ 55 dB

Ripples in the pass band < 0.5 dB

Adjacent channel sound trap at 47.25 MHz

Adjacent channel picture trap at 41.25 MHz.

The response is symmetrical in the frequency range 44.25 - 47.25 MHz around the frequency 45.75 MHz which is dB below the pass band level.

PHASE RESPONSE:

Linear phase response (i.e. constant group delay) is desirable in the TV-IF filter. For a total time delay of 660 ns, the deviation must be within ± 5 ns. Such a small time delay is difficult to achieve by SAW filters. However, a linear phase filter with a relatively large time delay still can be implemented with some adjustments in the circuitry.

The non symmetric amplitude response could be split into two symmetric responses as shown in Fig.5.2a. The two filters are shown schematically in Fig.5.2b & c. Their total response should approximate the response of Fig.5.1b. These two linear phase, symmetric band pass filters could be easily achieved individually by apodized SAW transducers. However, two such apodized transducers cannot be placed side by side to give a total response equal to the product of their individual responses as it was explained in Chapter V. This could be done only by introducing a Multistrip Coupler (MSC) between the two transducers, as shown schematically in Fig.5.3. In this case the total response

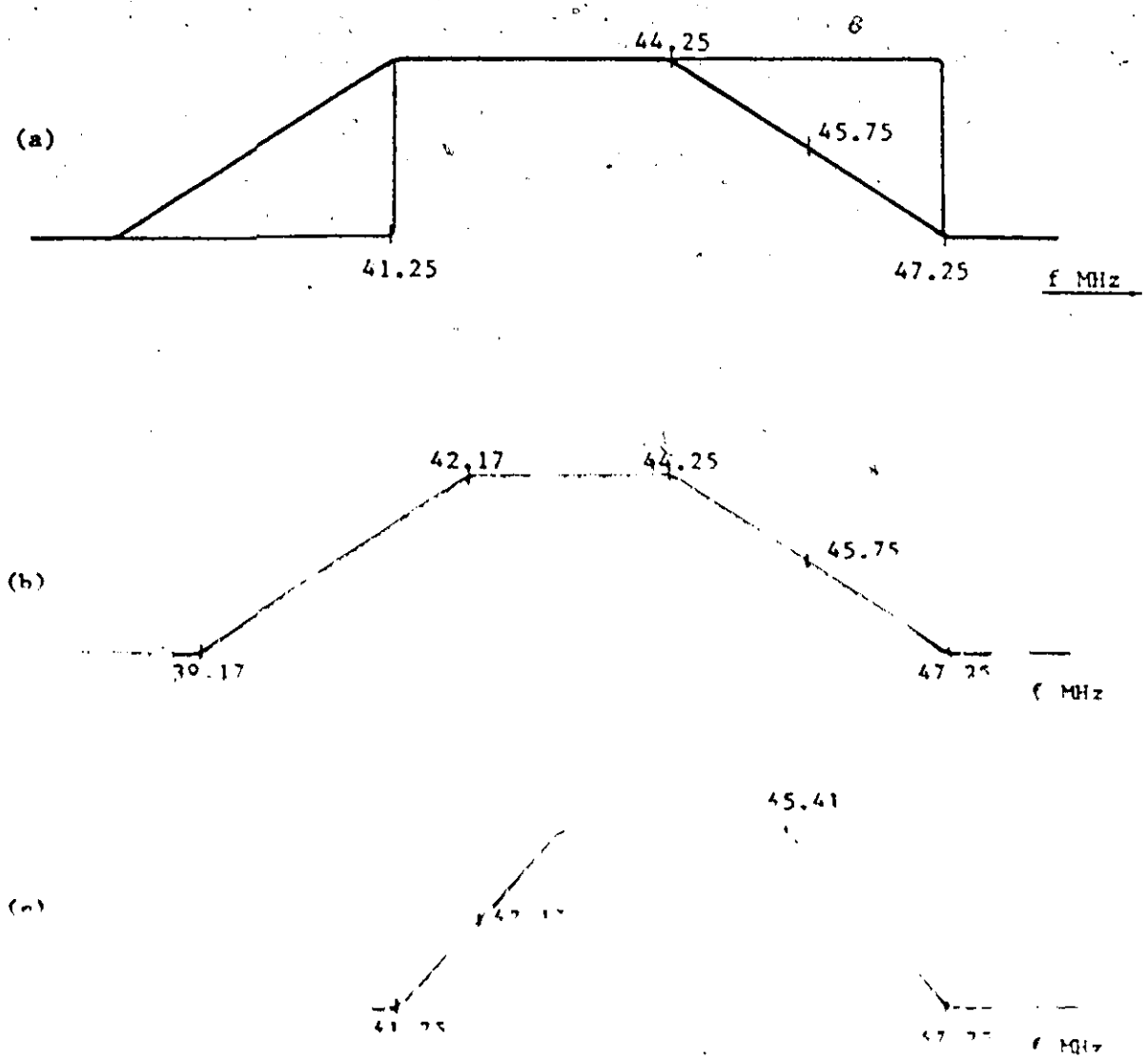

Fig 5.2 (a) Realization of the filter response of Fig 5.1a by two symmetric responses,
(b)&(c) The two symmetric responses approximating the response of Fig 5.1b.

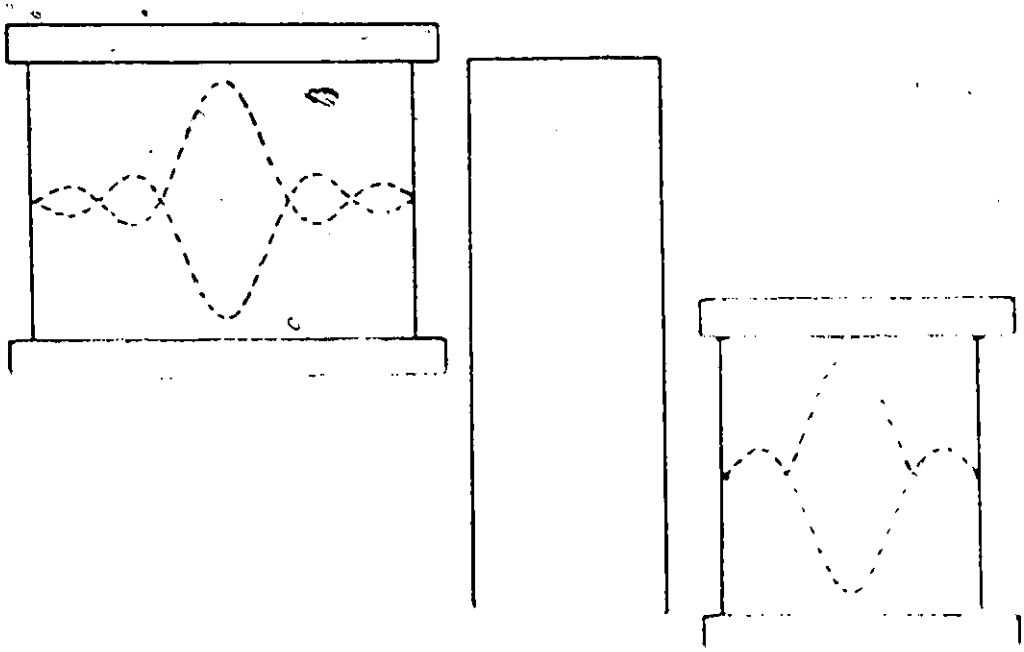

is equal to the product of the individual responses [Chapter III].

Introducing the MSC in the design will also eliminate many of the secondary effects of the SAW transducers such as wave diffraction, multiple wave reflections or the Triple Transit Echo (TTE), bulk waves, etc. The advantages of using the MSC in SAW devices were explained in detail in Chapter III.

5.3 The Impulse Response:

The interdigital transducers having the responses of Fig.5.2b & c, will be referred to as transducers number 1 and 2 respectively. All the variables related to transducer number 1 will be suffixed 1, so also all variables related to transducer number 2 will be suffixed 2. In the design of these two transducers the optimization scheme described in Chapter IV will be used to find the corresponding impulse response.

Double electrode transducers will be used and hence the sampling frequency will be taken as $8f_o$ [Sec.4.3], where f_o is the filter center frequency. All frequencies will be normalized with respect to the sampling frequency for each transducer. The frequency range from zero to $4f_o$ is divided into 3 bands: two stop bands and one pass band. The amplitude specifications in these bands are given in the form of a desired amplitude and a weighting function to define the relative ripple size in the different bands. The weighting function might be a fixed number or a varying function along the frequency band. In both transducers, special weighting functions in the stop bands are provided to ensure higher insertion loss at the band edges which will

be the adjacent picture and sound traps of the IF filter.

After a number of trials it was found that the best values for the lengths of the filter impulse responses are:

$$(NFILT)_1 = 364$$

$$(NFILT)_2 = 564$$

It should be noticed that the sampling frequency is 8 f_o, hence for split electrodes the corresponding number of finger pairs should be

$$N_1 = \frac{(NFILT)_1}{4} = 91$$

$$N_2 = \frac{(NFILT)_2}{4} = 141$$

These values, however, are much larger than the values predicted by (4.9). As it will be seen, a number of approximations should be done on the optimized impulse response before implementing it on the transducer design. The input data, the weighting function subroutine and the resulting impulse response for each transducer are listed in Appendix B.

Examining the resulting responses, it is seen that they change signs in quadruples and also there is a 180° change of phase at the sidelobes as should be expected. However at the ends of the responses there are a number of elements whose signs are changing in a different scheme and also their amplitudes are changing very rapidly. These elements are difficult to implement by a SAW transducer. Excluding these elements from the response will increase the ripple amplitude (non-optimum). After truncation the number of finger pairs will be

$$N_1 = 79$$

$$N_2 = 131$$

Still this truncated response cannot be realized by a SAW transducer.

Consider half a period of 4 impulses of the truncated impulse response (Fig.5.4a). These 4 impulses are "approximated" by the impulses of Fig.5.4b in which

$$A' = D' = 0$$

$$B' = -C' = \frac{|B| + |C|}{2}$$

this last response is the one which could be realized by a double electrode transducer.

These approximations increase the ripple amplitude in both the passband and the stop bands. However, this could always be compensated by increasing the length of the filter response. The approximated impulse responses together with their corresponding frequency responses are shown in Figs.5.5, 5.6, 5.7, 5.8. The total filter response which is the multiplication of the responses of Figs.5.6 & 5.8, is shown in Fig.5.9.

5.4 Design Specifications

Design specifications can be divided into specifications on:

* The crystal substrate

** The multistrip coupler

*** The apodized transducers.

The substrate is a Y cut- Z propagation Lithium Niobate ($LiNbO_3$) crystal having the dimensions 0.5" x 0.04" x 1" along the x and y axes respectively. The crystal has a very high quality polished surface on one

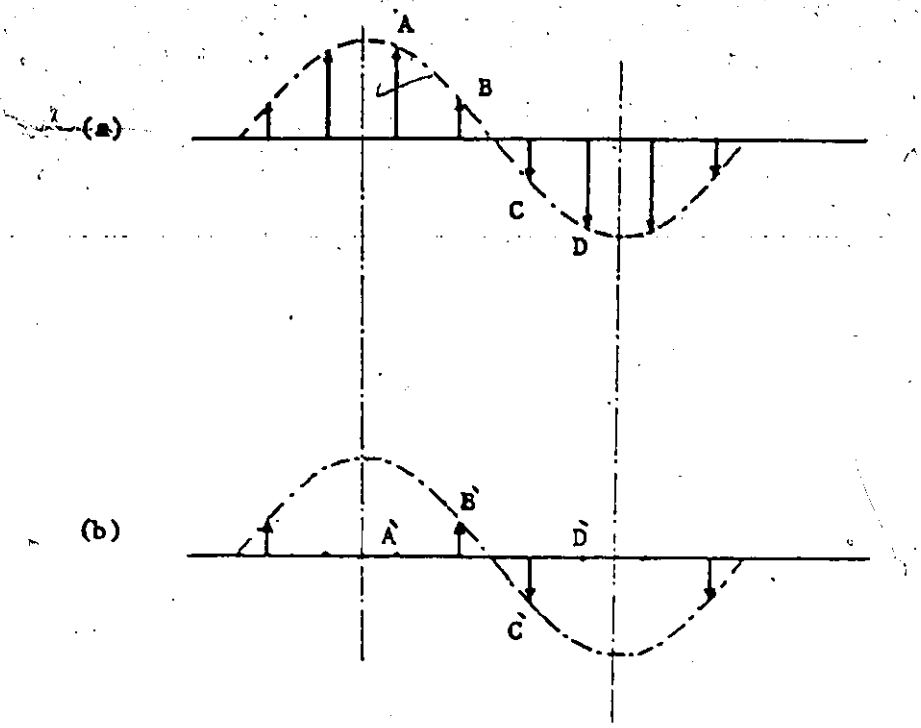

Fig 5.4 Optimized (a) and approximated (b) impulse responses along one Interdigital period.

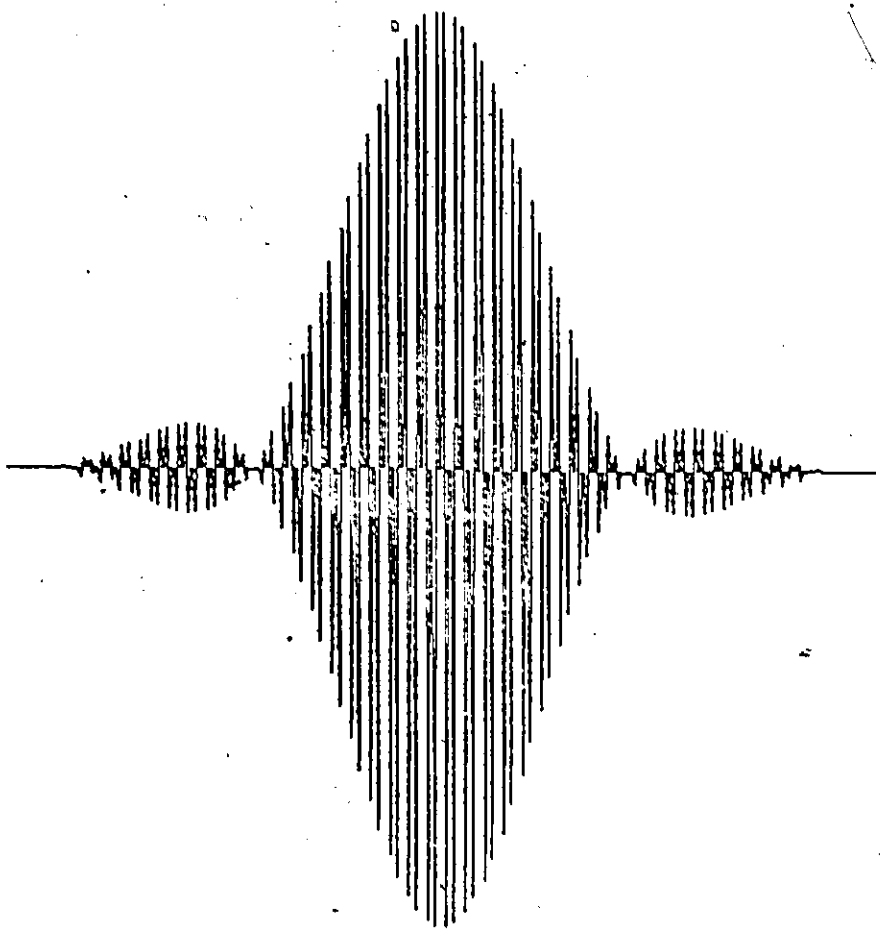

Fig 5.5 OPTIMIZED IMPULSE RESPONSE OF TRANSDUCER NO.1

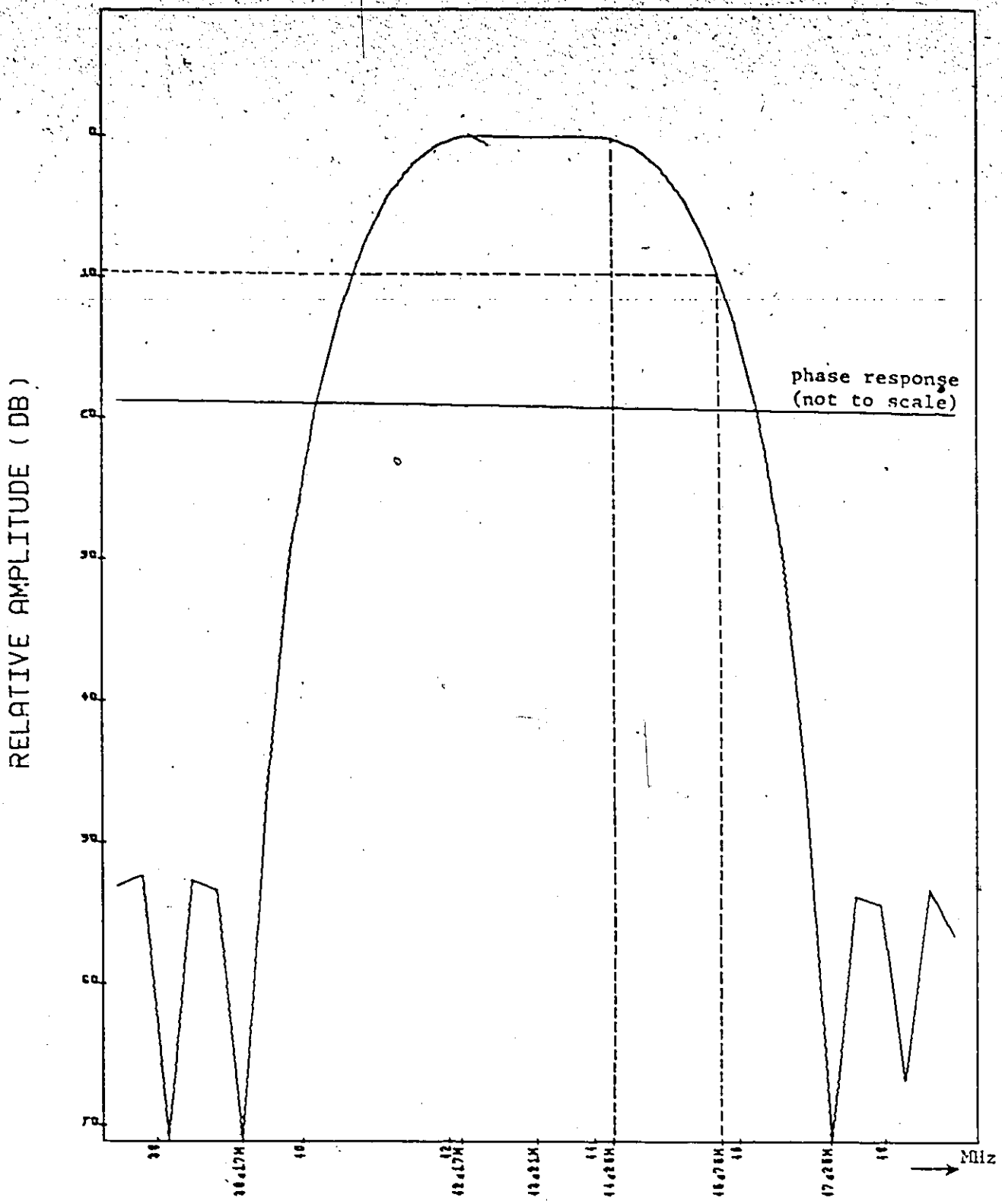

Fig 5.6 OPTIMIZED AMPLITUDE AND PHASE RESPONSES OF TRANSDUCER NO.1

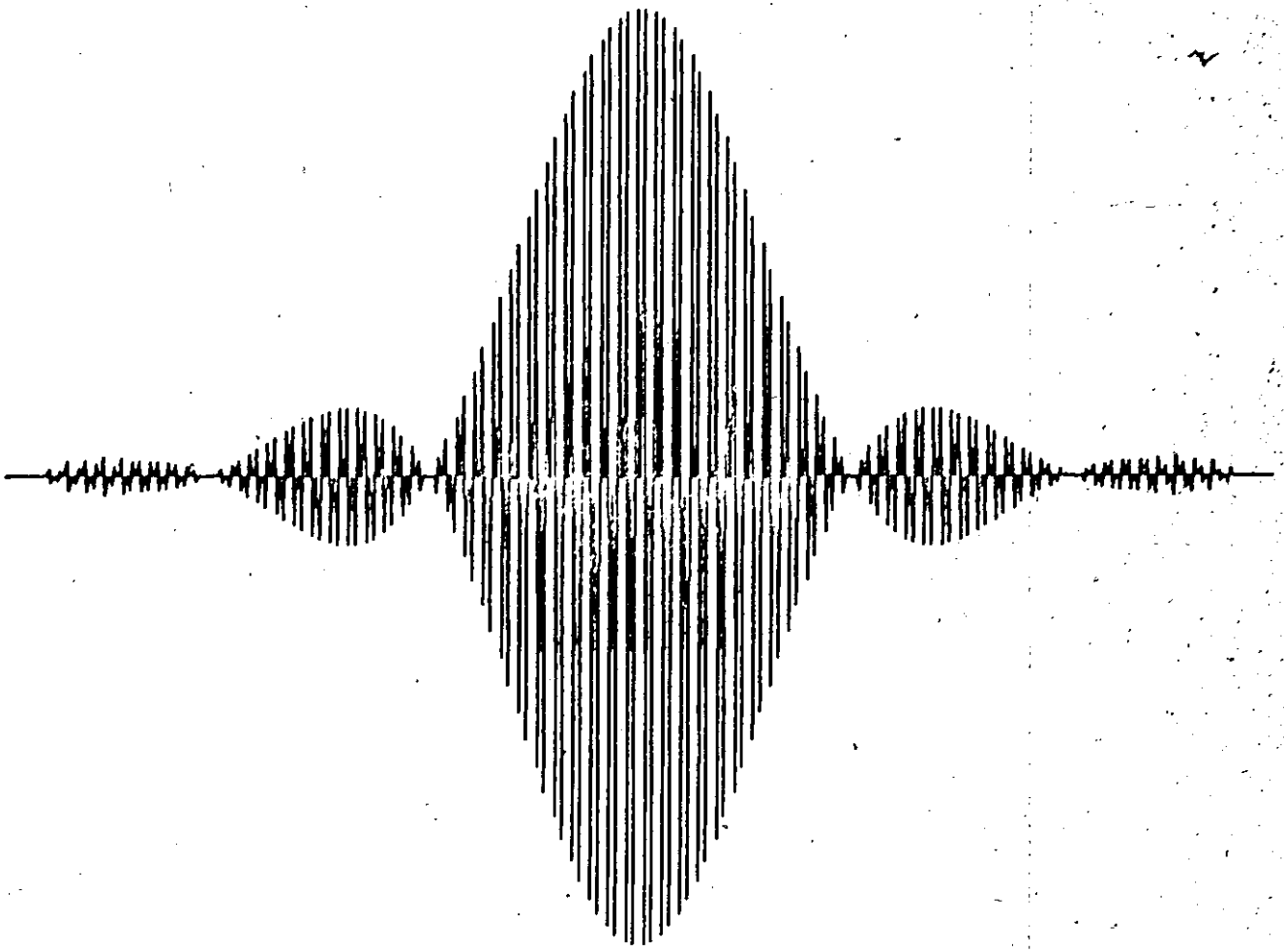

Fig 5.7 OPTIMIZED IMPULSE RESPONSE OF TRANSDUCER NO.2

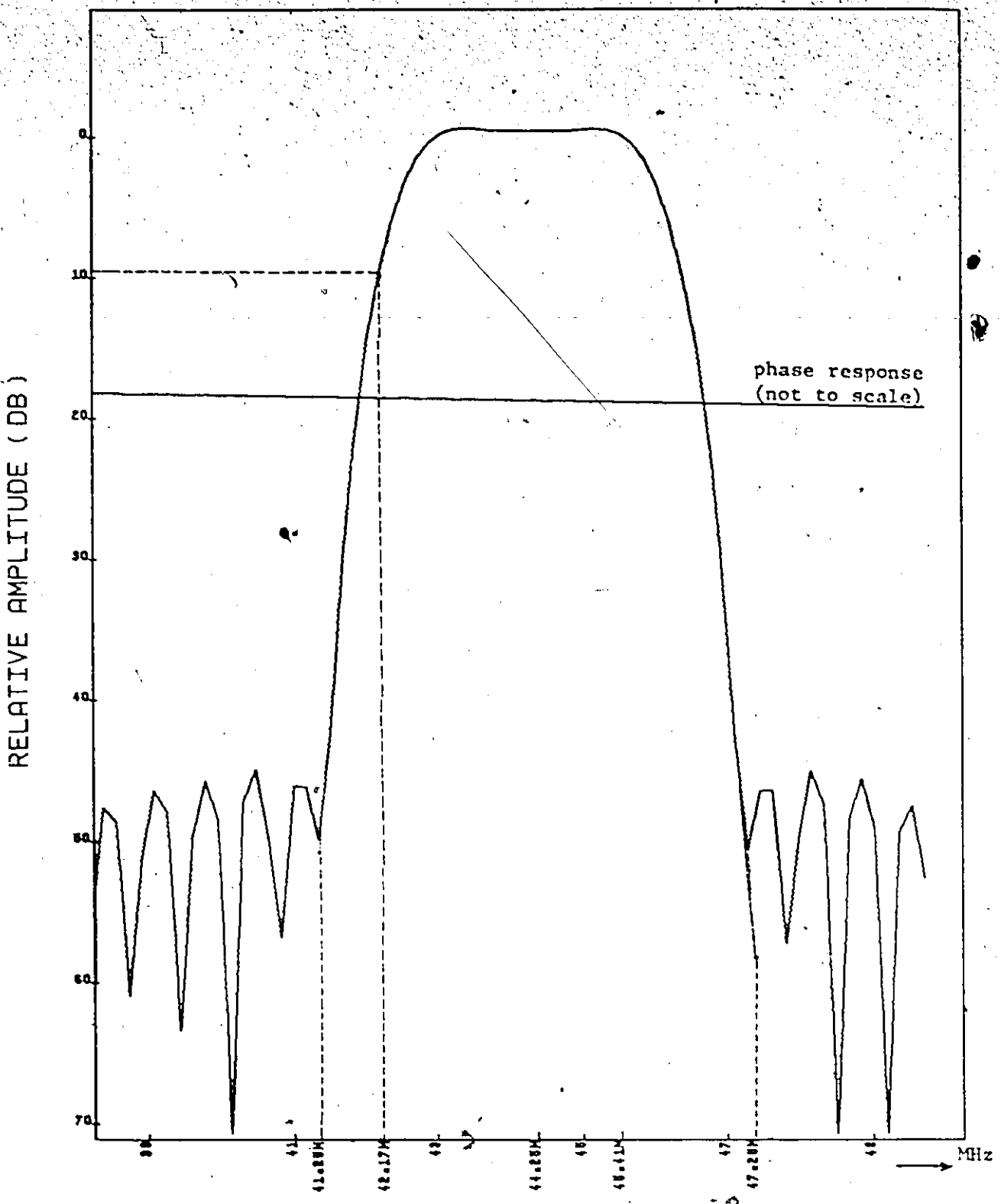

Fig 5.8 OPTIMIZED AMPLITUDE AND PHASE RESPONSES OF TRANSDUCER NO.2

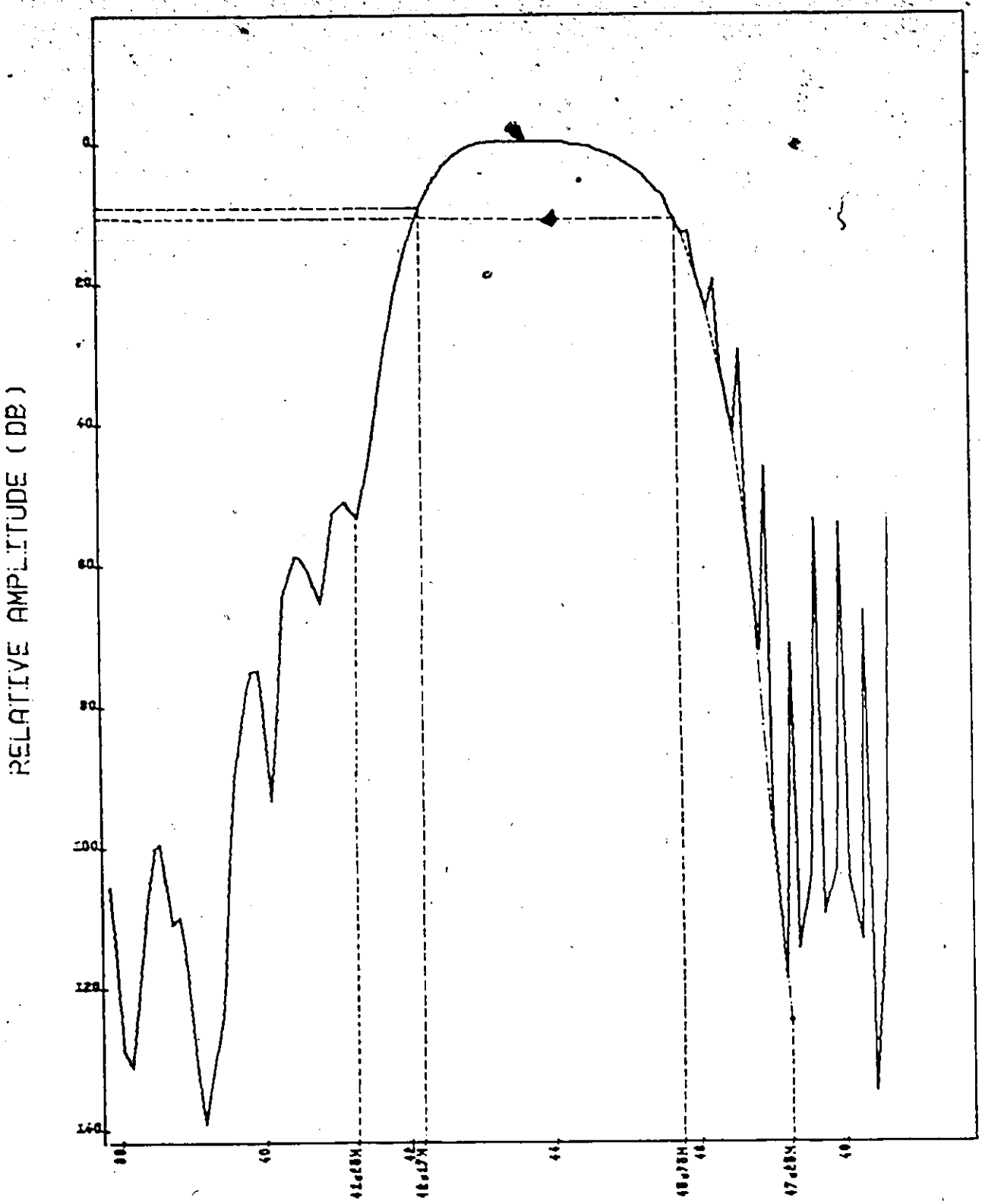

Fig 5.9 TOTAL FILTER RESPONSE

side while the other side is left rough.

The multistrip coupler described in Chapter III as a design example, will be used for coupling the SAW transducers as shown in Fig.5.3. The length of the coupler which is the only parameter to be specified is determined by the width of the acoustic channels. Specifications of the MSC are summarized in Table 5.1.

A SAW transducer is specified by its center frequency and overlapping function. Since the impulse response gives only the relative overlapping, this response should be scaled to a maximum value. The choice of maximum finger overlapping will affect both the input impedance and the wave diffraction of the transducer. The input impedance of an apodized transducer as a function of the maximum overlapping length can be found by modelling the transducer using the equivalent circuit model. Such procedures might not be necessary since in a case like the TV-IF filter, it is always possible to adjust the output impedance of the preceding stage to the filter to match its input impedance. However, an estimate for the input impedance can be obtained by approximating the apodized input transducer into a uniform transducer whose finger overlapping is equal to the maximum overlapping of the apodized transducer. The number of fingers of the equivalent uniform transducer is chosen such that the active area or the overlapping area is the same in both transducers. From Fig.5.5 & 5.7, the number of fingers of the equivalent uniform transducers are approximately 24 and 30 finger pairs (pairs of split electrodes) for transducers No.1 and 2 respectively. The error in this estimate is less than ± 4 finger pairs. If the maximum over-

lapping is taken equal to 0.18" which is almost the maximum allowed by the substrate dimensions, then from equations (2.2) and (2.5), the input capacitances C_{T_1} and C_{T_2} for transducers No.1 and 2 respectively will be

$$C_{T_1} \simeq 50 \text{ pF} \pm 10 \text{ pF}$$

$$C_{T_2} \simeq 60 \text{ pF} \pm 10 \text{ pF}$$

From (2.5) and (2.6d), the corresponding input conductances

$$G_1 \simeq 9.6 \text{ mU} \pm \frac{4}{3} \text{ mU}$$

$$G_2 \simeq 15.2 \text{ mU} \pm \frac{4.4}{3.6} \text{ mU}$$

The coupling coefficient $k^2 = 0.045$ and the metallization ratio $\eta = 0.5$ were adopted in the above calculations.

Wave diffraction due to finite beam width is negligible if the output transducer (in our case the MSC) lies inside the Fresnel Region of the radiating electrodes. With maximum beam width of 0.18", a relatively small beam width of 0.02" will have an effective Fresnel distance (Equation (2.14) of $\simeq$ 0.3". The MSC, then, is likely to be inside the Fresnel Region of the different radiating elements of the input transducer [see the block diagram of Fig.5.11]. However, the multistrip coupler itself will further reduce the effect of wave diffraction.

Now with the maximum overlap being specified it is possible to determine the transducer dimensions. Consider the two finger pairs of Fig.5.10, which correspond to the half period of Fig.5.4. Let the values of B' and C' of Fig.5.4b be the elements W(J) and W(J+1) res-

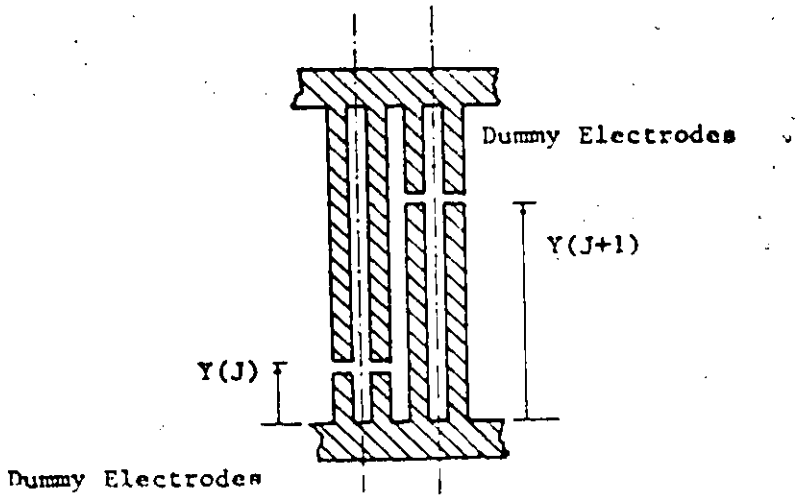

Fig 5.10 Two finger electrode pairs
of an apodized transducer.

pectively of some array W(I), whose elements are the generated impulses from the transducer. The corresponding lengths Y(J) and Y(J+1) of Fig.5.10 will be given by:

$$Y(J) = Y(J+1) + W(J+1) \times \text{Scale Factor.}$$

where the scale factor is equal to the chosen value of the maximum overlap length (0.18") divided by the value of the central element (the largest of the array W(I)). The array Y(I) for the two transducers are listed in Appendix C, with element values one hundred times their real values and in inches.

Assuming a metalization ratio n = 0.5 the finger width will then be = $\lambda_o/8$, where λ_o is the wave length at the transducer center frequency calculated with a wave velocity v = 3488 m/sec. The design specifications are summarized in Table 5.1, with the block diagram shown in Fig.5.11. In the block diagram of Fig.5.11, two broad band dummy transducers are included with two dummy loads. These transducers will absorb any incident residual wave due to the incomplete transfer of energy by the MSC.

5.5 Fabrication Procedures

There are several techniques for fabrication of SAW devices which are based on photolithography [21]. The choice between these techniques depends finally on the required pattern resolution, i.e. the smallest line width to be produced and the final device area. These techniques differ in two aspects; the photoresist pattern formation and the pattern definition techniques. The photoresist pattern formation can be done either by using contact mask techniques or other

TABLE 5.1

SUMMARY OF FILTER SPECIFICATIONS

THE SUBSTRATE

Material	Dimensions X, Y, Z.	Coupling Coefficient	Wave Velocity (Free Surface)	Metallization
Y-Cut-Z Prop $LiNbO_3$	0.5"x0.04"x1"	4.5%	3488 m/sec	3000 Å Aluminum Thin Film

THE MULTISTRIP COUPLER

Synchronous Frequency	Metallization Ratio η	Strip Width $\lambda_o / 4$	Number of Strips N_T	Other Specifications
58.3 MHz	0.5	14.955 μm 0.5888x10^{-3}in.	103	See Fig. 5.11

THE TRANSDUCERS

	Transducer No.1	Transducer No.2
Center Frequency (Synchronous Frequency)	43.21 MHz	44.22 MHz
Number of Finger Pairs (Pairs of Split Electrodes)	50	101
The Optimized Impedance and Frequency Responses	Fig 5.5 & 5.6	Fig 5.7 & 5.8
Maximum Finger Overlapping	0.18"	0.18"
The Arrays Y(J) [Fig.5.10].	Appendix C	Appendix C
Finger Width $\lambda_o/8$ (v = 3488 m/sec., η = 0.5	10.01 μm 0.3973x10^{-3}in.	9.853 μm 0.3879x10^{-3}in.
Other Specifications [See Fig.5.11]		

TABLE 5.1
(Cont)

THE DUMMY TRANSDUCERS (Identical Transducers)

Center Frequency (Synchronous Frequence)	44.25 MHz
Number of Finger pairs	10

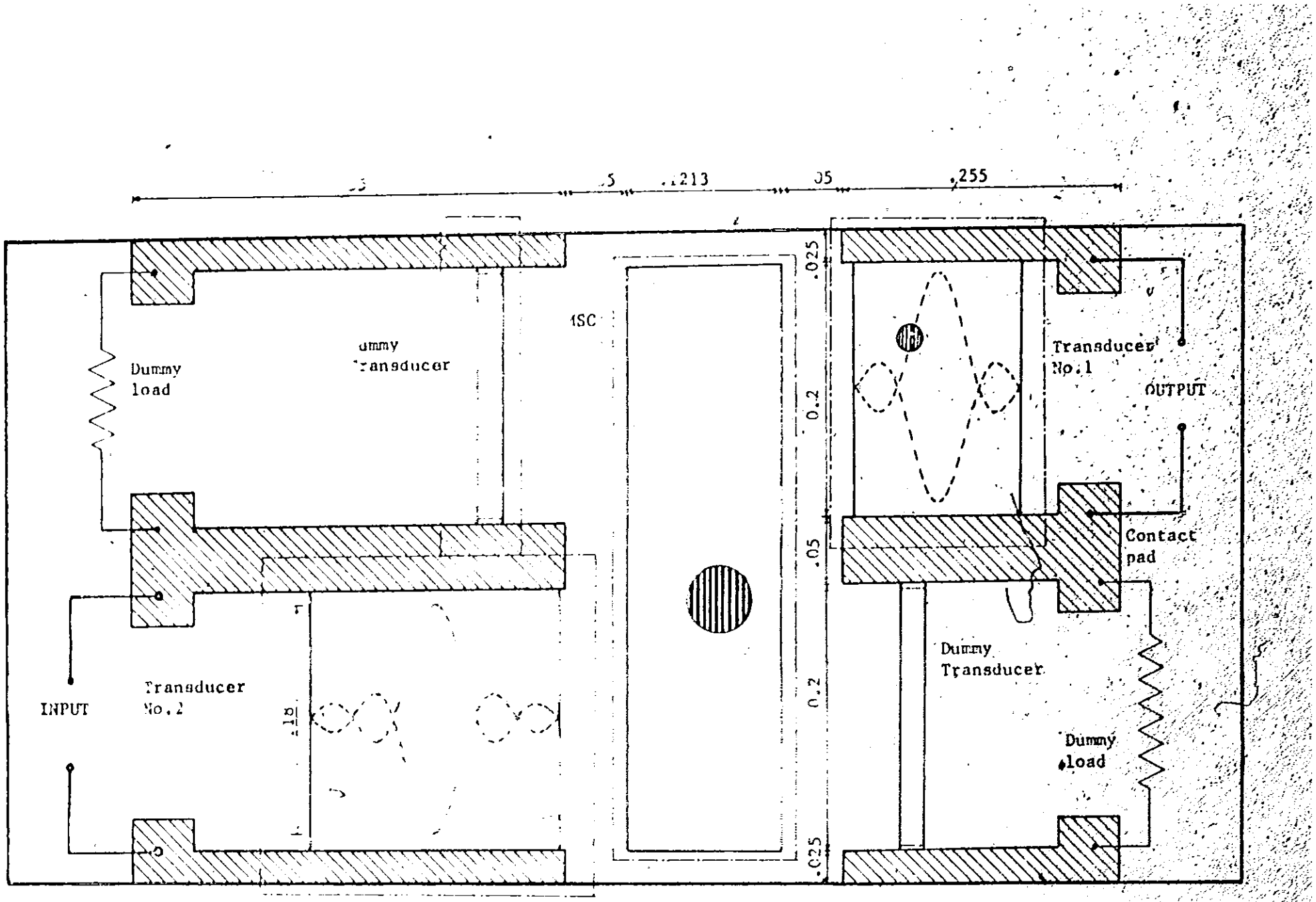

Fig 5.11 Block Diagram of the Device.
(All dimensions in inches)

techniques which do not use contact masks such as image projection or electron beam techniques.

Ordinary contact mask technique is only capable of reproducing patterns with minimum line width of 4 μm[23]. This limit is imposed by the limited degree of contact between the substrate and the mask. Special masks, known as conformable masks are made of very thin glass plates, such that when the space between the substrate and the mask is evacuated very close contact is achieved over relatively large areas. Using conformable masks it was possible to reproduce patterns with line widths in the submicron region.

The electron beam and image projection techniques [21], [23], which do not use contact masks, are most efficient in the submicron region. A practical resolution for electron-beam lithography is about 0.1 μm. However, the field of view over which this resolution can be obtained is limited. Hence very accurate step-and-repeat mechanism is required if the pattern exceeds the field of view which is usually the case for SAW devices.

The desired metallic pattern can be "defined" either by "Chemical etching" or "lift off" techniques [23]. The chemical etching is practical for producing patterns having line widths as small as 4 or 5 μm. The limit is caused by the difficulty in controlling etch rates so that excessive undercutting does not occur. The lift off technique is always used to produce patterns having submicron line widths and covering large areas. The smallest line width in the filter to be fabricated is approximately 9 μm. At this width the contact mask technique, together with chemical etching technique, can be used

adequately for fabrication. The fabrication process consists of four major processes:

5.5.1 Artwork and Mask Generation.

5.5.2 Metallization.

5.5.3 Pattern Formation and Definition.

5.5.4 Wiring and Matching the Device.

5.5.1 Artwork and Mask Generation:

SAW devices are characterized by the relatively large area they cover and at the same time the accuracy of the finger widths required. The mask is generated by cutting an oversize version of the pattern on "Rubylith" and then by photoreduction the required mask is obtained. The accuracy of the resulting pattern is determined by the cutting errors on Rubylith. High accuracy usually requires cutting the original pattern at a large size which might exceed the field of view of the reduction camera. For the pattern shown in Fig.5.11, the smallest finger width is approximately 0.4×10^{-3} in. [see Table 5.1]. The "rounding off" error of the cutting table is theoretically 0.0005" and practically 0.001". Hence cutting the pattern at 100 times the original size, an error in finger positions of 0.001" will produce a phase error less than 3% which is an acceptable level. The total size of the pattern of Fig.5.11 at that scale will be approximately 80" x 50", which is very large to be drawn on the cutting table and also requires a very special camera system which has such large field of view. The photomask of the pattern of Fig.5.11 is produced by two photoreduction steps as follows:

(1) The pattern is divided into separate parts (as shown in Fig.5.11 by the dotted lines) such that the size of each part is small enough [at the cutting scale] to be handled by the cutting table and the first reduction camera. Also the pattern should be divided into complete units such as a complete transducer or a MSC.

(2) The transducers are cut on Rubylith at a scale of 100 times. The size of the drawing of each transducer does not exceed 21" x 25" which is an average size drawing. The MSC is cut on Rubylith at a scale of 50 only because of its relatively large size. However, at this scale the phase error due to the cutting "rounding off" does not exceed 3%. The size of the drawing of the MSC is approximately 8" x 25". The drawing specifications for the transducer and the multistrip coupler are given in Table 5.1.

(3) The photoreduction is done in two steps. First the drawings are photoreduced separately into a common size [20 x the original size]. The sub-patterns are then reassembled on a second sheet of Rubylith where the contact pads are added. The assembly is then photoreduced by a factor of 20 to produce the required photomask.

Using the Nuarc STT1418 camera system [a facility of the McMaster University Audio Visual Center], the drawings of the transducer are reduced by a factor of 5 while the MSC is reduced by a factor of 2.5. The field of view of the camera is approximately 25" x 22" to which the drawings can be fitted. The drawings are reduced on 8" x 11.5" high resolution Kodak films. In the second reduction the Microkon 1700 camera was used to produce the required photomask on 2 x 2 x 0.060" high resolution Kodak plates.

Fig 5.12 The separate drawings of the Transducers and the Multistrip Coupler on the cutting table.

Fig 5.13 A picture for the assembly of the Transducers and the Multistrip Coupler before the second photoreduction.

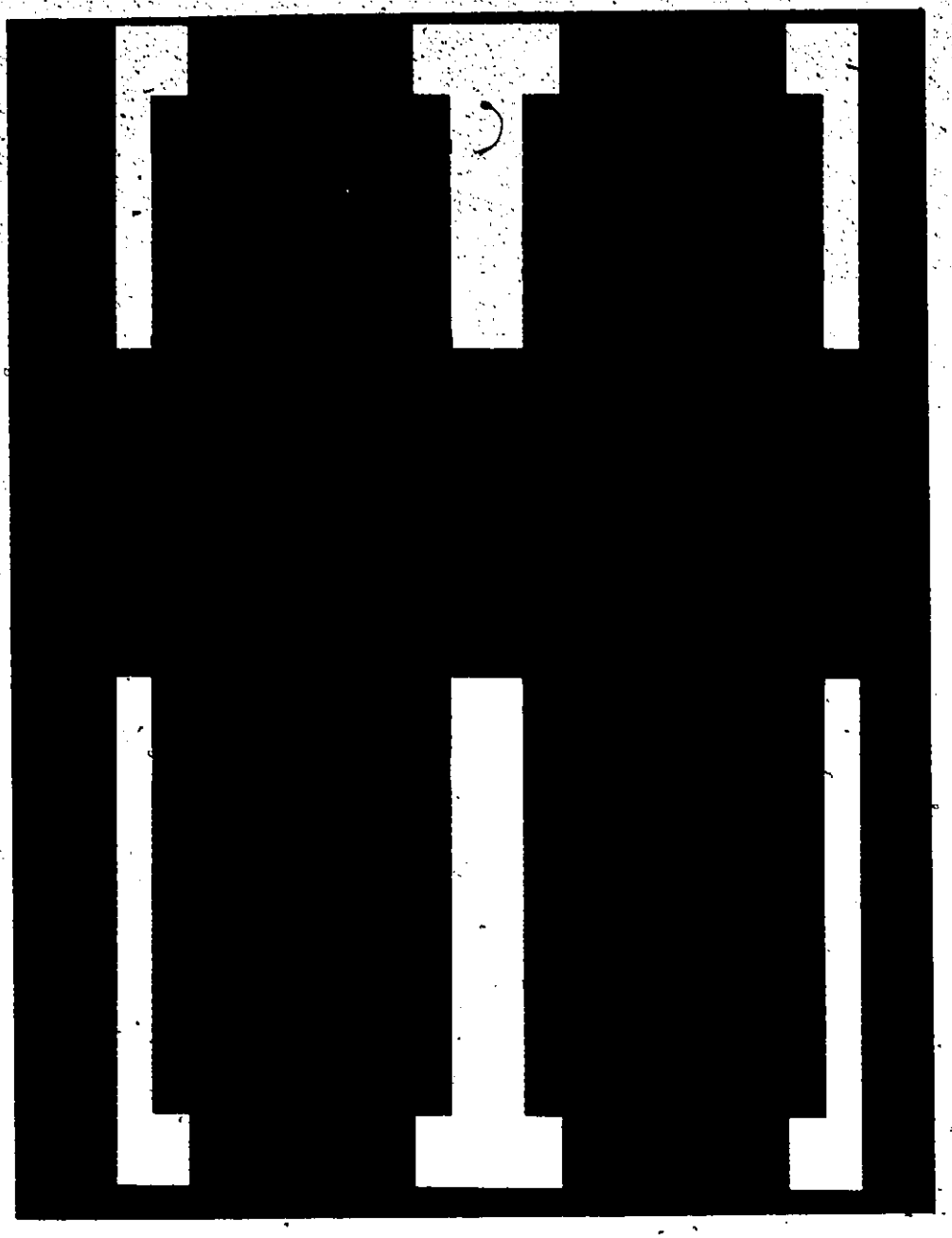

The percentage error of the reduction ratio is directly proportional to the percentage error in the center frequency and the filter band width. In our case an error of 1% in the reduction ratio will produce an error of approximately 0.5 MHz in the center frequency and 0.06 MHz in the band width. Such an error in the center frequency cannot be tolerated and hence very precise adjustment of the reduction ratio is required. On the first reduction both transducers should be reduced by the same ratio which need not be accurately the exact ratio. This is because on the second reduction the ratio can be accurately adjusted to compensate for the error in the first reduction. However, this will introduce error in the reduction ratio of the MSC since it was drawn at a different scale. Fortunately the error in the synchronous frequency of the MSC, as it was discussed in Chapter III, does not affect its performance seriously except for wide band pass filters. An error of 1 or 2 MHz in the synchronous frequency of the MSC is admissable. Using the telescope accessory of the Microkon 1700 camera, it was possible to adjust the reduction ratio for an error in the center frequency of both transducers of less than 0.05 MHz.

5.5.2 Metallization

The second step in the fabrication process of SAW devices is the deposition of a metallic thin film on the piezoelectric substrate. Gold and aluminum are the most common metals used for films ranging from a few hundred to a few thousand angstroms. Most of the defects in the resulting device are actually due to the defects in the thin film.

There are two deposition techniques usually used for SAW devices,

the thermal evaporation and the RF sputtering [23]. The sputtering is more preferable since it produces more uniform and adherent thin films over large areas. However, the thermal evaporation was used for fabrication since sputtering was not an available facility. The metallization process consists of two steps:

(1) Preparation of the Substrate.

(2) The Vacuum Deposition.

(1) Preparation of the Substrate:

The polished surface of the crystal has to be "atomically" cleaned. Actually the quality of the deposited thin film depends to a large extent on the cleanliness of the surface. Deposition on an uncleaned surface causes pin holes in the thin film and poor adherence of the thin film to the surface.

The crystal is cleaned first in an acid to etch out any residual metal from any previous "unsuccessful" deposition on the substrate. The substrate is then immersed in a deionized water bath and agitated in an ultrasonic cleaner for about 10 minutes at a temperature of approximately 80°C. After the ultrasonic cleaning, the substrate is dried using compressed air and then flushed several times using acetone to dissolve any organic matter (skin, oils, etc.) on the surface. The substrate is then placed in a vapour degreaser using 95% Ethanol Alcohol for a few minutes. The substrate is now clean and ready for the vacuum deposition.

In all the above steps the substrate should be handled with extreme care using a clean plastic tweezer and only at the corners of the substrate. The amount of dust in the surrounding medium

should be kept to a minimum. Also the cleaned substrate should not be left in the open air, while loading it in the vacuum unit, for more than one minute.

(2) The Vacuum Deposition [21]:

Evaporation from a resistance heated filament using the Edwards High Vacuum Coating Unit 12E3 was used for the deposition of the aluminum thin film. The substrate is held inside the vacuum chamber by a substrate holder which allows most of the substrate area to be exposed to the aluminum vapour stream. The substrate temperature during deposition was left at room temperature; i.e. substrate heating was not necessary during the vacuum deposition. The deposition process is carried out as follows:

(i) The vacuum chamber is cleaned first from any dust and if it had been used previously for deposition of any other metal, an aluminum deposition should be made first before inserting the substrate into the vacuum chamber. This is to prevent contamination in the deposited aluminum film

(ii) Pure (99.99%) aluminum wire (0.062"Dia.) is cut into small bars and loaded into the standard Tungsten helixial wire. Two such loaded filaments would be enough for the deposition of the required thickness.

(iii) The substrate is taken from the vapour degreaser and inserted quickly in its substrate holder and placed inside the vacuum chamber. Since the substrate area is relatively small, a uniform thin film can be obtained with the substrate at approximately 5 inches vertically

above the evaporation source. Extreme care should be taken while loading the substrate in its holder because any stress in forcing the substrate into its groove can break the brittle edges.

(iv) Once the substrate is placed inside the vacuum chamber, the "roughing" process should be started to reduce the pressure inside the chamber. The time period after getting the substrate out of the vapour degreaser, during which the substrate is exposed directly to the air should be kept to a minimum.

(v) At a pressure of approximately 10^{-5} torr.(mm Hg), the deposition can be started. First the filament is heated with relatively low current for about 5 minutes with the shutter between the filament and substrate closed. This is to prevent the dust particles near the evaporation source from reaching the substrate by convection. The current is then increased until the aluminum starts to "wet" the filament. The shutter is then opened to start the deposition on the substrate.

(vi) A deposition rate between 100 Å /sec and 200 Å /sec has been used for a thickness of approximately 3000 Å. The thickness and the deposition rate are monitored by measuring the frequency of oscillations of a quartz crystal placed inside the vacuum chamber beside the substrate [21]. At the end of deposition, the shutter is closed and the substrate is left for about 30 minutes to cool down before opening the

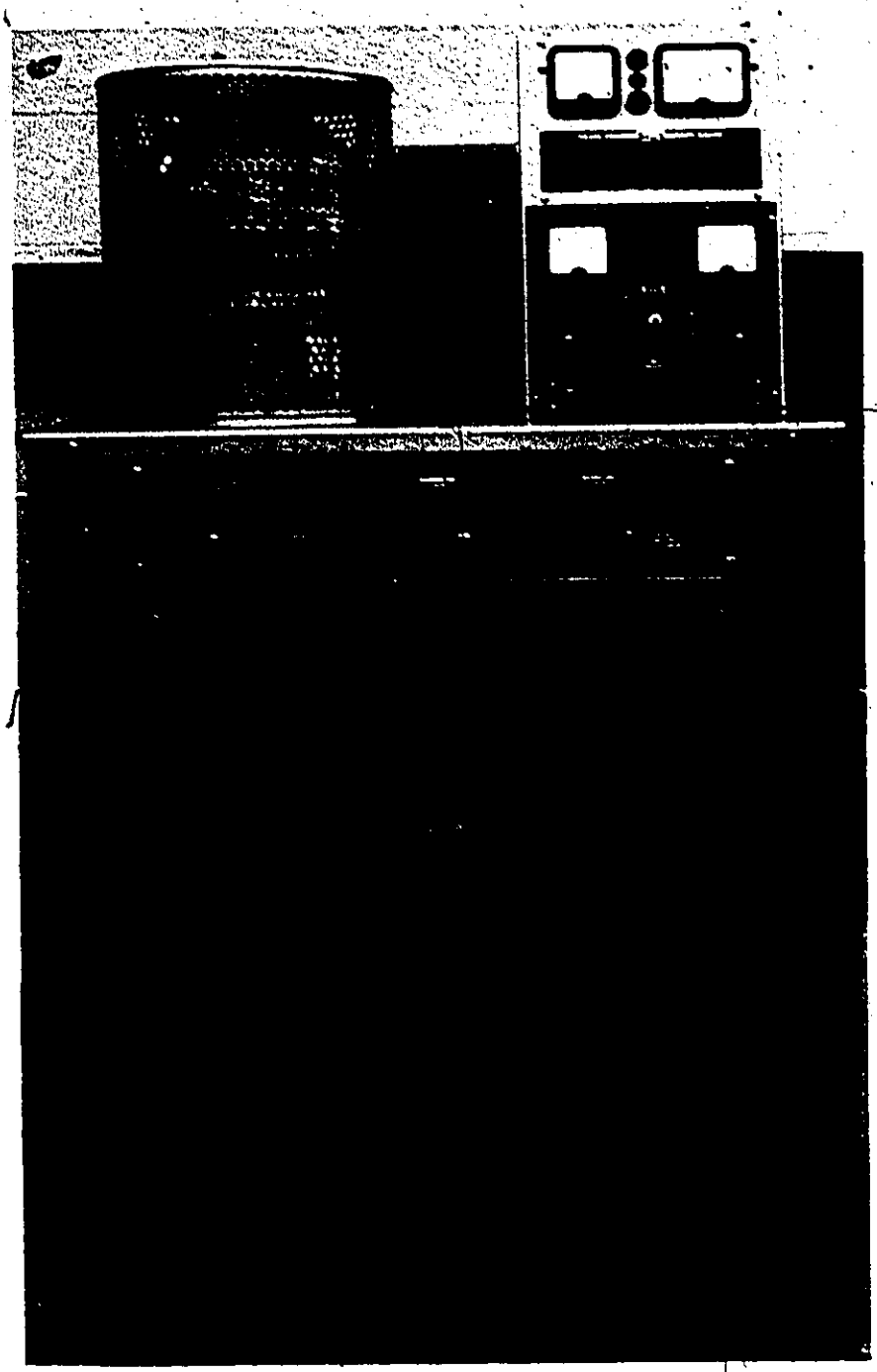

air admittance valve. The metallized substrate is then taken to the dark room for pattern formation and definition. The thin film should always be kept away from dust or any object that might scratch the surface.

5.5.3 Pattern Formation and Definition [21] and [23].

To form the required pattern on the aluminum thin film, positive photoresist was used. After developing the pattern, chemical etching was used to define the pattern on the substrate. The procedures are as follows:

(1) A filtered specimen of a few cc's of Shipley AZ 1350 J positive photoresist is prepared immediately before using it.

(2) The substrate is mounted on the "spinner" such that all its edges are free or otherwise these edges will trap the photoresist on spinning and form a thick resist layer along the edges. The variations in thickness over the optimum exposure to vary over the substrate

(3) A few drops of the photoresist are applied on the substrate until it flows over the edges. Full speed (3000 RPM) continuous spinning for about 3 or 4 minutes is required. This will make the variations of the photoresist thickness very localized near the edges of the substrate. Fortunately the areas near the edges are of less interest since these areas will be covered with the transducers' pads. The substrate is then pre baked for about 25 minutes at approximately 80°C.

(4) After the pre-baking, the substrate is taken out of the oven and left until it cools down. The mask is then placed over the substrate

surface lightly and the edges of both the substrate and the mask are aligned together carefully under the microscope. On alignment the crystal and the substrate are brought into pressured contact. This precaution is taken so that neither the mask nor the photoresist layer are scratched. Since the exposing light source is usually somewhat divergent, it follows from geometrical optics that any gap between the emulsion of the mask and the resist coat causes spreading of the exposed region. Hence the finger widths or the finger to space ratio of the resulting pattern will be smaller than that of the mask. Light spreading under dark mask areas is also caused by diffusion scattering of light in the resist and by reflection from the film or substrate surface underneath [21]. The alignment of the mask to the substrate axis is essential in SAW devices, as was explained in Chapter II.

(5) The substrate and the mask are exposed to ultraviolet light from a distance of approximately 20 inches with a Norelco EVY 650 watt projection lamp for about 1.5 minutes. The exposure time is determined by the thickness of the photoresist, the pattern resolution and the distance from the light source.

(6) The pattern is developed in the AZ 1350 Shipley developer for about one minute until all photoresist is removed from exposed areas. The substrate is rinsed in water and dried using compressed air.

(7) After post baking for approximately one hour, the substrate is immersed in the etchant to etch out the exposed areas. The etchant used is a warm solution of phosphoric, acetic and nitric acids mixed volumetrically in the ratio 25 : 5 : 1 [22]. The etching process is

observed under the microscope so that immediately upon completion the substrate is rinsed carefully several times in water. This is to prevent excessive undercutting which is a usual phenomenon in chemical etching [21]. Before removing the photoresist a check under the microscope should be made to make sure that there is no residual metal to be etched, especially between the electrode fingers.

(8) The photoresist finally is removed using acetone and the substrate is ready for wiring if the etched pattern is acceptable. Any short circuit between two electrode fingers makes the circuit completely unacceptable. This could be checked by measuring the electrical resistance between the electrode pads. Open circuits, i.e. cuttings in the electrode fingers, in the etched pattern might be tolerated to a certain extent depending on the number and location of these open circuits. If the circuit is not acceptable the whole process should be started from the beginning.

This process was developed by producing approximately 150 different circuits using different masks until acceptable results were obtained. In Fig.5.15 the final device with its leads are shown.

5.5.4 Wiring and Matching the device

Bad wiring or mounting can produce a response which is completely different from that of the device itself. The leads of the device should be kept as short as possible. In the temporary mounting shown in Fig.5.16 the Eccobond Solder 56 G was used to bind the two 0.001" diameter gold wire leads to the transducers' pads. The leads are approximately 1.5 millimeters in length and their free ends are connected to two OSM 204CC coaxial bullhead connectors using either the same Eccoband solder or else low temperature soldering (i.e. ind-

alloy solders). Soldering gives better ohmic contact but it should not be used on the surface of the substrate because of the locally produced heat which may break the substrate. The Ultrasonic bonder may also be used in such cases.

The last step in the fabrication process after the required response is obtained is to match the device. First the input and output admittances of the filter are measured. The input and output capacitances are then tuned out by series or parallel inductors. The input conductance of the filter is better matched by adjusting the output conductance of the preceding stage to the filter in the electronic circuit rather than adjusting the filter input conductance. Similarly, the output conductance is matched by adjustment of the input conductance of the following stage. Matching reduces the insertion loss. However, accurate measurement of the response can be done without matching the device.

Fig 5.15 Photograph of the final device.

Fig 5.16 Photograph of the temporary mounting of the device.

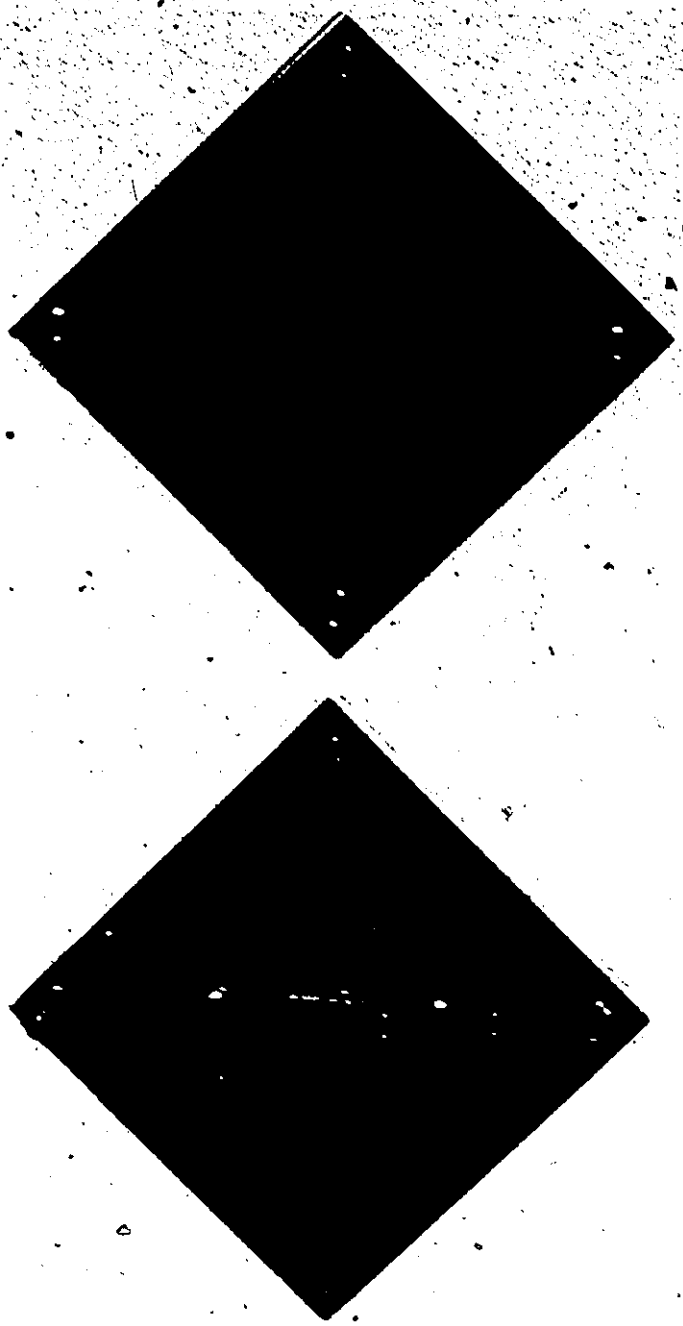

CHAPTER VI

EXPERIMENTAL RESULTS AND CONCLUSIONS

6.1 General

A number of patterns have been cut on "Rubylith" having principally the same design described in Chapter V. Two of these patterns were cut using the HP 9100 Calculator/Plotter at a scale of 20 x. The plotter had been provided with a special knife instead of its usual pen. The two masks gave approximately the same results, part of which is presented in this chapter.

A third pattern, consisting of two transducers, one apodized and the other uniform, was cut on Rubylith at a scale of 100 using the cutting table. The results of this pattern are also shown.

The results of the final design described in Chapter V is presented finally in this chapter.

6.2 Instrumentation

The well known filters standard measurements can be classified into two sets of measurements.

Transmission Properties:

* Insertion loss
* Phase Delay
* Group Delay

Reflection Properties:

* Complex Impedance
* Reflection Coefficient
* VSWR

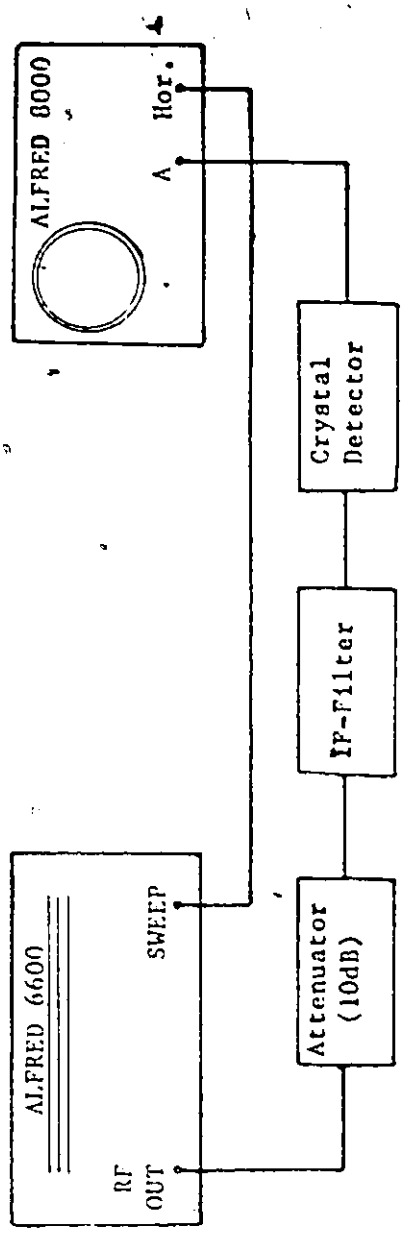

Fig 6.1 Circuit diagram for measuring the filter amplitude response.

These standard measurements are well instrumented for the different frequency ranges. In the range 0.1 - 110 MHz, for example, the HP 8407 Network Analyzer gives very accurate measures for all of the above quantities. However in this chapter only the amplitude response and the complex impedance of the filter will be considered.

The amplitude response of the filter is measured by using a Singer Alfred Sweep Oscillator 6600 and a Singer Alfred Sweep Network Analyzer 8000/7051. The circuit diagram is shown in Fig.6.1. The RF output of the generator is applied to the filter through a 10 dB attenuator to reduce the effect of the reflections due to mismatch on the filter response. The output of the filter is detected by a crystal detector and displayed on the oscilloscope. The sweep output of the generator is used to drive the horizontal sweep of the oscilloscope. The oscilloscope has two channels and is provided with counters for measuring either the loss or gain in the display of both channels. The insertion loss will be the difference in the oscilloscope counter readings for the two cases when the filter is connected as shown in Fig.6.1 and when the filter is omitted and the crystal is connected directly to the attenuator. It should be noticed that the filter is a reciprocal device whose input and output leads are exchangeable. The only resulting difference is the change of the input and output impedances.

The sweep range and the center frequency of the RF signal can be varied simultaneously. A sweep range of approximately 10 MHz and a center frequency about 42 MHz are used for displaying the IF filter response. An X-Y recorder can be connected to the oscilloscope through

Fig 4.2 Photograph of the Singer 8000/7051 Sweep Network Analyzer shown wired for measuring the filter amplitude response

its auxiliary outputs on the rear panel.

Measurements on the horizontal axis, i.e. the frequency axis can be done by using either the Frequency Markers of the sweeper or switching to the sweep mode and measuring the frequency at the required points on the response by a frequency counter directly connected to the RF output. For accurate measurements of the frequency, the latter method is used. A photograph of the instrumentation is shown in Fig.6.2.

The input and output admittances of the filter were measured using a WAYNE KERR VHF Admittance Bridge B801B. The frequency range of the bridge is from 1 to 100 MHz with an accuracy of approximately ± 2% in measuring both the conductance and capacitance. The bridge is driven from a GR 1001 A standard signal generator with an RF amplitude modulated signal at 100 [illegible] used as a detector.

Preliminary Results

Part of the preliminary results are shown in this section. A pattern having principally the same design described in Chapter V was output on Polylith at a scale of 20 using the HP 9100 Calculator Plotter. The plotter was provided with a special cutting knife instead of its usual pen. The plotting instructions are programmed and fed to the calculator memory in advance. The pattern (Fig.6.3) consists of 100 and 62 single electrode finger transducers and another two dummy transducers. The response of each transducer can be measured alone by blanking the MSC in the original negative mask and using

Fig 6.3 Photograph of a pattern cut on Rubylith using the HP 9100 Calculator/Plotter at a scale of 20x.

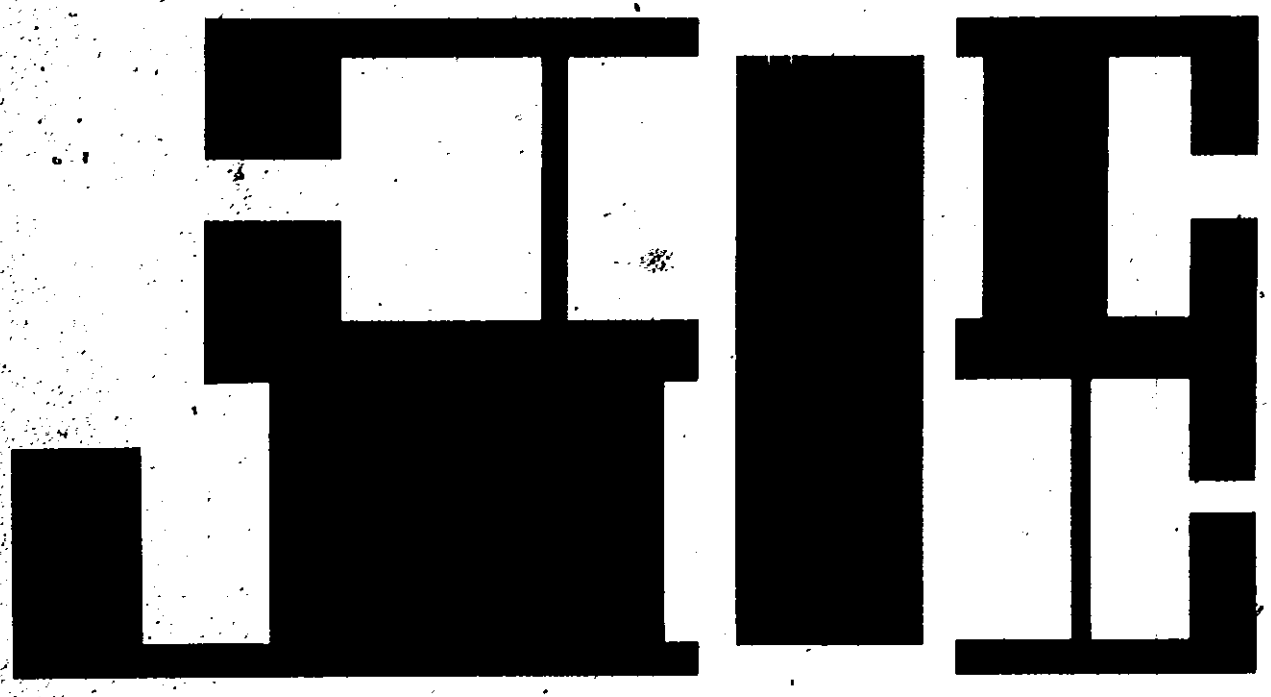

the opposite dummy transducer as an output transducer. The impulse response and the frequency response of the smaller transducer are shown in Fig.6.4. The frequency response of the longer transducer, symmetrically around its center frequency and along the frequency band 0.1-110 MHz, are shown in Fig.6.5. The ripples in the pass band of both transducers are due to the phase error in finger positioning. The phase error is a result of the round-off error of the "plotter". Also the irregularities in the finger edges produced by the cutting knife give non-uniform wave fronts. It should be noticed that the phase cancellation is more effective in the longer transducer than in the shorter one. Also the phase error becomes more significant at the synchronous frequency where these errors add in-phase (either in positive or negative) causing a serious drop or peak in the response at the center frequency.

The non-symmetry of the impulse response in Fig.6.4 is clearly due to the Triple Transit Echo (TTE). The TTE causes the non-symmetry in the amplitude response and distortion in the phase response. The total filter response with the MSC included is shown in Fig.6.6. Additional ripples in the frequency response are introduced by the MSC. Again these ripples are due to the phase error in positioning the coupler strips.

The inband insertion loss (without matching) for all responses is approximately 25 dB. Both the center frequency and the band width for each of these responses are off the design values. A simple SAW filter consists of an apodized transducer and a broad band uniform transducer. The pattern was cut on Rubylith at a scale of 100

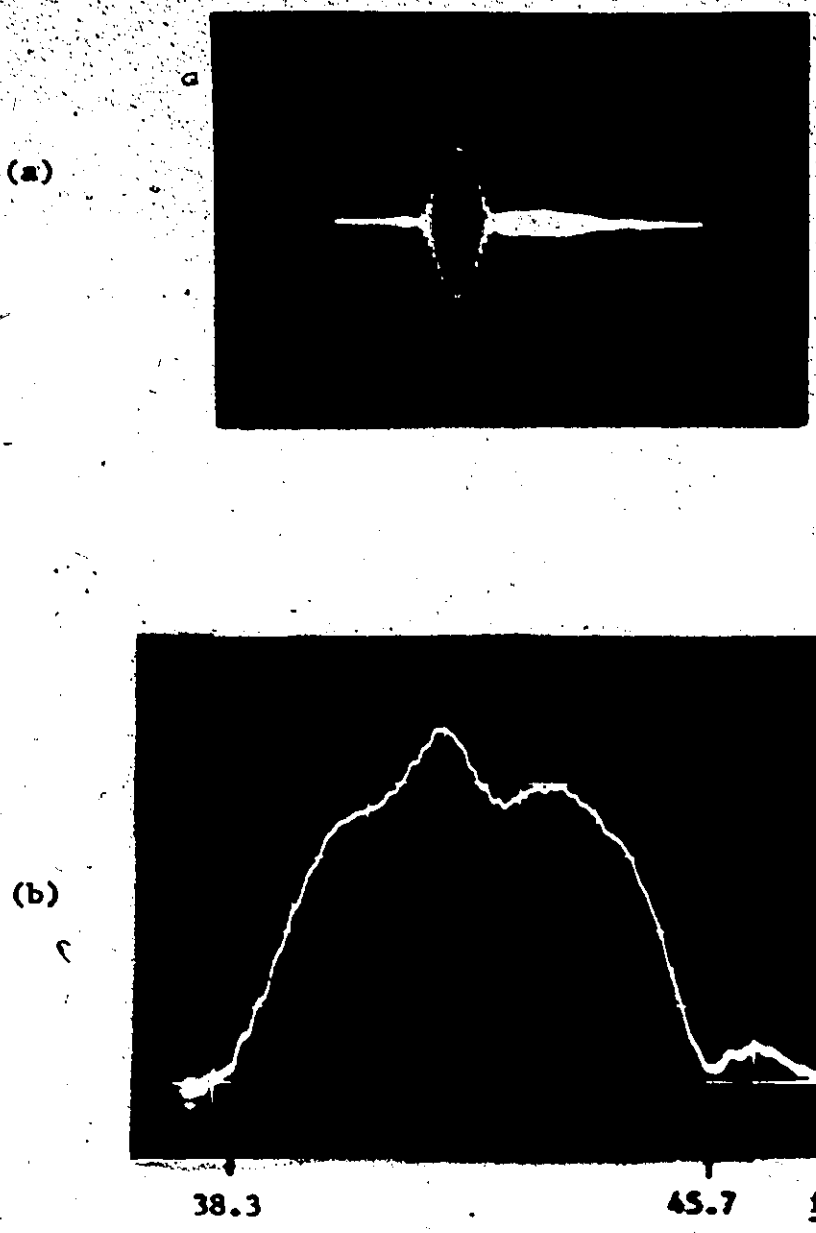

Fig 6.4 (a) The Impulse Response of the small transducer of Fig 6.3,
(b) The corresponding frequency response.

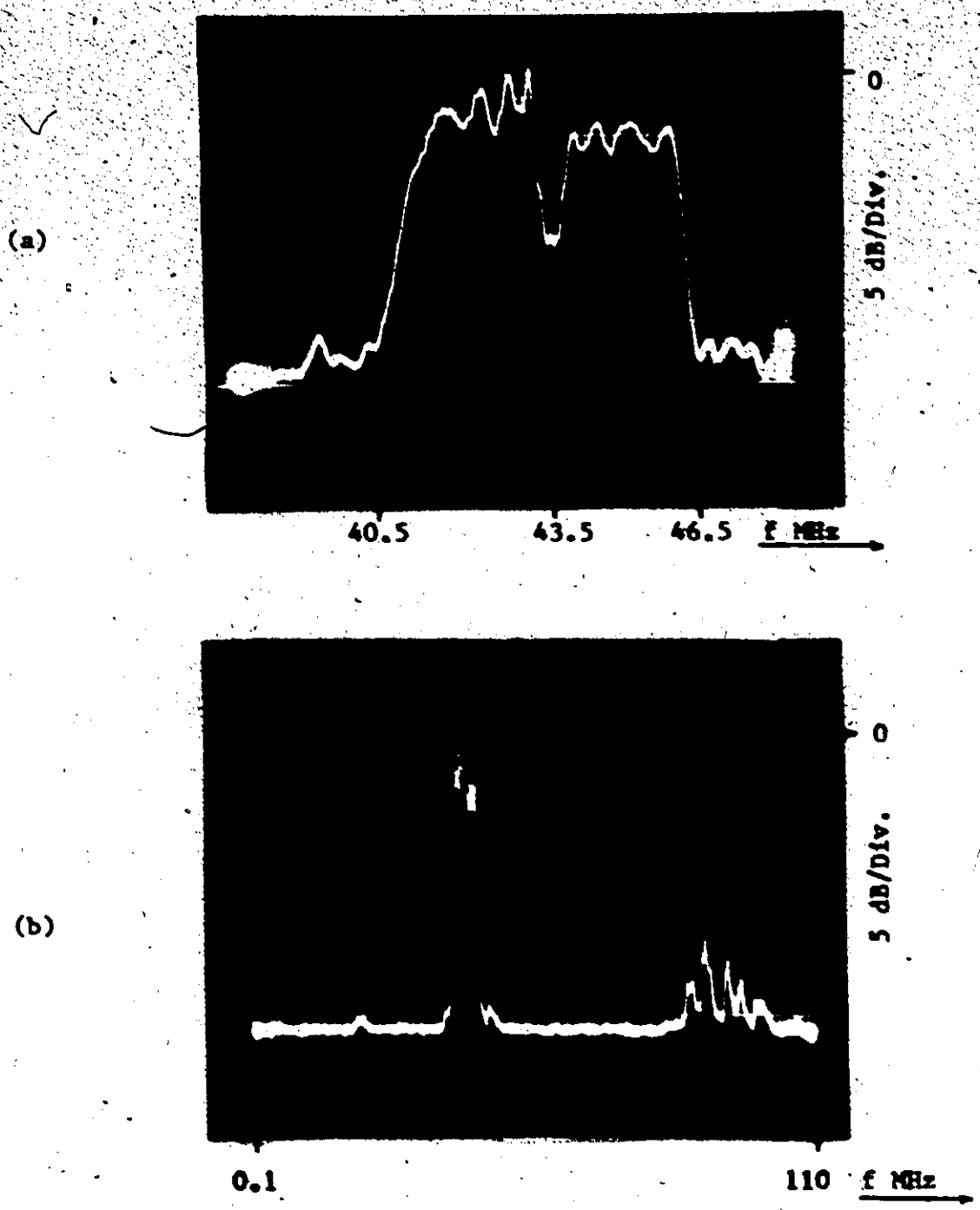

Fig 6.5 The frequency response of the large transducer of Fig 6.3,
(a) In the frequency band 40–50 MHz,
(b) In the frequency band 0.1–110 MHz.

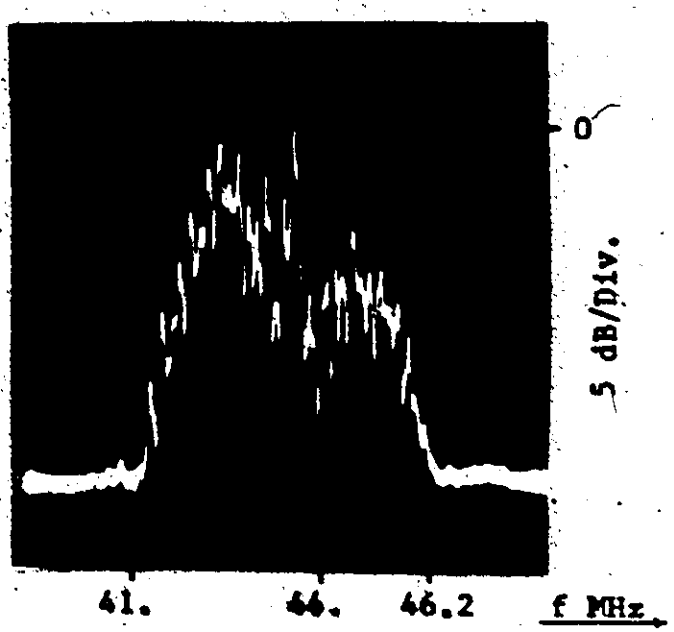

Fig 6.6 The total frequency response Of the filter,using the mask of Fig6.3.

using the cutting table withsplit electrode fingers (Sec.2.4.1). The pattern is shown in Fig.6.7. The input-output wiring of the transducers is shown diagramatically in Fig.6.8a. The corresponding amplitude response is shown in Fig.6.8b. It is seen that the response has high frequency ripples and other low frequency ripples. The total response along the whole frequency range is shown in Fig.6.8c. The capacitive coupling between the input and output transducer pads [feed through] causes the increase in the output level. Absorbing the wave reflections from the substrate edges by covering the substrate edges with a thin layer of paraffin wax, the corresponding response is shown in Fig.6.8d. Changing the input and output termination as shown in Fig.6.9a, the corresponding response is given in Fig.6.9b. The feed through is not a serious problem in the final design when the MSC is used since the capacitive coupling between the input and output transducers is almost negligible. However, the response of Fig.6.9b is not the desired response because the overlapping function used in the design corresponds to the case of a single finger electrode transducer.

6.4 Final Results

The frequency response of the resulting non-matched device is shown in Fig.6.10 and 6.11. Deviation of the resulting response from the theoretical response of Fig.5.9 is obvious in both the band width and the shape of the response itself. Keeping in mind that the total response is the product of two responses given theoretically by Fig. 5.6. and 5.8, the deviation can be easily explained as follows. First it is noticed that the resulting response is not symmetric and it has

Fig 6.7 Photograph of a pattern cut on Rubylith using the cutting table at a scale of 100x.

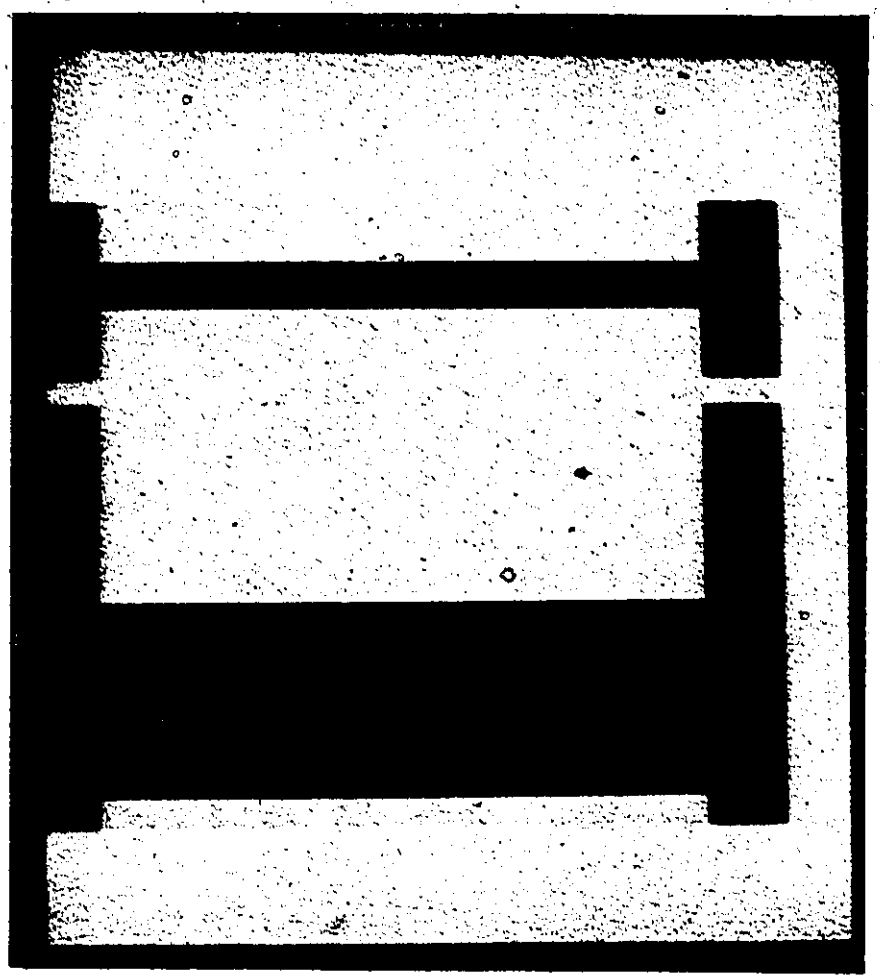

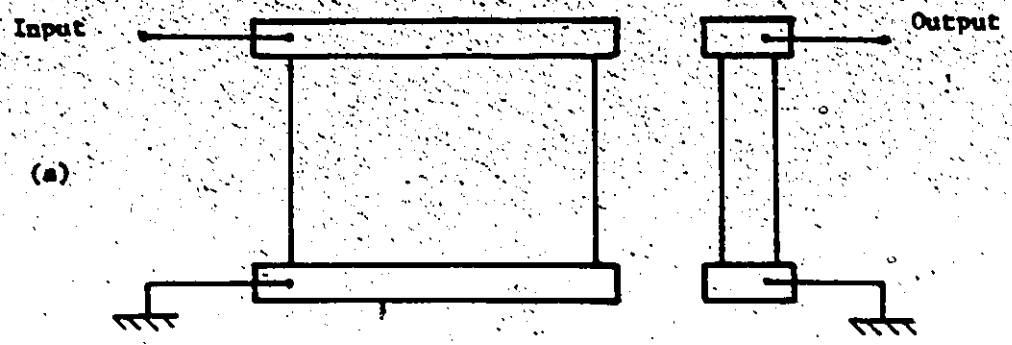

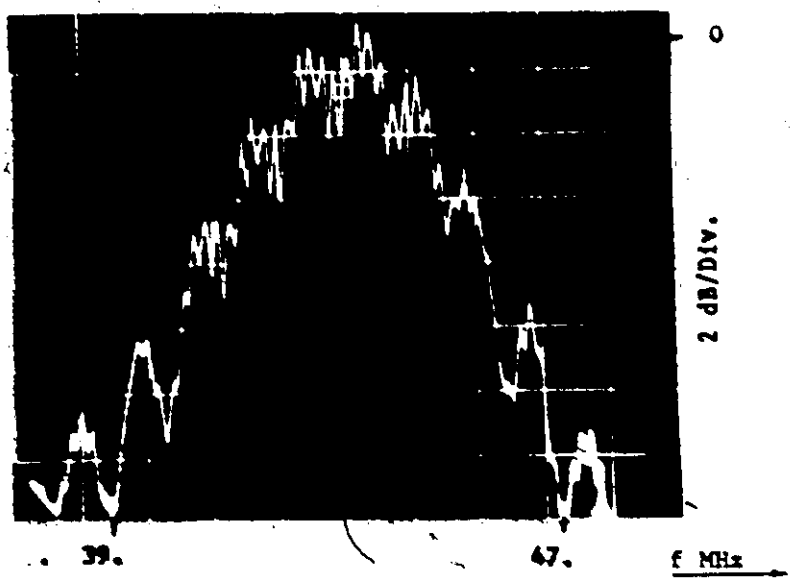

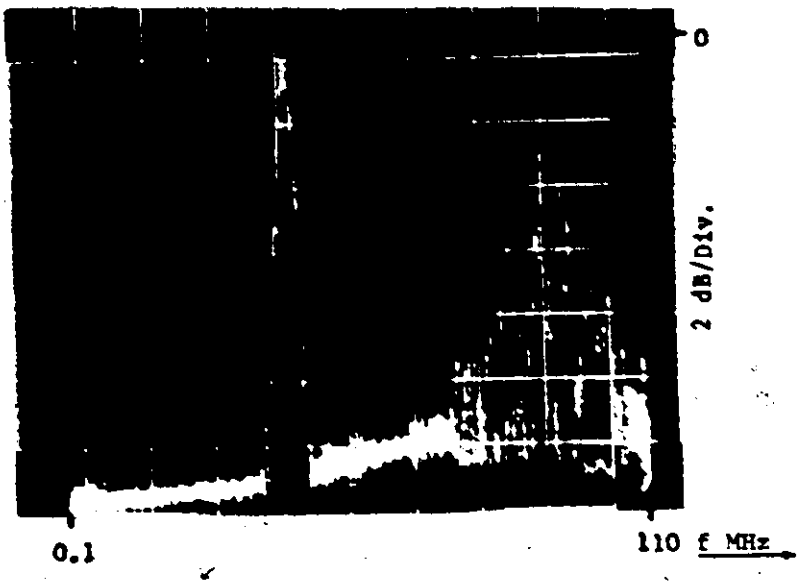

Fig. 6.8

(Cont. Fig 6.8)

(d)

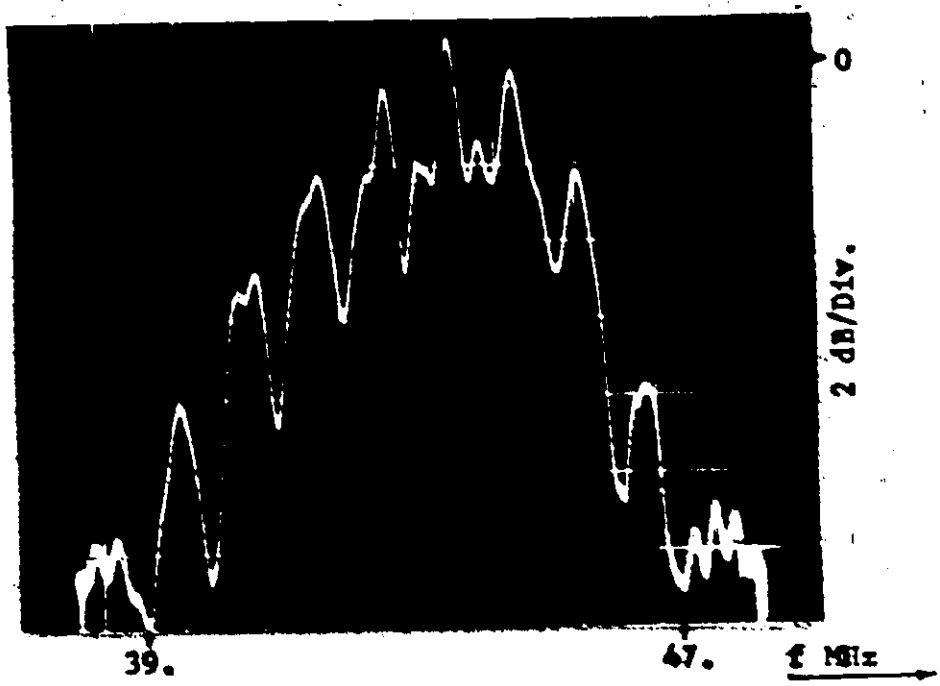

Fig 6.8 The frequency response of the filter of Fig6.7 .
(a) The wiring configuration of the device,
(b)&(c) The corresponding frequency response,
(d) The response after absorbing wave reflections from the substrate edges.

(a)

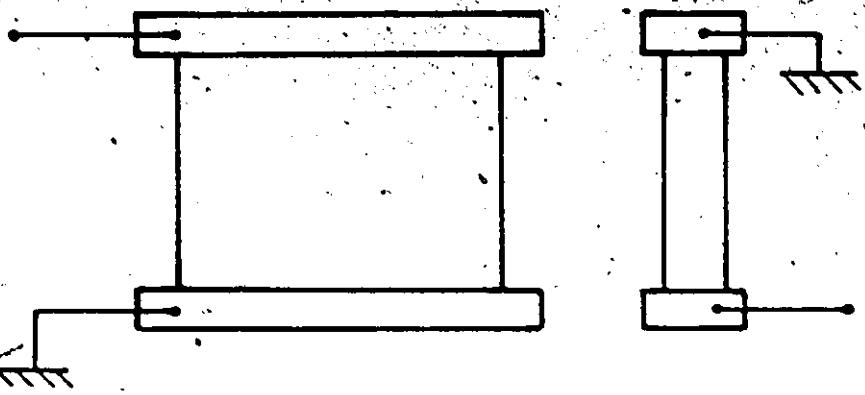

(b)

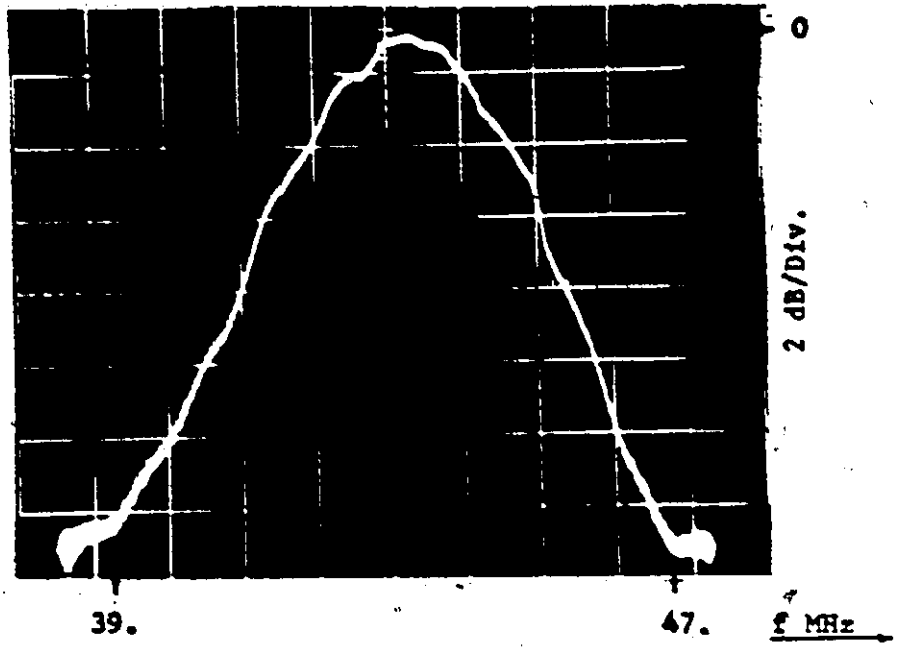

Fig 6.9 The frequency response of the filter of Fig6.7 ,
(a) The wiring configuration of the device.
(b) The corresponding frequency response.

a smaller transition width on its high frequency edge. Comparing with the responses of Fig.5.6, 5.8 and 5.9, it is seen that if the response of transducer No.1 is moved by approximately 2 MHz to the right, while the response of transducer No.2 is moved to the left by approximately 1.5 MHz then their product will be the same as the resulting response of Fig.6.11.

The deviation of the frequency bands of the transducers is due to two different reasons. First the SAW velocity of a metallized surface is different from that of a free surface. This will lead to deviation in the center frequency of both transducers since the finger spacings were calculated using the SAW velocity of a free surface. However this should produce (approximately) the same deviation in the center frequency since the surface metallization conditions are almost the same in the two transducer regions. Surface metallization reduces the SAW velocity and hence causes a drop in the center frequency. The deviation of the frequency band of each transducer with respect to the other is due to the deviation in their reduction ratio during the first reduction. The drawings of the transducers should be reduced by exactly the same ratio as was mentioned before an error of 1% in the reduction ratio results in a frequency shift of approximately 4 MHz.

The frequency response can be corrected by adjusting the reduction ratio in the two photoreduction steps. The production of a master mask requires high precision equipment and also a number of perturbations on the reduction ratio until the exact response is obtained.

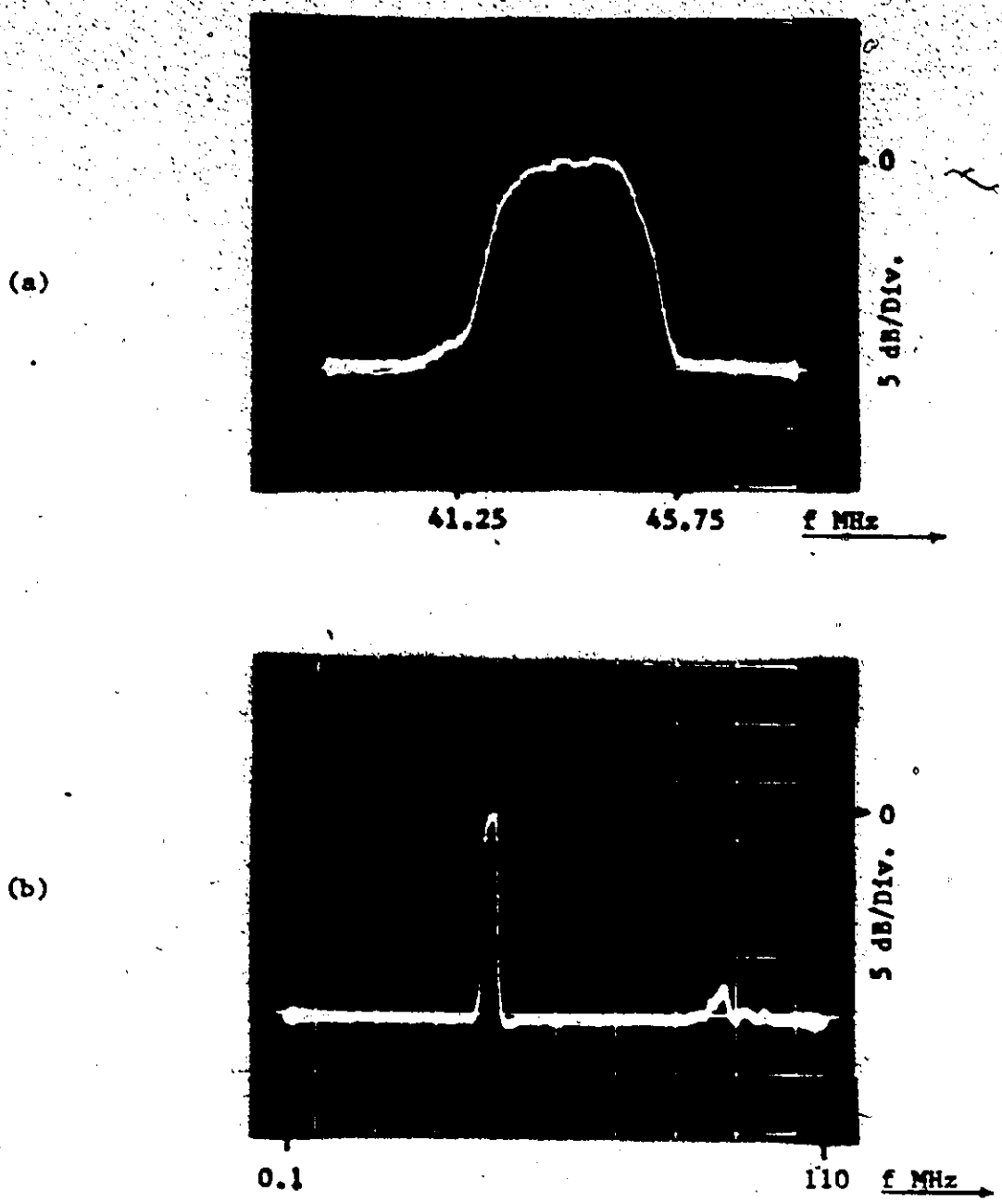

Fig 6.10 The resulting filter response of the mask of Fig 5.13,
(a) In the frequency band 35-50 MHz,
(b) In the frequency band 0.1-110MHz.

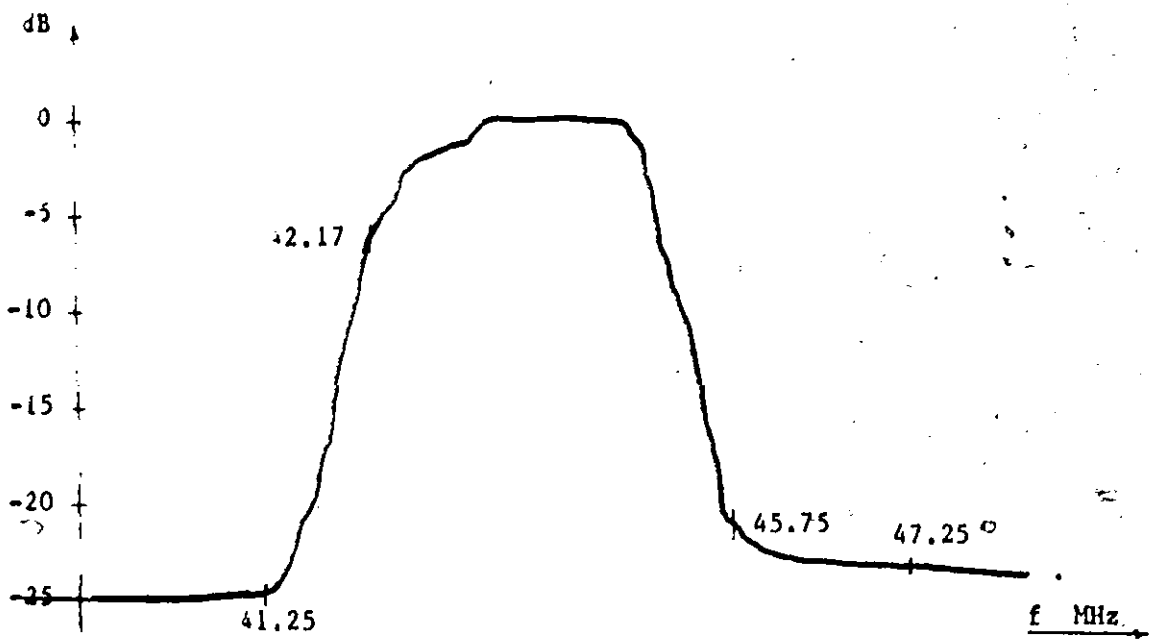

Fig 6.11 The filter response as given by the XY Recorder (the response of Fig 6.10(a)).

Measurements of the input admittance of each transducer are shown in Fig.6.12. The measurements were performed under open circuit conditions of the output transducer. However, the differences between the measured values under the open circuit and short circuit conditions, were less than 3%. A comparison between the estimated and measured values of the input admittance of each transducer at its resonance frequency is shown in Table 6.1.

TABLE 6.1.

	Transducer No.1		Transducer No.2.	
	Estimated	Measured	Estimated	Measured
Conductance (millimhos)	9.6 ± 4	2.5	15.2 ± 5	5.1
Capacitance (pF)	50 ± 10	38	60 ± 10	47

The estimated values in Table 6.1 were derived in Sec.5.4. The calculations were based on a metallization ratio $\eta = 0.5$. However, the measured value of η(the finger to space ratio) was only 0.375. This will cause a drop in both the conductance and capacitance by a factor of approximately 0.84 as given by (2.2), (2.5) and (2.6d). The larger part in the drop of the measured values from the estimated values of the conductance is due to the additional resistance introduced by the binding solder used to connect the wire leads to the device.

The inband insertion loss of the response of Fig.6.10 is approximately 25 dB. This value can be reduced considerably by decreasing

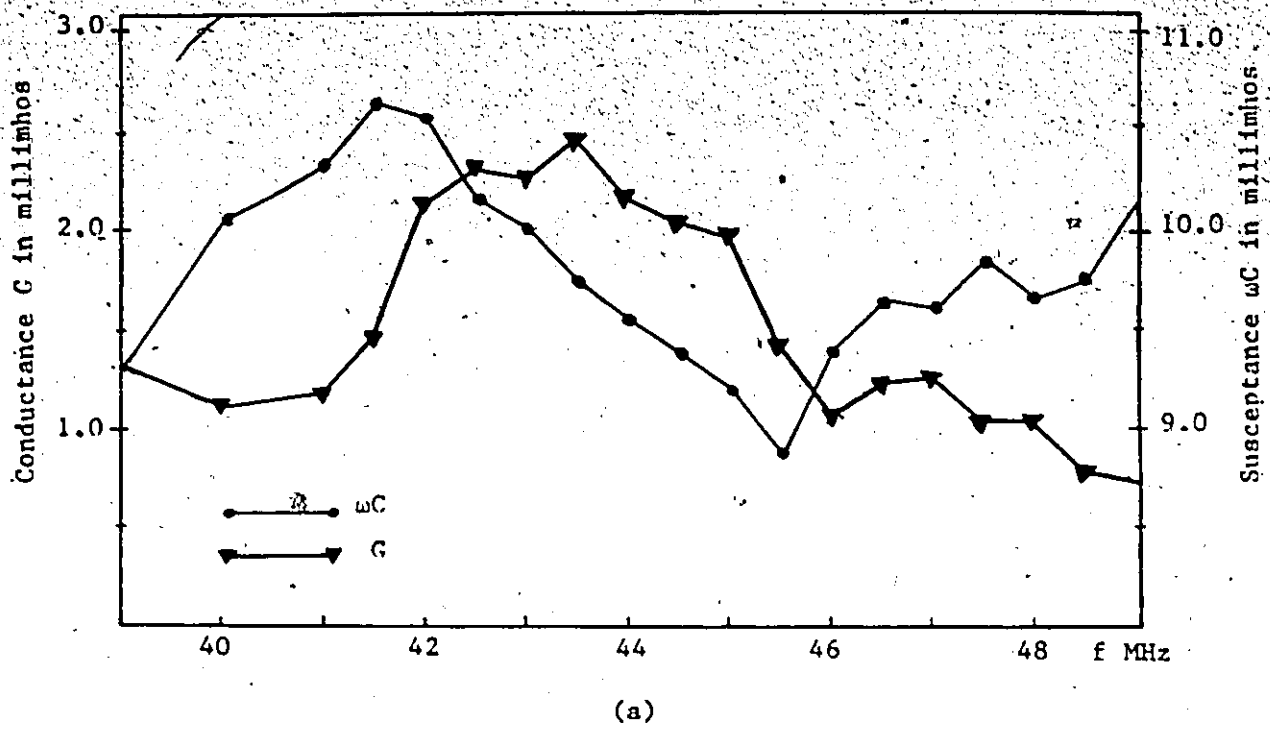

(a)

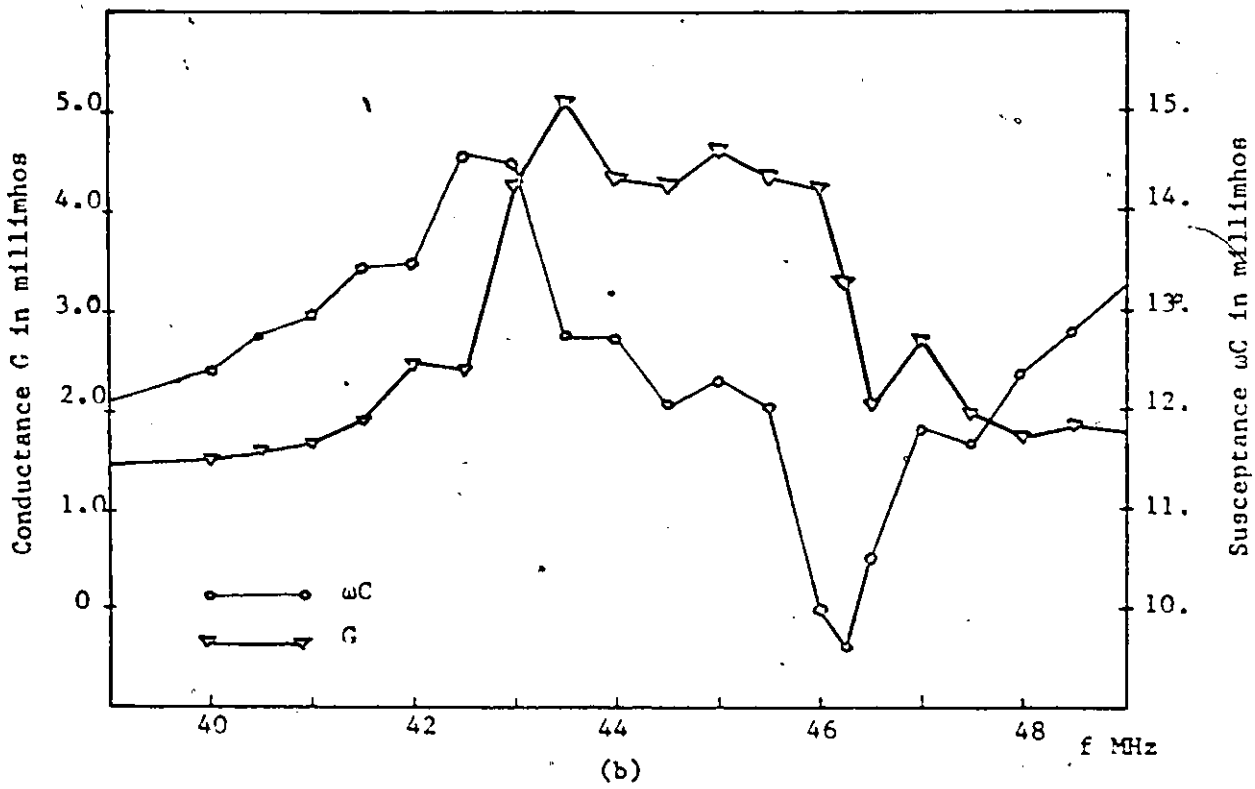

(b)

Fig 6.12 Measured input admittance Y=G+ωC,
(a) For transducer No. 1,
(b) For transducer No. 2.

the ohmic losses in the wire leads of the device and by matching the device with shunt coils at the input and output terminals.

CHAPTER VII

GENERAL CONCLUSIONS AND RECOMMENDATIONS

A SAW TV-IF filter was designed and fabricated. The required filter response is achieved using two apodized transducers coupled with a Multi-strip Coupler. The total frequency response of the filter is the product of the individual frequency responses of the transducers. Deviation of the experimental results from theory is caused by errors in mask production.

(1) The reduction ratio of the two transducers patterns must be exactly the same, i.e., the oversize drawings of the transducers must be reduced simultaneously in the first reduction step. This usually requires a special camera system with a high-resolution lens covering a large field of view. If such a camera is not feasible, a high precision camera can be used instead, such that each drawing is reduced separately with the same reduction ratio.

(2) After the second reduction step, the resulting mask "will" produce the required response but with a slight shift in the frequency band. In such a case a number of iterations on the second reduction ratio is required before the exact response is obtained. It should be noticed that such changes in the reduction ratio have a negligible effect on the filter bandwidth.

Other perfections in the fabrication process are required to produce a defectless device. Perfections in the substrate cleaning, vacuum deposition, mask alignment and device wiring and matching, reduce the distortion in the resulting filter response and also decrease the insertion loss of the device.

APPENDIX A

Computer Program Listing for the Optimization Program

MONIR

```
HSAA,T777.
FTN.
LGO.
      6400 END OF RECORD
      PROGRAM TST (INPUT,OUTPUT,PUNCH,TAPE5=INPUT,TAPE6=OUTPUT,
     1TAPE7=PUNCH)
C     PROGRAM FOR THE DESIGN OF LINEAR PHASE FINITE IMPULSE RESPONSE
C     (FIR) FILTERS USING THE REMEZ EXCHANGE ALGORITHM.
C
C     THE INPUT DATA CONSISTES OF 5 CARDS
C
C     CARD 1- FILTER LENGTH,NUMBER OF BANDS ,CARD PUNCH DESIRED, AND
C     GRID DENSITY.
C
C     CARD 2- BAND EDGES ,LOWER AND UPPER EDGES FOR EACH BAND WITH
C     A MAXIMUM OF 10 BANDS.
C
C     CARD 3- DESIRED FUNCTION FOR EACH BAND.
C
C     CARD 4- WEIGHT FUNCTION IN EACH BAND.
C
      COMMON PI2,AD,DEV,X,Y,GRID,DES,WT,ALPHA,IEXT,NFCNS,NGRID
      DIMENSION IEXT(284),AD(284),ALPHA(284),X(284),Y(284)
      DIMENSION  DES(2272),GRID(2272),WT(2272)
      DIMENSION H(284)
      DIMENSION EDGE(20),FX(10),WTX(10),DEVIAT(10)

      PI=4.*ATAN2(1.,1.)
      PI2=2.*PI

      NFMAX=564
  100 CONTINUE

C  PROGRAM INPUT SECTION

      READ(5,101) NFILT,NBANDS,JPUNCH,LGRID
      IF(NFILT.GT.NFMAX.OR.NFILT.LT.3)  CALL ERROR
      IF(NBANDS.LE.0)  NBANDS=1
  101 FORMAT (4I5)
      IF (LGRID.LE.0)  LGRID=16
      JE=2*NBANDS

      READ(5,105)(EDGE(J), J=1,JE)
      READ(5,105)(FX(J) ,J=1,NBANDS)
      READ(5,105)(WTX(J), J=1,NBANDS)
  105 FORMAT(5E16.8)

      NFCNS=NFILT/2
```

```
C  SET UP THE DENSE GRID. THE NUMBER OF POINTS IN THE GRID IS (FILTER
C  LENGTH +1)*GRID DENSITY/2

      GRID(1) =EDGE(1)
      DELF =LGRID*NFCNS
      DELF =0.5/DELF
  135 CONTINUE
      J =1
      L =1
      LBAND =1
  140 FUP =EDGE(L+1)
  145 TEMP =GRID(J)

C  CALCULATE THE DESIRED MAGNITUDE RESPONSE AND THE WEIGHT FUNCTION OF
C  THE GRID

      DES(J) =EFF(TEMP,FX,WTX,LBAND)
      WT(J)=WATE(TEMP,FX,WTX,LBAND)
      J =J+1
      GRID(J) =TEMP+DELF
      IF(GRID(J).GT.FUP) GO TO 150
      GO TO 145
  150 GRID(J-1) =FUP
      DES(J-1) =EFF(FUP,FX,WTX,LBAND)
      WT(J-1) =WATE(FUP,FX,WTX,LBAND)
      LBAND =LBAND+1
      L =L+2
      IF(LBAND.GT.NBANDS) GO TO 160
      GRID(J) = EDGE(L)
      GO TO 140
  160 NGRID =J-1
      IF(GRID(NGRID).GT.(0.5-DELF))  NGRID=NGRID-1

C  SET UP A NEW APPROXIMATION PROBLEM WHICH IS EQUIVILANT TO THE
C  ORIGINAL PROBLEM

      DO 175 J=1,NGRID
      CHANGE = COS(PI*GRID(J))
      DES(J) = DES(J)/CHANGE
  175 WT(J) = WT(J)*CHANGE

C  INITIAL GUESS FOR THE EXREMAL FREQUENCIES - EQUALLY SPACED
C  ALONG THE GRID
  200 TEMP =FLOAT(NGRID-1)/FLOAT(NFCNS)
      DO 210 J=1,NFCNS
  210 IEXT(J) =(J-1)*TEMP +1
      IEXT(NFCNS+1) =NGRID
      NM1 =NFCNS-1
      NZ =NFCNS+1

C  CALL THE REMEZ EXCHANGE ALGORITHM TO DO THE APPROXIMATION PROBLEM

      CALL REMEZ(EDGE,NBANDS)

C  CALCULATE THE IMPULSE RESPONSE

  310 H(1) =0.25*ALPHA(NFCNS)
```

```
      DO 315 J=2,NM1
  315 H(J) =0.25*(ALPHA(NZ-J)+ALPHA(NFCNS+2-J))
      H(NFCNS) =0.5*ALPHA(1)+0.25*ALPHA(2)

C  PROGRAM OUTPUT SECTION

  350 WRITE(6,360)
  360 FORMAT(1H1,70(1H*)//25X,*FINITE IMPULSE RESPONSE (FIR)*/25X,*
     1LINEAR PHASE    FILTER    DESIGN*/25X,*REMEZ EXCHANGE ALGORITHM*
     2/)
      WRITE(6,365)
  365 FORMAT(25X,*BANDPASS FILTER*/)
      WRITE(6,378) NFILT
  380 FORMAT(15X,*.....IMPULSE RESPONSE.....*)
  378 FORMAT(15X,*FILTER LENGTH=*,I3/)
      WRITE(6,380)
      DO 381 J=1,NFCNS
      K =NFILT+1-J
      WRITE(6,382) J,H(J),K
  381 CONTINUE
  382 FORMAT(20X,*H(*,I3,*)=*,E15.8,*=H(*,I4,*)*)
      DO 450 K=1,NBANDS,4
      KUP =K+3
      IF(KUP.GT.NBANDS) KUP =NBANDS
      WRITE(6,385) (J ,J=K,KUP)
  385 FORMAT(/24X,4(*BAND*,I3,8X))
      WRITE(6,390)(EDGE(2*J-1),J=K,KUP)
  390 FORMAT(2X,*LOWER BAND EDGE*,5F15.9)
      WRITE(6,395) (EDGE(2*J), J=K,KUP)
  395 FORMAT(2X,*UPPER BAND EDGE*,5F15.9)
      WRITE(6,400) (FX(J), J=K,KUP)
  400 FORMAT(2X,*DESIRED VALUE*,2X,5F15.9)
      WRITE(6,410) (WTX(J), J=K,KUP)
  410 FORMAT(2X,*WEIGHTING*,6X,5F15.9)
      DO 420 J=K,KUP
  420 DEVIAT(J) = DEV/WTX(J)
      WRITE(6,425) (DEVIAT(J), J=K,KUP)
  425 FORMAT(2X,*DEVIATION*,6X,5F15.9)
      DO 430 J=K,KUP
  430 DEVIAT(J) =20.0*ALOG10(DEVIAT(J))
      WRITE(6,435) (DEVIAT(J), J=K,KUP)
  435 FORMAT(2X,*DEVIATION IN DB*,5F15.9)
  450 CONTINUE
      WRITE(6,455) (GRID(IEXT(J)), J=1,NZ)
  455 FORMAT(/2X,*EXTREMAL FREQUENCIES*/(2X,5F12.7))
      WRITE(6,460)
  460 FORMAT(/1X,70(1H*)/1H1)
      IF(JPUNCH.EQ.0) GO TO 470
      WRITE(7,465)(H(J),J=1,NFCNS)
  465 FORMAT(E15.8)
  470 CONTINUE
      STOP
      END
      FUNCTION EFF(TEMP,FX,WTX,LBAND)
C
C    FUNCTION TO CALULATE THE DESIRED MAGNITUDE RESPONSE AS A FUNCTION
C    OF FREQUENCY.
C
```

```
      DIMENSION FX(5),WTX(5)
      EFF=FX(LBAND)
      RETURN
      END
      FUNCTION WATE(TEMP,FX,WTX,LBAND)
C
C     FUNCTION TO CALULATE THE WEIGHT FUNCTION AS A FUNCTION OF FREQUENCY.
C
      DIMENSION FX(5),WTX(5)
      GO TO (11,12,13) LBAND
   11 WATE=10./(1.148728813-9.*TEMP)**2.
      GO TO 14
   12 WATE=WTX(LBAND)
      GO TO 14
   13 WATE=10./(9.*TEMP-1.101271185)**2.
   14 CONTINUE
      RETURN
      END
      SUBROUTINE ERROR
      WRITE (6,1)
    1 FORMAT (1H ,*.......... ERROR IN INPUT DATA ..........*)
      STOP
      END

      SUBROUTINE REMEZ(EDGE,NBANDS)
C     THIS SUBROUTINE IMPLEMENTS THE REMEZ EXCHANGE ALGORITHM FOR THE
C     WEIGHTED CHEBYCHEV APPROXIMATION OF A CONTINUOUS FUNCTION WITH
C     A SUM OF COSINES. INPUTS TO THE SUBROUTINE ARE A DENSE GRID WHICH
C     REPLACES THE FREQUENCY AXIS,THE DESIRED FUNCTION ON THIS GRID,
C     THE WEIGHT FUNCTION ON THE GRID , THE NUMBER OF COSINES ,AND AN
C     INITIAL GUESS OF THE EXTREMAL FREQUENCIES. THE PROGRAM MINIMIZES THE
C     CHEBYCHEVERROR BY DETERMINING THE BEST LOCATION OF THE EXTREMAL
C     FREQUENCIES (POINTS OF MAXIMUM ERROR) AND THEN CALCULATES THE
C     COEFFICIENTS OF THE BEST APPROXIMATION.

      COMMON PI2,AD,DEV,X,Y,GRID,DES,WT,ALPHA,IEXT,NFCNS,NGRID
      DIMENSION EDGE(20)
      DIMENSION  DES(2272),GRID(2272),WT(2272)
      DIMENSION IEXT(284),AD(284),ALPHA(284),X(284),Y(284)
      DIMENSION A(284),P(284),Q(284)
C
C     THE PROGRAM ALLOWS A MAXIMUM NUMBER OF ITERATIONS OF 25
C
      ITRMAX=25
      DEVL=-1.0
      NZ=NFCNS+1
      NZZ=NFCNS+2
      NITER=0
  100 CONTINUE
      IEXT(NZZ)=NGRID+1
      NITER=NITER+1
      IF(NITER.GT.ITRMAX) GO TO 400
      DO 110 J=1,NZ
      DTEMP=GRID(IEXT(J))
      DTEMP=COS(DTEMP*PI2)
  110 X(J)=DTEMP
      JET=(NFCNS-1)/15+1
      DO 120 J=1,NZ
```

```
      120 AD(J)=D(J,NZ,JET)
          DNUM=0.0
          DDEN=0.0
          K=1
          DO 130 J=1,NZ
          L=IEXT(J)
          DTEMP=AD(J)*DES(L)
          DNUM=DNUM+DTEMP
          DTEMP=K*AD(J)/WT(L)
          DDEN=DDEN+DTEMP
      130 K=-K
          DEV=DNUM/DDEN
          NU=1
          IF(DEV.GT.0.0) NU=-1
          DEV=-NU*DEV
          K=NU
          DO 140 J=1,NZ
          L=IEXT(J)
          DTEMP=K*DEV/WT(L)
          Y(J)=DES(L)+DTEMP
      140 K=-K
          IF(DEV.GE.DEVL) GO TO 150
          CALL OUCH
          GO TO 400
      150 DEVL=DEV
          JCHNGF=0
          K1=IEXT(1)
          KNZ=IEXT(NZ)
          KLOW=0
          NUT=-NU
          J=1
C
C     SEARCH FOR THE EXTREMAL FREQUENCIES OF THE BEST APPROXIMATION
C
      200 IF(J.EQ.NZZ) YNZ=COMP
          IF(J.GE.NZZ) GO TO 300
          KUP=IEXT(J+1)
          L=IEXT(J)+1
          NUT=-NUT
          IF(J.EQ.2) Y1=COMP
          COMP=DEV
          IF(L.GE.KUP) GO TO 220
          ERR=GEE(L,NZ)
          ERR=(ERR-DES(L))*WT(L)
          DTEMP=NUT*ERR-COMP
          IF(DTEMP.LE.0.0) GO TO 220
          COMP=NUT*ERR
      210 L=L+1
          IF(L.GE.KUP) GO TO 215
          ERR=GEE(L,NZ)
          ERR=(ERR-DES(L))*WT(L)
          DTEMP=NUT*ERR-COMP
          IF(DTEMP.LE.0.0) GO TO 215
          COMP=NUT*ERR
          GO TO 210
      215 IEXT(J)=L-1
          J=J+1
          KLOW=L-1
```

```
      JCHNGE=JCHNGE+1
      GO TO 200
  220 L=L-1
  225 L=L-1
      IF(L.LE.KLOW) GO TO 250
      ERR=GEE(L,NZ)
      ERR=(ERR-DES(L))*WT(L)
      DTEMP=NUT*ERR-COMP
      IF(DTEMP.GT.0.0) GO TO 230
      IF(JCHNGE.LE.0) GO TO 225
      GO TO 260
  230 COMP=NUT*ERR
  235 L=L-1
      IF(L.LE.KLOW) GO TO 240
      ERR=GEE(L,NZ)
      ERR=(ERR-DES(L))*WT(L)
      DTEMP=NUT*ERR-COMP
      IF(DTEMP.LE.0.0) GO TO 240
      COMP=NUT*ERR
      GO TO 235
  240 KLOW=IEXT(J)
      IEXT(J)=L+1
      J=J+1
      JCHNGE=JCHNGE+1
      GO TO 200
  250 L=IEXT(J)+1
      IF(JCHNGE.GT.0) GO TO 215
  255 L=L+1
      IF(L.GE.KUP) GO TO 260
      ERR=GEE(L,NZ)
      ERR=(ERR-DES(L))*WT(L)
      DTEMP=NUT*ERR-COMP
      IF(DTEMP.LE.0.0) GO TO 255
      COMP=NUT*ERR
      GO TO 210
  260 KLOW=IEXT(J)
      J=J+1
      GO TO 200
  300 IF(J.GT.NZZ) GO TO 320
      IF(K1.GT.IEXT(1)) K1=IEXT(1)
      IF(KNZ.LT.IEXT(NZ1)) KNZ=IEXT(NZ)
      NUT1=NUT
      NUT=-NU
      L=0
      KUP=K1
      COMP=YNZ*(1.-WT(1))
      LUCK=1
  310 L=L+1
      IF(L.GE.KUP) GO TO 315
      ERR=GEE(L,NZ)
      ERR=(ERR-DES(L))*WT(L)
      DTEMP=NUT*ERR-COMP
      IF(DTEMP.LE.0.0) GO TO 310
      COMP=NUT*ERR
      J=NZZ
      GO TO 210
  315 LUCK=6
      GO TO 325
```

```
  320 IF(LUCK.GT.9) GO TO 350
      IF(COMP.GT.Y1) Y1=COMP
      K1=IEXT(NZZ)
  325 L=NGRID+1
      KLOW=KNZ
      NUT=-NUT1
      COMP=Y1*(1.00001)
  330 L=L-1
      IF(L.LE.KLOW) GO TO 340
      ERR=GEE(L,NZ)
      ERR=(ERR-DES(L))*WT(L)
      DTEMP=NUT*ERR-COMP
      IF(DTEMP.LE.0.0) GO TO 330
      J=NZZ
      COMP=NUT*ERR
      LUCK=LUCK+10
      GO TO 235
  340 IF(LUCK.EQ.6) GO TO 370
      DO 345 J=1,NFCNS
  345 IEXT(NZZ-J)=IEXT(NZ-J)
      IEXT(1)=K1
      GO TO 100
  350 KN=IEXT(NZZ)
      DO 360 J=1,NFCNS
  360 IEXT(J)=IEXT(J+1)
      IEXT(NZ)=KN
      GO TO 100
  370 IF(ICHNGE.GT.3) GO TO 100


C     CALCULATION OF THE BEST APP
C     CALCULATION OF THE COEFFICIENTS OF THE
C     THE INVERSE DISCRETE
C

  400 CONTINUE
      NM1=NFCNS-1
      FSH=1.0E-06
      GTEMP=GRID(1)
      X(NZZ)=-2.0
      CN=2*NFCNS-1
      DELF=1.0/CN
      L=1
      KKK=0
      IF(EDGE(1).EQ.0.0.AND.EDGE(2)
      IF(NFCNS.LE.3) KKK=1
      IF(KKK.EQ.1) GO TO 405
      DTEMP=COS(PI2*GRID(1))
      DNUM=COS(PI2*GRID(NGRID))
      AA=2.0/(DTEMP-DNUM)
      BB=-(DTEMP+DNUM)/(DTEMP-DNUM)
  405 CONTINUE
      DO 430 J=1,NFCNS
      FT=(J-1)*DELF
      XT=COS(PI2*FT)
      IF(KKK.EQ.1) GO TO 410
      XT=(XT-BB)/AA
      FT=ACOS(XT)/PI2
  410 XE=X(L)
```

```
      IF(XT.GT.XE) GO TO 420
      IF((XE-XT).LT.FSH) GO TO 415
      L=L+1
      GO TO 410
  415 A(J)=Y(L)
      GO TO 425
  420 IF((XT-XE).LT.FSH) GO TO 415
      GRID(1)=FT
      A(J)=GEE(1,NZ)
  425 CONTINUE
      IF(L.GT.1) L=L-1
  430 CONTINUE
      GRID(1)=GTEMP
      DDEN=PI2/CN
      DO 510 J=1,NFCNS
      DTEMP=0.0
      DNUM=(J-1)*DDEN
      IF(NM1.LT.1) GO TO 505
      DO 500 K=1,NM1
  500 DTEMP=DTEMP+A(K+1)*COS(DNUM*K)
  505 DTEMP=2.0*DTEMP+A(1)
  510 ALPHA(J)=DTEMP
      DO 550 J=2,NFCNS
  550 ALPHA(J)=2*ALPHA(J)/CN
      ALPHA(1)=ALPHA(1)/CN
      IF(KKK.EQ.1) GO TO 545
      P(1)=2.0*ALPHA(NFCNS)*DD+ALPHA(NM1)
      P(2)=2.0*AA*ALPHA(NFCNS)
      Q(1)=ALPHA(NFCNS-2)-ALPHA(NFCNS)
      DO 540 J=2,NM1
      IF(J.LT.NM1)
      AA=0.5*AA
      BB=0.5*BB
      CONTINUE
      P(J+1)=0.0
      DO 520 K=1,J
      A(K)=P(K)
      P(K)=2.0*BB*A(K)
      P(2)=P(2)+A(1)
      JM1=J-1
      DO 525 K=1,JM1
      P(K)=P(K)+AA*A(K+1)
      JP1=J+1
      DO 530 K=3,JP1
      P(K)=P(K)+AA*A(K-1)
      IF(J.EQ.NM1)
      DO 535 K=1,J
      Q(K)=-A(K)
      Q(1)=Q(1)+ALPHA(
  540 CONTINUE
      DO 543 J=1,NFCNS
  543 ALPHA(J)=P(J)
  545 CONTINUE
      IF(NFCNS.GT.3) RETURN
      ALPHA(NFCNS+1)=0.0
      ALPHA(NFCNS+2)=0.0
      RETURN
      END
```

```
      FUNCTION D(K,N,M)
C
C     FUNCTION TO CALULATE THE LAGRANGE INTERPOLATION COEFFICIENTS
C     FOR USE IN THE FUNCTION GEE.
      COMMON PI2,AD,DEV,X,Y,GRID,DES,WT,ALPHA,IEXT,NFCNS,NGRID
      DIMENSION IEXT(284),AD(284),ALPHA(284),X(284),Y(284)
      DIMENSION  DES(2272),GRID(2272),WT(2272)
      D=1.0
      Q=X(K)
      DO 3 L=1,M
      DO 2 J=L,N,M
      IF(J-K)1,2,1
    1 D=2.0*D*(Q-X(J))
    2 CONTINUE
    3 CONTINUE
      D=1.0/D
      RETURN
      END

      FUNCTION GEE(K,N)
C
C     FUNCTION TO EVALUATE THE FREQUENCY RESPONSE USING THE LAGRANGE
C     INTERPOLATION FORMULA IN THE BARYCENTRIC FORM
C
      COMMON PI2,AD,DEV,X,Y,GRID,DES,WT,ALPHA,IEXT,NFCNS,NGRID
      DIMENSION IEXT(284),AD(284),ALPHA(284),X(284),Y(284)
      DIMENSION  DES(2272),GRID(2272),WT(2272)
      P=0.0
      XF=GRID(K)
      XF=COS(PI2*XF)
      D=0.0
      DO 1 J=1,N
      C=XF-X(J)
      C=AD(J)/C
      D=D+C
    1 P=P+C*Y(J)
      GEE=P/D
      RETURN
      END

      SUBROUTINE OUCH
      WRITE(6,1)
    1 FORMAT (*..... FAILURE TO CONVERGE .....*/
     1*PROBABLY CAUSED BY MACHINE ROUNDING ERROR*/
     2* THE IMPULSE RESPONSE MAY BE CORRECT*/
     3*CHECK WITH A FREQUENCY RESPONSE*)
      RETURN
      END
         6600 END OF RECORD
 564      3       1       8
  0.0              0.1169254222     .1217221628       0.1282768361     0.1334745762
 0.5
   0.0            1.0                       0.0
    1.0                 15.0               1.0
            END OF FILE
```

APPENDIX B

B.1. Weighting Function Subroutines & Input Data Cards:

(1) Transducer No. 1

```
      FUNCTION WATE(TEMP,FX,WTX,LBAND)
C
C     FUNCTION TO CALULATE THE WEIGHT FUNCTION AS A FUNCTION OF FREQUENCY.
C
      DIMENSION FX(5),WTX(5)
      GO TO (11,12,13) LBAND
   11 WATE=10./(1.119816-9.*TEMP)**2.
      GO TO 14
   12 WATE=WTX(LBAND)
      GO TO 14
   13 WATE=10./(9.*TEMP-1.130184)**2.0
   14 CONTINUE
      RETURN
      END
```

```
364    3    1    8
 0.0          0.1133128905    0.1219914371    0.1280065628    0.1366871094
0.5
   0.0          1.0             0.0
   1.0          15.0            1.0
```

(2) Transducer No. 2

```
      FUNCTION WATE(TEMP,FX,WTX,LBAND)
C
C     FUNCTION TO CALULATE THE WEIGHT FUNCTION AS A FUNCTION OF FREQUENCY.
C
      DIMENSION FX(5),WTX(5)
      GO TO (11,12,13) LBAND
   11 WATE=10./(1.14[illegible]-9.*TEMP)**2.
      GO TO 14
   12 WATE=WTX(LBAND)
      GO TO 14
   13 WATE=10./(9.*TEMP-1.10127[illegible])**2.
   14 CONTINUE
      RETURN
      END
```

```
564    3    1    8
 0.0          0.1165254237    .1217231638     0.1282742341    0.1334745762
0.5
   0.0          1.0             0.0
   1.0          15.0            1.0
```

B.2 The Optimized Impulse Response of the Transducers:

(1) Transducer No. 1

```
*****************************************************************************

                    FINITE IMPULSE RESPONSE (FIR)
                       LINEAR PHASE    FILTER        DESIGN
                    REMEZ EXCHANGE ALGORITHM

                    BANDPASS FILTER

FILTER LENGTH=364

.....IMPULSE RESPONSE.....
     H(   1)=   .39761713E-02=H( 364)
     H(   2)=  -.13814238E-01=H( 383)
     H(   3)=   .18626689E-01=H( 362)
     H(   4)=  -.16114834E-01=H( 361)
     H(   5)=   .77197956E-02=H( 360)
     H(   6)=  -.47844735E-02=H( 359)
     H(   7)=   .21073432E-02=H( 358)
     H(   8)=  -.25280086E-02=H( 357)
     H(   9)=   .67924734E-03=H( 356)
     H(  10)=  -.15451216E-02=H( 355)
     H(  11)=   .30545871E-03=H( 354)
     H(  12)=  -.96751862E-03=H( 353)
     H(  13)=   .20500951E-03=H( 352)
     H(  14)=  -.63602409E-03=H( 351)
     H(  15)=   .12930070E-03=H( 350)
     H(  16)=  -.48714146E-03=H( 349)
     H(  17)=   .11757609E-03=H( 348)
     H(  18)=  -.29943786E-03=H( 347)
     H(  19)=   .16049795E-03=H( 346)
     H(  20)=  -.22282440E-03=H( 345)
     H(  21)=   .46075536E-04=H( 344)
     H(  22)=  -.32243248E-03=H( 343)
     H(  23)=  -.72002836E-04=H( 342)
     H(  24)=  -.24589746E-03=H( 341)
     H(  25)=   .12467966E-03=H( 340)
     H(  26)=   .53886753E-04=H( 339)
     H(  27)=   .27900321E-03=H( 338)
     H(  28)=  -.12846573E-04=H( 337)
     H(  29)=  -.32737824E-04=H( 336)
     H(  30)=  -.[illegible]723679E-03=H( 335)
     H(  31)=  -.29626151E-03=H( 334)
     H(  32)=  -.25499150E-03=H( 333)
     H(  33)=   .16573751E-03=H( 332)
     H(  34)=   .35679125E-03=H( 331)
     H(  35)=   .54056875E-03=H( 330)
     H(  36)=   .11754377E-03=H( 329)
     H(  37)=  -.20776670E-03=H( 328)
     H(  38)=  -.59659781E-03=H( 327)
     H(  39)=  -.66975370E-03=H( 326)
     H(  40)=  -.32879669E-03=H( 325)
     H(  41)=   .35439980E-03=H( 324)
     H(  42)=   .65884694E-03=H( 323)
     H(  43)=   .91776334E-03=H( 322)
     H(  44)=   .24449243E-03=H( 321)
     H(  45)=  -.30077851E-03=H( 320)
     H(  46)=  -.10930468E-02=H( 319)
     H(  47)=  -.97859910E-03=H( 318)
     H(  48)=  -.49614479E-03=H( 317)
     H(  49)=   .[illegible]3210E-03=H( 316)
     H(  50)=   .11642156E-02=H( 315)
```

H(51)= .12369981E-02=H(314)	H(112)= .74285159E-03=H(253)
H(52)= .52805364E-03=H(313)	H(113)= -.85573334E-03=H(252)
H(53)= -.57765948E-03=H(312)	H(114)= -.24015846E-02=H(251)
H(54)= -.14094367E-02=H(311)	H(115)= -.26583567E-02=H(250)
H(55)= -.14816300E-02=H(310)	H(116)= -.12491729E-02=H(249)
H(56)= -.61756939E-03=H(309)	H(117)= .13764207E-02=H(248)
H(57)= .64229263E-03=H(308)	H(118)= .36102287E-02=H(247)
H(58)= .16404214E-02=H(307)	H(119)= .39506513E-02=H(246)
H(59)= .16642275E-02=H(306)	H(120)= .17569429E-02=H(245)
H(60)= .71436907E-03=H(305)	H(121)= -.19230254E-02=H(244)
H(61)= -.76970398E-03=H(304)	H(122)= -.50009810E-02=H(243)
H(62)= -.18496995E-02=H(303)	H(123)= -.53296231E-02=H(242)
H(63)= -.19055499E-02=H(302)	H(124)= -.23675186E-02=H(241)
H(64)= -.79432454E-03=H(301)	H(125)= .25501286E-02=H(240)
H(65)= .83117854E-03=H(300)	H(126)= .64995003E-02=H(239)
H(66)= .20487404E-02=H(299)	H(127)= .68600012E-02=H(238)
H(67)= .20581008E-02=H(298)	H(128)= .29581333E-02=H(237)
H(68)= .85942414E-03=H(297)	H(129)= -.31747315E-02=H(236)
H(69)= -.91278837E-03=H(296)	H(130)= -.80654146E-02=H(235)
H(70)= -.22052191E-02=H(295)	H(131)= -.84325255E-02=H(234)
H(71)= -.22390827E-02=H(294)	H(132)= -.36540634E-02=H(233)
H(72)= -.91612394E-03=H(293)	H(133)= .38739535E-02=H(232)
H(73)= .97175925E-03=H(292)	H(134)= .96966568E-02=H(231)
H(74)= .22276886E-02=H(291)	H(135)= .10107565E-01=H(230)
H(75)= .23272559E-02=H(290)	H(136)= .43305319E-02=H(229)
H(76)= .94042729E-03=H(289)	H(137)= -.45571746E-02=H(228)
H(77)= -.10056835E-02=H(288)	H(138)= -.11401451E-01=H(227)
H(78)= -.23364986E-02=H(287)	H(139)= -.11792036E-01=H(226)
H(79)= -.23804533E-02=H(286)	H(140)= -.50441696E-02=H(225)
H(80)= -.95105341E-03=H(285)	H(141)= .52855768E-02=H(224)
H(81)= .98775821E-03=H(284)	H(142)= .13097459E-01=H(223)
H(82)= .23182022E-02=H(283)	H(143)= .13506851E-01=H(222)
H(83)= .22954479E-02=H(282)	H(144)= .57278440E-02=H(221)
H(84)= .89616515E-03=H(281)	H(145)= -.59889637E-02=H(220)
H(85)= -.93434633E-03=H(280)	H(146)= -.14501931E-01=H(219)
H(86)= -.22211527E-02=H(279)	H(147)= -.15161172E-01=H(218)
H(87)= -.21217550E-02=H(278)	H(148)= -.64349164E-02=H(217)
H(88)= -.85196178E-03=H(277)	H(149)= .66747411E-02=H(216)
H(89)= .80572624E-03=H(276)	H(150)= .16410699E-01=H(215)
H(90)= .19571876E-02=H(275)	H(151)= .16794924E-01=H(214)
H(91)= .18033159E-02=H(274)	H(152)= .70723570E-02=H(213)
H(92)= .72042033E-03=H(273)	H(153)= -.73043645E-02=H(212)
H(93)= -.72741706E-03=H(272)	H(154)= -.17974196E-01=H(211)
H(94)= -.15915154E-02=H(271)	H(155)= -.18290749E-01=H(210)
H(95)= -.14750447E-02=H(270)	H(156)= -.77132613E-02=H(209)
H(96)= -.53560628E-03=H(269)	H(157)= .79262455E-02=H(208)
H(97)= .52673480E-03=H(268)	H(158)= .19375933E-01=H(207)
H(98)= .11007033E-02=H(267)	H(159)= .19696138E-01=H(206)
H(99)= .92720324E-03=H(266)	H(160)= .82571237E-02=H(205)
H(100)= .31141443E-03=H(265)	H(161)= -.84489100E-02=H(204)
H(101)= -.27739659E-03=H(264)	H(162)= -.20556186E-01=H(203)
H(102)= -.45799638E-03=H(263)	H(163)= -.20909880E-01=H(202)
H(103)= -.25553433E-03=H(262)	H(164)= -.87517049E-02=H(201)
H(104)= -.18259314E-04=H(261)	H(165)= .89293123E-02=H(200)
H(105)= -.43861597E-04=H(260)	H(166)= .21733753E-01=H(199)
H(106)= -.35808977E-03=H(259)	H(167)= .21965542E-01=H(198)
H(107)= -.56035991E-03=H(258)	H(168)= .91653334E-02=H(197)
H(108)= -.35117030E-03=H(257)	H(169)= -.93001011E-02=H(196)
H(109)= .42386296E-03=H(256)	H(170)= -.22619426E-01=H(195)
H(110)= .12817037E-02=H(255)	H(171)= -.22784594E-01=H(194)
H(111)= .15532354E-02=H(254)	H(172)= -.94975133E-02=H(193)

H(173)= .95969568E-02=H(192)
H(174)= .23269371E-01=H(191)
H(175)= .23384522E-01=H(190)
H(176)= .97251336E-02=H(189)
H(177)= -.97551748E-02=H(188)
H(178)= -.23675967E-01=H(187)
H(179)= -.23740073E-01=H(186)
H(180)= -.98465981E-02=H(185)
H(181)= .98665534E-02=H(184)
H(182)= .23537437E-01=H(183)

	BAND 1	BAND 2	BAND 3
LOWER BAND EDGE	0.000000000E	.121991437	.176687109
UPPER BAND EDGE	.113312391	.128008563	.500000000
DESIRED VALUE	0.000000000	1.000000000	0.000000000
WEIGHTING	1.000000000	15.000000000	1.000000000
DEVIATION	.136215211	.009081014	.136215211
DEVIATION IN DB	-17.31548787C	-40.837313051	-17.315487870

(2) Transducer No. 2

FINITE IMPULSE RESPONSE (FIR)
LINEAR PHASE FILTER DESIGN
REMEZ EXCHANGE ALGORITHM

BANDPASS FILTER

FILTER LENGTH=564

.....IMPULSE RESPONSE.....

H(1) =	-.51014962E-02	=H(564)
H(2) =	.17063043E-01	=H(563)
H(3) =	-.21636557E-01	=H(562)
H(4) =	.18187751E-01	=H(561)
H(5) =	-.83821348E-02	=H(560)
H(6) =	.53084211E-02	=H(559)
H(7) =	-.24367666E-02	=H(558)
H(8) =	.27940237E-02	=H(557)
H(9) =	-.68050837E-03	=H(556)
H(10) =	.19117419E-02	=H(555)
H(11) =	-.15097831E-03	=H(554)
H(12) =	.11708443E-02	=H(553)
H(13) =	-.31766256E-03	=H(552)
H(14) =	.49504310E-03	=H(551)
H(15) =	-.40033163E-03	=H(550)
H(16) =	.41713678E-03	=H(549)
H(17) =	-.91985380E-05	=H(548)
H(18) =	.66143366E-03	=H(547)
H(19) =	.18713455E-03	=H(546)
H(20) =	.41318581E-03	=H(545)
H(21) =	-.21837004E-03	=H(544)
H(22) =	-.94656044E-04	=H(543)
H(23) =	-.40218075E-03	=H(542)
H(24) =	-.56027075E-04	=H(541)
H(25) =	.99723138E-04	=H(540)
H(26) =	.52835534E-03	=H(539)
H(27) =	.32069437E-03	=H(538)
H(28) =	.28378152E-03	=H(537)
H(29) =	-.21680671E-03	=H(536)
H(30) =	-.30121748E-03	=H(535)
H(31) =	-.47450421E-03	=H(534)
H(32) =	-.88250767E-04	=H(533)
H(33) =	.18341978E-03	=H(532)
H(34) =	.56544767E-03	=H(531)
H(35) =	.37842101E-03	=H(530)
H(36) =	.30815323E-03	=H(529)
H(37) =	-.22865284E-03	=H(528)
H(38) =	-.51199957E-03	=H(527)
H(39) =	-.45418117E-03	=H(526)
H(40) =	-.20308312E-03	=H(525)
H(41) =	.22804117E-03	=H(524)
H(42) =	.62232545E-03	=H(523)
H(43) =	.47612624E-03	=H(522)
H(44) =	.33507822E-03	=H(521)
H(45) =	-.34668656E-03	=H(520)
H(46) =	-.46189245E-03	=H(519)
H(47) =	-.66958850E-03	=H(518)
H(48) =	-.12645446E-03	=H(517)
H(49) =	.18747367E-03	=H(516)
H(50) =	.68890136E-03	=H(515)

H(51) =	.5496093 4E-03=H(514)	H(112) =	.4404554 0E-03=H(453)		
H(52) =	.3010441 5E-03=H(513)	H(113) =	-.4603650 2E-03=H(452)		
H(53) =	.1039894 3E-03=H(512)	H(114) =	-.1217122 2E-02=H(451)		
H(54) =	-.5793091 5E-03=H(511)	H(115) =	-.1261822 2E-02=H(450)		
H(55) =	-.9353542 9E-03=H(510)	H(116) =	-.5493604 5E-03=H(449)		
H(56) =	-.2075666 0E-03=H(509)	H(117) =	.5811047 1E-03=H(448)		
H(57) =	.2627225 7E-03=H(508)	H(118) =	.1455610 4E-02=H(447)		
H(58) =	.6507151 7E-03=H(507)	H(119) =	.1515744 4E-02=H(446)		
H(59) =	.6061768 7E-03=H(506)	H(120) =	.6481995 2E-03=H(445)		
H(60) =	.2573345 6E-03=H(505)	H(121) =	-.6749585 6E-03=H(444)		
H(61) =	-.2700540 4E-03=H(504)	H(122) =	-.1705677 0E-02=H(443)		
H(62) =	-.6073172 0E-03=H(503)	H(123) =	-.1742861 1E-02=H(442)		
H(63) =	-.6053969 4E-03=H(502)	H(124) =	-.7557636 6E-03=H(441)		
H(64) =	-.2232999 2E-03=H(501)	H(125) =	.7946182 5E-03=H(440)		
H(65) =	.2762708 4E-03=H(500)	H(126) =	.1925230 6E-02=H(439)		
H(66) =	.5932789 9E-03=H(499)	H(127) =	.1957385 6E-02=H(438)		
H(67) =	.5688758 7E-03=H(498)	H(128) =	.8346600 1E-03=H(437)		
H(68) =	.2364770 2E-03=H(497)	H(129) =	-.6753981 8E-03=H(436)		
H(69) =	-.2464734 9E-03=H(496)	H(130) =	-.2165918 1E-02=H(435)		
H(70) =	-.5530772 3E-03=H(495)	H(131) =	-.2204624 4E-02=H(434)		
H(71) =	-.5007707 4E-03=H(494)	H(132) =	-.1297797 5E-03=H(433)		
H(72) =	-.2045127 9E-03=H(493)	H(133) =	.9648388 5E-03=H(432)		
H(73) =	.2279857 5E-03=H(492)	H(134) =	.2372600 2E-02=H(431)		
H(74) =	.5064065 4E-03=H(491)	H(135) =	.2404481 8E-02=H(430)		
H(75) =	.4464427 8E-03=H(490)	H(136) =	.1007260 6E-02=H(429)		
H(76) =	.1900976 8E-03=H(489)	H(137) =	-.1049601 0E-02=H(428)		
H(77) =	-.1936530 4E-03=H(488)	H(138) =	-.2547190 1E-02=H(427)		
H(78) =	-.4032294 8E-03=H(487)	H(139) =	-.2586122 9E-02=H(426)		
H(79) =	-.3584018 2E-03=H(486)	H(140) =	-.1069400 7E-02=H(425)		
H(80) =	-.1431950 9E-03=H(485)	H(141) =	.1111446 1E-02=H(424)		
H(81) =	.1685158 2E-03=H(484)	H(142) =	.2659881 9E-02=H(423)		
H(82) =	.2899426 1E-03=H(483)	H(143) =	.2723572 3E-02=H(422)		
H(83) =	.2736657 2E-03=H(482)	H(144) =	.1122980 0E-02=H(421)		
H(84) =	.8044896 7E-04=H(481)	H(145) =	-.1162176 8E-02=H(420)		
H(85) =	-.9613779 9E-04=H(480)	H(146) =	-.2811471 0E-02=H(419)		
H(86) =	-.1771396 5E-03=H(479)	H(147) =	-.2818067 3E-02=H(418)		
H(87) =	-.1440375 6E-03=H(478)	H(148) =	-.1162236 4E-02=H(417)		
H(88) =	-.1797450 1E-04=H(477)	H(149) =	.1196651 1E-02=H(416)		
H(89) =	.2787527 0E-04=H(476)	H(150) =	.2869814 5E-02=H(415)		
H(90) =	.5116408 7E-04=H(475)	H(151) =	.2872861 2E-02=H(414)		
H(91) =	-.2732464 5E-04=H(474)	H(152) =	.1171206 9E-02=H(413)		
H(92) =	-.1339403 3E-04=H(473)	H(153) =	-.1199895 4E-02=H(412)		
H(93) =	.1734685 4E-04=H(472)	H(154) =	-.2892784 1E-02=H(411)		
H(94) =	.1433935 3E-03=H(471)	H(155) =	-.2855664 0E-02=H(410)		
H(95) =	.1741089 8E-03=H(470)	H(156) =	-.1178651 6E-02=H(409)		
H(96) =	.1161878 8E-03=H(469)	H(157) =	.1198398 0E-02=H(408)		
H(97) =	-.1060792 2E-03=H(468)	H(158) =	.2828550 5E-02=H(407)		
H(98) =	-.3116965 5E-03=H(467)	H(159) =	.2802512 3E-02=H(406)		
H(99) =	-.3678183 7E-03=H(466)	H(160) =	.1135615 7E-02=H(405)		
H(100) =	-.1765037 2E-03=H(465)	H(161) =	-.1151349 7E-02=H(404)		
H(101) =	.1887649 8E-03=H(464)	H(162) =	-.2718650 4E-02=H(403)		
H(102) =	.5232129 2E-03=H(463)	H(163) =	-.2664490 4E-02=H(402)		
H(103) =	.5903124 0E-03=H(462)	H(164) =	-.1082058 4E-02=H(401)		
H(104) =	.2604172 1E-03=H(461)	H(165) =	.1085222 4E-02=H(400)		
H(105) =	-.2669654 9E-03=H(460)	H(166) =	.2552963 7E-02=H(399)		
H(106) =	-.7356163 1E-03=H(459)	H(167) =	.2468076 0E-02=H(398)		
H(107) =	-.7934361 6E-03=H(458)	H(168) =	.9798327 0E-03=H(397)		
H(108) =	-.3528795 3E-03=H(457)	H(169) =	-.9716074 4E-03=H(396)		
H(109) =	.3846814 2E-03=H(456)	H(170) =	-.2274834 5E-02=H(395)		
H(110) =	.9633835 6E-03=H(455)	H(171) =	-.2178655 2E-02=H(394)		
H(111) =	.1046084 8E-02=H(454)	H(172) =	-.8639492 2E-03=H(393)		

H(173) = .84641491E-03=H(392)	H(234) = -.11484113E-01=H(331)	
H(174) = .19262856E-02=H(391)	H(235) = -.17357455E-01=H(330)	
H(175) = .18263512E-02=H(390)	H(236) = .49553919E-02=H(329)	
H(176) = .70441698E-03=H(389)	H(237) = -.51264636E-02=H(328)	
H(177) = -.67564352E-03=H(388)	H(238) = -.12589916E-01=H(327)	
H(178) = -.15027217E-02=H(387)	H(239) = -.12837730E-01=H(326)	
H(179) = -.13243515E-02=H(386)	H(240) = -.54082220E-02=H(325)	
H(180) = -.51167331E-03=H(385)	H(241) = .55759393E-02=H(324)	
H(181) = .46753224E-03=H(384)	H(242) = .13659332E-01=H(323)	
H(182) = .99999140E-03=H(383)	H(243) = .13899910E-01=H(322)	
H(183) = .85322452E-03=H(382)	H(244) = .56391608E-02=H(321)	
H(184) = .29203529E-03=H(381)	H(245) = -.59991462E-02=H(320)	
H(185) = -.23463619E-03=H(380)	H(246) = -.14680585E-01=H(319)	
H(186) = -.40644375E-03=H(379)	H(247) = -.14900430E-01=H(318)	
H(187) = -.24607618E-03=H(378)	H(248) = -.62522856E-02=H(317)	
H(188) = -.32182866E-04=H(377)	H(249) = .64029255E-02=H(316)	
H(189) = -.40933749E-04=H(376)	H(250) = .15631781E-01=H(315)	
H(190) = -.26373440E-03=H(375)	H(251) = .15837081E-01=H(314)	
H(191) = -.44793617E-03=H(374)	H(252) = .66325375E-02=H(313)	
H(192) = -.25682190E-03=H(373)	H(253) = -.67706184E-02=H(312)	
H(193) = .34514604E-03=H(372)	H(254) = -.16506455E-01=H(311)	
H(194) = .10216377E-02=H(371)	H(255) = -.16692071E-01=H(310)	
H(195) = .12197610E-02=H(370)	H(256) = -.69788559E-02=H(309)	
H(196) = .57876663E-03=H(369)	H(257) = .71066244E-02=H(308)	
H(197) = -.67789712E-03=H(368)	H(258) = .17291843E-01=H(307)	
H(198) = -.18543134E-02=H(367)	H(259) = .17458710E-01=H(306)	
H(199) = -.20587936E-02=H(366)	H(260) = .72867075E-02=H(305)	
H(200) = -.94014707E-03=H(365)	H(261) = -.73949766E-02=H(304)	
H(201) = .10565059E-02=H(364)	H(262) = -.17977656E-01=H(303)	
H(202) = .27505455E-02=H(363)	H(263) = -.18119789E-01=H(302)	
H(203) = .29803592E-02=H(362)	H(264) = -.75488979E-02=H(301)	
H(204) = .13224130E-02=H(361)	H(265) = .76419881E-02=H(300)	
H(205) = -.14490230E-02=H(360)	H(266) = .18559626E-01=H(299)	
H(206) = -.37169992E-02=H(359)	H(267) = .18670357E-01=H(298)	
H(207) = -.39537587E-02=H(358)	H(268) = .77236031E-02=H(297)	
H(208) = -.17312963E-02=H(357)	H(269) = -.78445837E-02=H(296)	
H(209) = .18725901E-02=H(356)	H(270) = -.19015595E-01=H(295)	
H(210) = .47403962E-02=H(355)	H(271) = -.19104398E-01=H(294)	
H(211) = .49906116E-02=H(354)	H(272) = -.79398220E-02=H(293)	
H(212) = .21612807E-02=H(353)	H(273) = .79642356E-02=H(292)	
H(213) = -.23094308E-02=H(352)	H(274) = .19358020E-01=H(291)	
H(214) = -.58113668E-02=H(351)	H(275) = .19411182E-01=H(290)	
H(215) = -.60637462E-02=H(350)	H(276) = .80641115E-02=H(289)	
H(216) = -.26116248E-02=H(349)	H(277) = -.80950241E-02=H(288)	
H(217) = .27706697E-02=H(348)	H(278) = -.19562723E-01=H(287)	
H(218) = .69175265E-02=H(347)	H(279) = -.19596844E-01=H(286)	
H(219) = .71790055E-02=H(346)	H(280) = -.81236249E-02=H(285)	
H(220) = .30731586E-02=H(345)	H(281) = .81365074E-02=H(284)	
H(221) = -.32395664E-02=H(344)	H(282) = .19646466E-01=H(283)	
H(222) = -.80468954E-02=H(343)		
H(223) = -.83191438E-02=H(342)		
H(224) = -.35390289E-02=H(341)		
H(225) = .37104814E-02=H(340)		
H(226) = .91993935E-02=H(339)		
H(227) = .94609310E-02=H(338)		
H(228) = .40164705E-02=H(337)		
H(229) = -.41898552E-02=H(336)		
H(230) = -.10343393E-01=H(335)		
H(231) = -.10611370E-01=H(334)		
H(232) = -.44837115E-02=H(333)		
H(233) = .46576988E-02=H(332)		

	BAND 1	BAND 2	BAND 3
LOWER BAND EDGE	0.000000000	.121723164	.133474576
UPPER BAND EDGE	.116525424	.128276836	.500000000
DESIRED VALUE	0.000000000	1.000000000	0.000000000
WEIGHTING	1.000000000	15.000000000	1.000000000
DEVIATION	.155244248	.010349617	.155244248
DEVIATION IN DB	-16.179689637	-39.701514818	-16.179689637

APPENDIX C

The Transducers finger overlapping functions(Fig 5.10)

(1) Transducer No. 1

Y(1)	=	9.06607474	= (79)
Y(2)	=	8.99701327	= (78)
Y(3)	=	9.40036340	= (77)
Y(4)	=	9.10330362	= (76)
Y(5)	=	9.72712779	= (75)
Y(6)	=	9.22924307	= (74)
Y(7)	=	10.12461400	= (73)
Y(8)	=	9.11480975	= (72)
Y(9)	=	10.26518517	= (71)
Y(10)	=	8.91008400	= (70)
Y(11)	=	10.39432434	= (69)
Y(12)	=	8.77705502	= (68)
Y(13)	=	10.49996853	= (67)
Y(14)	=	8.72242664	= (66)
Y(15)	=	10.49239259	= (65)
Y(16)	=	8.82994935	= (64)
Y(17)	=	10.34935344	= (63)
Y(18)	=	9.06734740	= (62)
Y(19)	=	10.03184315	= (61)
Y(20)	=	9.49698117	= (60)
Y(21)	=	9.56370352	= (59)
Y(22)	=	10.26140139	= (58)
Y(23)	=	8.80092590	= (57)
Y(24)	=	11.19324599	= (56)
Y(25)	=	7.83625542	= (55)
Y(26)	=	12.32691375	= (54)
Y(27)	=	6.71779119	= (53)
Y(28)	=	13.59159335	= (52)
Y(29)	=	5.46713304	= (51)
Y(30)	=	14.89918327	= (50)
Y(31)	=	4.21887482	= (49)
Y(32)	=	16.18923179	= (48)
Y(33)	=	3.06149719	= (47)
Y(34)	=	17.34135672	= (46)
Y(35)	=	2.08764399	= (45)
Y(36)	=	18.24124123	= (44)
Y(37)	=	1.37961355	= (43)
Y(38)	=	18.81478934	= (42)
Y(39)	=	1.00000000	= (41)
Y(40)	=	19.00000000	= (40)

(2) Transducer No. 2

Y(1)	=	10.88929471	=	(131)
Y(2)	=	11.06171052	=	(130)
Y(3)	=	10.50755932	=	(129)
Y(4)	=	10.80829417	=	(128)
Y(5)	=	10.21405275	=	(127)
Y(6)	=	10.69130422	=	(126)
Y(7)	=	9.93659321	=	(125)
Y(8)	=	10.23411162	=	(124)
Y(9)	=	9.61555037	=	(123)
Y(10)	=	10.13615175	=	(122)
Y(11)	=	9.55234150	=	(121)
Y(12)	=	10.09872535	=	(120)
Y(13)	=	9.55409914	=	(119)
Y(14)	=	10.04287491	=	(118)
Y(15)	=	9.61806207	=	(117)
Y(16)	=	9.94273391	=	(116)
Y(17)	=	9.76722585	=	(115)
Y(18)	=	9.81798264	=	(114)
Y(19)	=	9.85201287	=	(113)
Y(20)	=	9.60596273	=	(112)
Y(21)	=	10.00598755	=	(111)
Y(22)	=	9.42217382	=	(110)
Y(23)	=	10.23365531	=	(109)
Y(24)	=	9.24144322	=	(108)
Y(25)	=	10.49283098	=	(107)
Y(26)	=	9.02409181	=	(106)
Y(27)	=	10.74435779	=	(105)
Y(28)	=	8.85132984	=	(104)
Y(29)	=	10.94867554	=	(103)
Y(30)	=	8.67172551	=	(102)
Y(31)	=	11.08593727	=	(101)
Y(32)	=	8.55623399	=	(100)
Y(33)	=	11.16755731	=	(99)
Y(34)	=	3.54274217	=	(98)
Y(35)	=	11.17414098	=	(97)
Y(36)	=	8.64246556	=	(96)
Y(37)	=	11.04001805	=	(95)
Y(38)	=	8.87954939	=	(94)
Y(39)	=	10.77292501	=	(93)
Y(40)	=	8.24513512	=	(92)
Y(41)	=	10.32937315	=	(91)
Y(42)	=	9.74637274	=	(90)
Y(43)	=	9.32731298	=	(89)
Y(44)	=	10.49369273	=	(88)
Y(45)	=	9.10256337	=	(87)
Y(46)	=	11.31285233	=	(86)
Y(47)	=	9.24487539	=	(85)
Y(48)	=	10.33433364	=	(84)
Y(49)	=	7.24529378	=	(83)
Y(50)	=	13.24351931	=	(82)
Y(51)	=	6.25531130	=	(81)
Y(52)	=	14.29053416	=	(80)
Y(53)	=	5.19611468	=	(79)
Y(54)	=	15.31567474	=	(78)
Y(55)	=	4.15503990	=	(77)
Y(56)	=	15.31453244	=	(76)
Y(57)	=	3.20950217	=	(75)
Y(58)	=	17.21984807	=	(74)
Y(59)	=	2.38152684	=	(73)
Y(60)	=	17.97423324	=	(72)
Y(61)	=	1.72143379	=	(71)
Y(62)	=	10.53788405	=	(70)
Y(63)	=	1.24916214	=	(69)
Y(64)	=	13.34819678	=	(68)
Y(65)	=	1.00000000	=	(67)
Y(66)	=	10.00000000	=	(66)

REFERENCES

1. Gordon S. Kino, John Shaw, "Acoustic Surface Waves", Scientific American, pp.50-68, Oct.1972.

2. Delamar T. Bell,JR., J.D. Holmes & R.V. Ridings, "Applications of Acoustic Surface-Wave Technology to Spread Spectrum Communications." IEEE Trans. on Microwave Theory and Techniques, vol.MTT-21,No.4, pp.263-271,April 1973.

3. J. Heighway and A. Thompson, "SAW Devices and Their Possible Implications for Noval Radar Systems Design", International Specialist Seminar on Component Performance and System Applications, Aviemore, Scotland,25-28 Sept.1973.

4. W.R. Smith, H.M. Gerard, J.H. Collins, T.M. Reeder, H.J. Shaw, "Analysis of Interdigital Surface Wave Transducers by Use of an Equivalent Circuit Model", IEEE Trans. on Microwave Theory and Techniques, vol.MTT-17, No,11, pp.856-864,Nov. 1969.

5. R.H. Tancrell, M.G. Holland,"Acoustic Surface Wave Filters", Proc. of the IEEE,vol.59, No.3, pp. 393-409,March 1971.

6. A.J. Slobodnik,JR.,"UHF and Microwave Frequency Acoustic Surface Wave Delay Lines: Design", Microwave Physics Lab. Project 5635, Air Force Cambridge Research Labs.

7. C.S. Hartman, D.T. Bell,JR., R.C. Rosenfeld, "Impulse Model Design of Acoustic Surface-Wave Filters", IEEE Trans.,vol.MTT-21,No.4, pp. 162-175,April 1973.

8. R.F. Michell," SAW Transversal Filters: Their Use and Limitations", International Specialist Seminar on Component Performance and System Applications of Surface Acoustic Wave Devices, Aviemore Scotland, 25-28 Sept.1973.

9. G.W. Farnell, E.L. Adler,"An Overview of Acoustic Surface-Wave Technology", Final Report to Communications Research Center on DSS Contract 36001-3-4406.

10. R.H. Tancrell, R.C. Williamson," Wavefront Distortion of Acoustic Waves from Apodized Interdigital Transducers",Appl.Phys.Lett.,vol.19, No. 11,pp.456-459,Dec.1971.

11. Helge Engan, "Excitation of Elastic Surface Waves by Spatial Harmonics of Interdigital Transducers",IEEE Trans. on Elecron Devices,vol.ED-16, No.12,pp.1014-1017,Dec.1969.

12. V.M. Ristic, "Excitation and Detection of Volume Elastic Modes With Surface Conducting Gratings", Jurnal of Applied Physics,vol.43,No.5, pp.2082-2085,May 1972.

13. J.C.Crabb, J.D. Maines,N.R. Ogg, "Surface-Acoustic Diffraction on LiNbO ", Electronics Letters, vol.7,No.10,pp.253-255,May 1971.

14. F.G. Marshall, "Multistrip Coupler Based Devices", International Specialist Seminar on Component Performance and System Applications on Surface Acoustic Wave Devices, Aviemore, Scotland, 25-28 Sept.1973.

15 F.G. Marshall, C.O. Newton, E.G.S. Paige,"Theory and Design of the Acoustic Wave Multistrip Coupler", IEEE Trans. on Microwave Theory and Techniques,vol. MTT 21, No.4, pp.206-215,April 1973.

16. F.G. Marshall, C.O. Newton, E.G.S. Paige, "Surface Acoustic Wave Multistrip Components and Their Applications", IEEE Trans. on Microwave Theory and Techniques, vol.MTT 21,No.4,pp.216-225,April 73.

17. R.H. Tancrell, "Analysis Design of Bandpass Filters",IEEE Trans. on Sonics and Ultrasonics, vol. SU-21, No.1,pp.12-22,Jan. 1974.

18. A. Papoulis, "The Fourier Integral and Its Applications", McGraw-Hill, Inc.1962(pp.121).

19. H.D. Helms, "Nonrecursive Digital Filters:Design Methods for Achieving Specifications on Frequency Response", IEEE Trans. on Audio and Electroacoustics vol. AU-16, No.3, pp.336-342,Sept.1968.

20. J.H. McClellan, T.W. Parks, L.R. Rabiner, "A Computer Program for Designing Optimum FIR Linear Phase Digital Filters", IEEE Trans. on Audio and Elecroacoustics, vol. AU-21, No.6,pp.506-525,Dec.73.

21. L.I. Maissel, R.Glang,"Handbook of Thin Film Technology" McGraw-Hill,1970(Chapter 7).

22. D.A.J. Dupuis,"Thin Film Coplanar T.L.", M.Eng. Thesis ,McMaster University, April 73.

23. A.J. Bahr," Fabrication Techniques for Surface Acoustic Wave Devices", International Specialist Seminar on Component Performance and Systems Applications of Surface Acoustic Wave Devices, Aviemore, Scotland, 25-28 Sept. 1973.

24. A.L.Nalamwar, M. Epstein," Immittance Characterization of Acoustic Wave Transducers", IEEE Proc. March 1972, pp 336.

25. Milton S. Kiver," Television Simplified", D.Van Nostrand Company, Inc.1955(pp.111).